Theoretical Oceanography
Lecture Notes Master AO-S28

Martin Schmidt

[1]*Leibniz Institute for Baltic Sea Research Warnemünde,*
Seestraße 15, D - 18119 Rostock, Germany,

Tel. +49-381-5197-121, e-mail: martin.schmidt@io-warnemuende.de

The general outline of this lesson is based on the lessons of Wolfgang Fennel and the book "Analytical theory of forced oceanic waves".

April 20, 2017

Contents

0

Chapter 1

Literature recommendations

This script is not a textbook, but shall serve as a guide into the field of theoretical oceanography. The discipline in the foreground is physics. We demonstrate how the complex phenomena of oceanic flow can be derived and understood from basic laws of hydrodynamics and thermodynamics. Hence, textbooks on "descriptive oceanography" are of limited help for this purpose, but may serve as an excellend supplement, since a detailed description of observations cannot be given in the limited frame of this lecture. Here the book *Descriptive Physical Oceanography* of L. Talley et al. [7] is strongly recommended. This book provides impressive insight in the beauty of our earth not to be gained with pure eyes. Also the book of M. Tomczak and J. Godfrey [8] gives a good overview. There is also a web based version, http://www.es.flinders.edu.au/~mattom/regoc/pdfversion.html.2

The lecture does not follow a specific textbook. Many sections are inpired by the recently published book *Ocean Dynamics* of D. Olbers, J. Willebrand and C. Eden, [6]. The analytical theory based on formal solutions of linear partial differential equations (Green functions) follows W. Fennel and H. U. Lass, [2]. Stimulating ideas but also some of the figures are from previous lectures of Wolfgang Fennel.

The books of

- G. Vallis, *Atmosphere and Ocean Fluid Dynamics*, [9],

- J. Apel, *Principles of Ocean Physics*, [1],

- A. Gill, *Atmosphere-Ocean Dynamics*, [3],

- P. Kundu, *Fluid Mechanics*, [4]

- J. Lighthill, *Waves in Fluids*, [5]

are also to be recommended. This is only a minor selection.

For a deeper understanding of the principles of small scale hydrodynamics, see any of the numerous textbooks on theoretical physics.

Chapter 2

Responses of a stratified ocean to wind forcing

2.1. Basic equations and approximations

2.1.1. The linearized Boussinesq approximation

The aim of this section is the simplification of the non-linear hydrodynamic equations toward a linearized version suitable for analytical solution. A main point is the inclusion of stratification. We recall the equations of motion for an in-compressible fluid on an rotating sphere,

$$\rho \frac{d}{dt} \vec{v} + 2\rho \vec{\Omega} \times \vec{v} = \rho \vec{g} - \nabla P + \eta_{vis} \Delta \vec{v} + \vec{F}^{ext}, \tag{2.1}$$

$$\frac{d}{dt}\rho = \frac{\partial}{\partial t}\rho + \vec{v} \cdot \nabla \rho = 0, \tag{2.2}$$

$$\nabla \cdot \vec{v} = 0. \tag{2.3}$$

$\vec{v}$ is the ocean velocity in a terrestrical reference system, ρ is the density of sea water, P the pressure, η_{vis} a Newtonian viscosity. There are two inertial forces on the earth rotating with respect to the system of fixed stars with an angular velocity $\vec{\Omega}$, the centrifugal force and the Coriolis force. Hence, $\vec{g}$ is the effective acceleration by earth's gravity modified by the centrifugal force, $2\rho \vec{\Omega} \times \vec{v}$ denotes the Coriolis force. This set of equations is completed by advection-diffusion equations for the potential or conservative temperature and salinity and the equation of state

$$\rho = \rho(T, S, P). \tag{2.4}$$

These equations of motion are non-linear and difficult to solve. The reason is not simply the complex geometry of a real ocean, but it is the physics behind the non-linearity. Generally, realistic solutions can be found with numerical methods only.

Exercise 2.1 Recall the meaning of all contributions of Eq. 2.3! What is the difference between the Lagrangian and the Eulerian description of fluid motion?

Exercise 2.2 How should the advection-diffusion equations for heat and salt look like? Why is in-situ temperature a bad choice to represent the heat transport?

Exercise 2.3 Consider the Marsigli experiment [1] designed to demonstrate the reason for the strong vertical shear in the flow through the Bosporus. Less saline surface water leaves the Black Sea towards the Mediterranean but more saline bottom water flows in the opposite direction. Marsigli verified the currents with a lot and designed a laboratory experiment with two basins initially filled with water of different salinity. After removing a barrier between the two basins, the horizontally different water bodies relax towards a vertically stratified state. The related vertical structure of the currents resembles roughly those observed in the Bosporus. Discuss the relation between salinity, density and pressure. Use the hydrostatic approximation, see Eq. (2.5) to understand the different role of the sea level and density. Is the flow direction in the initial state and near the final state the same? Use a simplified form of Eq. (2.3) to discuss the relaxation process.

From observations we know that the ocean state variables $\mathbf{u}$, T and S are changing slowly and vary only slightly around some "average" state. We are interested in the deviations from this "average" state, which is usually much smaller than the state variable itself. Hence, our Marsigli-experiment fulfills this condition only when the original horizontal gradients are nearly equilibrated. This helps us to develop systematic approximations to simplify our equations. Later, after introducing also simplifications for the ocean geometry, even analytical solution can be gained, which are of great value to understand the basic principles of ocean dynamics.

In previous lessons we considered mostly elevations of the ocean surface. Now we elevate also internal surfaces, i.e. isopycnals. Hence, let us start the consideration with an "ocean at rest". The variables corresponding to this special state are denoted with a subscript '0'. For an ocean at rest a vertical "background" stratification is established and the remaining equation of motion reads

$$\rho_0 \overrightarrow{g} = \nabla P = \nabla p_0. \tag{2.5}$$

The gravity force is balanced by the vertical pressure gradient and the horizontal pressure gradient vanishes. This balance of forces is called *hydrostatic balance*. It implies, that the density depends on the vertical coordinate only,

$$\frac{\partial}{\partial z}p_0 = -g\rho_0(z), \qquad \frac{\partial}{\partial x}p_0 = 0, \qquad \frac{\partial}{\partial y}p_0 = 0, \qquad \frac{\partial}{\partial t}\rho_0 = 0. \tag{2.6}$$

Because of diffusion of heat and salt, the equilibrium density would change with time too. But this is a very slow process and the adiabatic approximation made to derive the continuity equation is well justified for the processes considered here. This excludes

---

[1]Luigi Fernando Marsigli (* 10. July 1658 in Bologna; †1. November 1730 in Bologna. Italian soldier, diplomat and scientist. Understood motions of the ocean in terms of small scale physics.

thermal expansion and haline compression. Note, the equilibrium state of sea water in a gravitaional potential is not a vertically uniform salt distribution but a vertically uniform temperature and chemical potential. So our ocean state is far away from any long term equilibrium.

We want to consider ocean responses to forces elevating isobars from this slowly changing "state of rest". As long as the elevation is small, the main density variation is still vertical and density and pressure variations are a small perturbation:

$$\rho(x, y, z, t) = \rho_0(z) + \rho'(x, y, z, t), \tag{2.7}$$
$$p(x, y, z, t) = p_0(z) + p'(x, y, z, t). \tag{2.8}$$

Hence, with

$$\rho = \rho_0 \left(1 + \frac{\rho'}{\rho_0}\right), \tag{2.9}$$

we have found a quantity suitable to linearize and, hence, to simplify the equations of motion. With

$$\frac{1}{\rho}\left(\rho\vec{g} - \nabla p\right) = \frac{1}{\rho}\left(\rho_0\vec{g} + \rho'\vec{g} - \nabla p_0 - \nabla p'\right) = \frac{1}{\rho}\left(\rho'\vec{g} - \nabla p'\right) \approx \frac{1}{\rho_0}\left(\rho'\vec{g} - \nabla p'\right), \tag{2.10}$$

the equations of motion can be linearized with respect to density perturbations,

$$\frac{d}{dt}\vec{v} + 2\vec{\Omega} \times \vec{v} = \frac{\rho'}{\rho_0}\vec{g} - \frac{1}{\rho_0}\nabla p' + \nu\Delta\vec{v} + \frac{1}{\rho_0}\vec{F}^{ext}. \tag{2.11}$$

Velocity is of the same order as the density perturbation. Hence, the linearized equation of continuity becomes

$$\frac{\partial}{\partial t}\rho' + w\frac{\partial}{\partial z}\rho_0 = 0, \tag{2.12}$$

changes in the density distribution are solely caused by vertical elevation of isopycnals.

Introducing the buoyancy,

$$b = -g\frac{\rho'}{\rho_0}, \tag{2.13}$$

as a measure for the perturbation of the density field and the Brunt-Väisälä frequency,

$$N^2 = -\frac{g}{\rho_0}\frac{\partial}{\partial z}\rho_0, \tag{2.14}$$

as a measure for stratification, the equations of motions linearized with respect to density perturbations read

$$\frac{d}{dt}u - fv + \frac{\partial}{\partial x}p = \eta_{vis}\Delta u + F_x^{ext}, \tag{2.15}$$

$$\frac{d}{dt}v + fu + \frac{\partial}{\partial y}p = \eta_{vis}\Delta v + F_y^{ext}, \tag{2.16}$$

$$\frac{d}{dt}w + \frac{\partial}{\partial z}p - b = \eta_{vis}\Delta w + F_z^{ext}, \tag{2.17}$$

$$\frac{\partial}{\partial t}b + wN^2 = 0. \tag{2.18}$$

$$\nabla \cdot \vec{v} = 0. \tag{2.19}$$

f is the locally vertical component of the angular velocity at latitude φ,

$$f = 2\Omega \sin \varphi. \tag{2.20}$$

The symbol p is introduced for the pressure perturbation divided by the equilibrium density, $p = p'/\rho_0$, not to be mistaken for the total pressure P in Eq. 2.1. In the vertical equation a term of the order

$$p\frac{N^2}{g} \tag{2.21}$$

is dropped. Note also the neglect of the vertical component of the Coriolis force.

This is a set of five equations defining five dynamic quantities, the zonal, meridional vertical velocity u, v and w, the elevation of isopycnals described by the buoyancy b and the pressure perturbation p.

Exercise 2.4 Recall the variability of the Coriolis parameter f in dependence of latitude φ! Find maxima and minima and maximum slope as well!

2.1.2. The hydrostatic balance
We introduce the hydrostatic balance as a commonly used approximation for the vertical momentum equation. This reduces the set of prognostic variables. We give two types of scale arguments to identify the limits of this approximation.
In many cases the vertical acceleration $\frac{d}{dt}w$ is small compared with the other terms in the system Eqs. 2.19. This leads us to the hydrostatic balance,

$$\frac{\partial}{\partial z}p - b \approx 0. \tag{2.22}$$

The pressure perturbation is defined solely from the elevation of isopycnals. This is a considerable simplification of our set of equations, which is very common in oceanography, but also in atmosphere physics.

Before we use it, we should investigate the limits for the applicability of this approximation. To this end we consider the Fourier transformed of the (linearized) vertical momentum equation and the buoyancy equation. With

$$A(t) = \int_{-\infty}^{+\infty} \frac{d\omega}{2\pi} e^{-i\omega t} A(\omega), \tag{2.23}$$

we find

$$-i\omega w + \frac{\partial}{\partial z}p - b = 0, \tag{2.24}$$
$$-i\omega b + N^2 w = 0. \tag{2.25}$$

and combining both equations,

$$\left(N^2 - \omega^2\right) w - i\omega \frac{\partial}{\partial z}p = 0. \tag{2.26}$$

High frequency corresponds to fast processes, low frequency and the limit $\omega \to 0$ to slowly changing or steady states. Hence, the hydrostatic approximation acts like a filter restricting the solution to frequencies $\omega^2 \ll N^2$. Hence, this approximation is a good choice when looking for slowly varying processes with frequencies below or near the inertial frequency, f. These will be of main interest in the next sections. In the Baltic Sea the Brunt-Väisälä frequency is much larger then the inertial frequency,

$$f \approx 10^{-4}\text{s}^{-1} \tag{2.27}$$
$$N \approx 10^{-2}\text{s}^{-1}, \tag{2.28}$$

and the hydrostatic approximation is well justified for $\omega^2 \le f^2$.

A more general discussion of the hydrostatic approximation could be based on scale arguments. Assume that the characteristic scale of vertical and horizontal velocity are W and U, the corresponding length scales are H and L. Buoyancy and pressure have scales B and P, earth rotation F.

From the continuity equation we derive the scaling relation

$$\frac{W}{H} = \frac{U}{L} \tag{2.29}$$

or,

$$W = U\frac{H}{L}. \tag{2.30}$$

Hence, the typical scale of the vertical motion, W, is by a factor H/L smaller than the scale of the horizontal motion, U. This factor is called "aspect ratio" and is usually much smaller than 1.

The buoyancy equation implies the scale equation

$$\frac{B}{T} + \frac{BU}{L} + \frac{BW}{H} + N^2W = 0. \tag{2.31}$$

If the time scale T is small enough that neither horizontal advection UT nor vertical advection WT exceeds the horizontal or the vertical length scale L and H respectively, non-linear terms are small,

$$\frac{UT}{L} \ll 1 \tag{2.32}$$
$$\frac{WT}{H} \ll 1. \tag{2.33}$$

In this case the scale B reads

$$B = N^2WT. \tag{2.34}$$

Using similar arguments for the vertical momentum equation in combination with Eq. 2.34 gives

$$\frac{W}{T} + FU + \frac{P}{H} + N^2WT = 0. \tag{2.35}$$

From the horizontal momentum equations an expression for the pressure scale can be gained,

$$P = UFL. \tag{2.36}$$

This corresponds to the geostrophic balance. Hence, in the vertical momentum equation the pressure term is by a factor L/H larger than the Coriolis term. This is the reason why the Coriolis term in the vertical equation is not considered.

Substituting

$$P \;\; = \;\; UFL = WF\frac{L}{H}, \tag{2.37}$$

the remaining terms are

$$\frac{W}{T} + FW\frac{L^2}{H^2} + N^2WT \;\; = \;\; 0. \tag{2.38}$$

or

$$\frac{1}{T} + F\frac{L^2}{H^2} + N^2T \;\; = \;\; 0. \tag{2.39}$$

We recall, the first term stems from the vertical acceleration, the second one from the vertical pressure gradient and the last one from the buoyancy. For

$$T \gg \frac{1}{F}\frac{H^2}{L^2}, \tag{2.40}$$

hence, for times larger than the inertial period the vertical acceleration is small compared with the pressure gradient. Actually the aspect ratio is usually small and this relation holds even at smaller time scales.

Finally, for time scales $T \gg N^{-1}$ the first term in Eq. 2.38 is small compared with the last term. The remaining balance is

$$\frac{P}{H} + N^2WT = 0. \tag{2.41}$$

Subsequently, we will focus on time scales near the inertial frequency or larger than the Brunt-Väisälä frequency. Hence, we will neglect the vertical acceleration.

Exercise 2.5 What is the meaning of "stratification"? Extract profiles of temperature and salinity from the World Ocean Atlas and calculate density and pressure! Recall the meaning of potential temperature and density.

Exercise 2.6 Demonstrate that the pressure does not "drive" (in the sense of "accelerate") any current, but pressure gradients do! Investigate, how horizontally varying temperature and salinity may be responsible for ocean currents.

2.1.3. The treatment of turbulence

Applying approximations like the Boussinesq approximation, linearisation and hydrostatic approximation filters out a large part of the solution spectrum, especially the irregular small scale motion mostly called "turbulence". With the aim to describe large scale motion this seems to be a great advantage and simplification. However, this way also the mechanism for wind forcing and bottom friction would be lost. We show a systematic way to overcome this dilemma.

To investigate the coupling between small-scale and large-scale processes we introduce a decomposition of all dynamic quantities a into a large scale part $\bar{a}$ and a small scale part a',

$$a = \bar{a} + a'. \tag{2.42}$$

$^{-}$ is a projection of a onto the large-scale part. This can be for example a time average over the typical time scale of the small-scale motion, but also a spatial average. This procedure is well defined only, if the time scale of both large-scale and small-scale processes are well separated. In the frequency space (Fourier transformed), there must exist a spectral gap in the power spectrum between the domain governed by large-scale and small-scale processes. We cannot discuss this in detail here, but assume simply that the spectral gap exists and large- and small-scale are well separated this way.

The operator $^{-}$ must be idempotent,

$$\bar{\bar{a}} = \bar{a} \tag{2.43}$$

and consequently

$$\overline{a'} = 0. \tag{2.44}$$

For application in on the equations of motion we postulate the Reynolds-rules

$$\overline{cu} = c\bar{u} \tag{2.45}$$
$$\overline{u+v} = \bar{u} + \bar{v} \tag{2.46}$$
$$\overline{\bar{u}\bar{v}} = \bar{u}\bar{v} \tag{2.47}$$
$$\overline{\bar{u}v'} = 0 \tag{2.48}$$
$$\overline{\overline{uv}} = \bar{u}\bar{v}. \tag{2.49}$$

Applying the operators $^{-}$ on the momentum equation we find

$$\frac{\partial \bar{u}}{\partial t} + \bar{u}\frac{\partial \bar{u}}{\partial x} + \bar{v}\frac{\partial \bar{u}}{\partial y} + \bar{w}\frac{\partial \bar{u}}{\partial z} - f\bar{v} + \frac{\partial \bar{p}}{\partial x}$$
$$= -\frac{\partial}{\partial x}\overline{u'u'} - \frac{\partial}{\partial y}\overline{v'u'} - \frac{\partial}{\partial z}\overline{w'u'}. \tag{2.50}$$

We see, that large-scale and small-scale processes are coupled from the non-linear parts of the momentum equations. The average action of turbulent (small-scale) motion has the same mathematical form like the molecular stress-tensor. They are often called *Reynolds stress*.

We can derive similar equations for $\overline{a'b'}$ but these contain terms of the form $\overline{a'b'c'}$ at the right hand side. This way, we end up with a hierachy of equation of growing order of products of the small-scale variables.

We need additional assumptions to find a closed set of equations.

- The most simple approximations is to negelect the terms of the order $\overline{a'b'}$. This leads us to the Euler equations.

- An improvement is the introduction of turbulent mixing coefficients and turbulent viscosity. This will be done below.

- Higher order terms lead to balance equations for the turbulent kinetic energie and its dissipation. This is the so called (k-ε-theorie).

The turbulent diffusion and viscosity is defined analogously to the dissipative terms in the Navier-Stokes equations

$$-\overline{u'u'} \;=\; 2A_H\frac{\partial\bar{u}}{\partial x} \tag{2.51}$$

$$-\overline{v'v'} \;=\; 2A_H\frac{\partial\bar{v}}{\partial y} \tag{2.52}$$

$$-\overline{w'w'} \;=\; 2A_V\frac{\partial\bar{w}}{\partial z} \tag{2.53}$$

$$-\overline{u'v'} \;=\; -\overline{v'u'} = A_H\left(\frac{\partial\bar{v}}{\partial x} + \frac{\partial\bar{u}}{\partial y}\right) \tag{2.54}$$

$$-\overline{u'w'} \;=\; -\overline{w'u'} = A_V\frac{\partial\bar{u}}{\partial z} + A_H\frac{\partial\bar{w}}{\partial x} \tag{2.55}$$

$$-\overline{v'w'} \;=\; -\overline{v'u'} = A_V\frac{\partial\bar{v}}{\partial z} + A_H\frac{\partial\bar{w}}{\partial y}. \tag{2.56}$$

Considering the momentum budget of a water column defined by the vertical integral it follows that the turbulent friction tensor at the sea surface and the bottom must be prescribed as a boundary condition. This boundary condition is formulated analogously to the boundary condition for molecular friction. The turbulent vertical momentum flux at the ocean surface is a continuous function, hence, the turbulent vertical momentum flux is equal to the turbulent stress$\overline{\tau}$,

$$-\overline{u'w'} \;=\; \frac{\overline{\tau}^{(x)}}{\rho_0)} \quad \text{für} \quad z = 0, \tag{2.57}$$

$$-\overline{v'w'} \;=\; \frac{\overline{\tau}^{(y)}}{\rho_0)} \quad \text{für} \quad z = 0. \tag{2.58}$$

For the sea surface $\overline{\tau}$ is the averaged wind stress, at the sea floor $\overline{\tau}$ is the bottom stress. The wind stress can be expressed in terms of the wind speed W,

$$\frac{\tau^{(x,y)}}{\rho_0} = C_{10}\frac{\rho_A}{\rho_0}W^{(x,y)}|W|. \tag{2.59}$$

The quantity C_{10} is called drag-coeffizient. A similar formula can be found for the bottom stress.

Exercise 2.7 What is the physical meaning of the wind stress in the budget of the horizontal momentum of the ocean? What is the unit of the wind stress? Plot the wind stress as function of the wind speed in 10 m height. Assume $C_{10} \approx 0.001$.

This parameterisation for the wind stress relates the vertical momentum flux (exactly spoken the vertical flux of horizontal momentum) to vertical shear. Especially near the sea surface this may be not realistic. Here the wind generates surface waves which carry horizontal momentum. An example is the Stokes drift. It is related to vertical shear but not to turbulent mixing.

Surface waves are breaking, which intrudes turbulent kinetic energy. This steeres mixing, works against stratification and dissipates tubulent energy to heat and potential energy. This permanent loss of turbulent energy limits this process to a surface layer of thickness H_{mix}. Here it is important to note, that the turbulent viscosity implies a downward propagation of the horizontal momentum entrained by the wind and carried by the surface gravity waves. For the momentum equations the vertical divergency of the momentum flux is the important quantity. The exact vertical profile is difficult to be measured and theory is complex. Nevertheless, the vertical integral of the divergency is well known, it is the momentum flux through the sea surface from the interaction of the wind with the surface waves. It is independent of the large scale flow. Hence, a simple, consistent approximation would be a volume force

$$X = -\frac{\partial}{\partial z}\overline{u'w'} = \frac{\tau^{(x)}}{\rho_0}\frac{\theta\left(z + H_{mix}\right)}{H_{mix}} \tag{2.60}$$

$$Y = -\frac{\partial}{\partial z}\overline{v'w'} = \frac{\tau^{(y)}}{\rho_0}\frac{\theta\left(z + H_{mix}\right)}{H_{mix}}. \tag{2.61}$$

X and Y are the divergence of the vertical momentum flux, the vertical integral is the momentum flux through the sea surface.

Exercise 2.8 Find the total momentum input by a volume force (X, Y)! Discuss the finding in relation to the vertical momentum flux!

Hence, with these approximations our Boussinesq-equations for the large-scale motion read

$$\frac{\partial \bar{u}}{\partial t} + \bar{\mathbf{u}} \cdot \nabla \bar{u} - f\bar{v} + \frac{\partial \bar{p}}{\partial x} = A_H \Delta \bar{u} + \frac{\partial}{\partial z} A_V \frac{\partial}{\partial z} \bar{u} + X \tag{2.62}$$

$$\frac{\partial \bar{v}}{\partial t} + \bar{\mathbf{u}} \cdot \nabla \bar{v} + f\bar{u} + \frac{\partial \bar{p}}{\partial y} = A_H \Delta \bar{v} + \frac{\partial}{\partial z} A_V \frac{\partial}{\partial z} \bar{v} + Y \tag{2.63}$$

$$-\bar{b} + \frac{\partial \bar{p}}{\partial z} = 0 \tag{2.64}$$

$$\frac{\partial \bar{b}}{\partial t} + \bar{\mathbf{u}} \cdot \nabla \bar{b} + N^2 \bar{w} = D \tag{2.65}$$

$$\frac{\partial \bar{u}}{\partial x} + \frac{\partial \bar{v}}{\partial y} + \frac{\partial \bar{w}}{\partial z} = 0. \tag{2.66}$$

These equations are completed by advection-diffusion equations for the temperature T and salinity s, which determine the diffusive term D at the right hand side of the bouyancy-equation.

These equations include both the expressions for the Reynolds stress, $\mathbf{X}$ stands for the entrainment of momentum into the mixed surface layer, A_V is the turbulent viscosity from all other small scale processes like breaking of internal waves, baroclinic instability and so on. For the surface boundary conditions we have to consider, that the total vertical flux of horizontal momentum has to be non-divergent at the surface. This includes the volume force $\mathbf{X}$ as well as the shear term. Because we have assumed, that the volume force stands for the wind stress, the internally generated stress must be zero at the sea surface, hence, for $z = 0$. This implies $u_z = 0$ for $z = 0$, which cannot be fulfilled exactly. However, the rigid-lid approximation introduced below will give consistent results.

2.1.4. Elimination of the buoyancy equation
Elimination of the buoyancy reduces the set of variables to 4. Three variables are defined by its time tendency, the horizontal velocity components and the pressure. The vertical velocity is diagnosed from the divergency of the horizontal velocity components. This motivates to call them "prognostic" and "diagnostic" variables.
We eliminate the buoyancy from the equations. The vertical velocity as function of the pressure reads

$$w = -\frac{1}{N^2}\frac{\partial}{\partial t}b \tag{2.67}$$

$$= -\frac{1}{N^2}\frac{\partial}{\partial z}\frac{\partial}{\partial t}p. \tag{2.68}$$

$$\frac{\partial}{\partial t}u - fv + \frac{\partial p}{\partial x} = A_H \Delta u + \frac{\partial}{\partial z}A_V \frac{\partial}{\partial z}u + X \tag{2.69}$$

$$\frac{\partial}{\partial t}v + fu + \frac{\partial p}{\partial y} = A_H \Delta \bar{v} + \frac{\partial}{\partial z}A_V \frac{\partial}{\partial z}\bar{v} + Y \tag{2.70}$$

$$\frac{\partial \bar{u}}{\partial x} + \frac{\partial \bar{v}}{\partial y} = \mathcal{Z}\frac{\partial}{\partial t}p. \tag{2.71}$$

The operator $\mathcal{Z}$ stands for

$$\mathcal{Z} = \frac{\partial}{\partial z}\frac{1}{N^2}\frac{\partial}{\partial z}. \tag{2.72}$$

2.1.5. Boundary conditions
Kinematic boundary conditions
To solve partial differential equations boundary conditions are needed. Sea floor and coastlines are like rigid walls where no flow may pass through. At the moving sea surface vertical velocity and time tendency of the elevation are related.
At fixed boundaries like coasts or the sea floor, the velocity component perpendicularly to

the boundary vanishes. Exceptions are under-water sources and sinks like ground water inflow or hydrothermal deep sea sources, so called "black smokers". A general form of the boundary condition reads

$$\vec{v} \cdot \vec{n} = 0, \tag{2.73}$$

where $\vec{n}$ is the normal vector to the boundary. For our purpose a more explicit form is preferred. The sea floor is described by the equation

$$z + H(x, y) = 0. \tag{2.74}$$

Application of the operator $\frac{d}{dt}$ yields

$$w + u \frac{\partial}{\partial x} + v \frac{\partial}{\partial y} H(x, y) = 0, \quad z = -H. \tag{2.75}$$

For a flat bottom we find

$$w = 0, \quad z = -H. \tag{2.76}$$

In the limit of a vertical boundary the velocity perpendicularly to this boundary vanishes.
    If the position of the boundary depends on time as for a moving sea surface,

$$z - \eta(x, y, t) = 0, \tag{2.77}$$

a similar method can be used. Application of the operator $\frac{d}{dt}$ yields

$$w - \frac{\partial}{\partial t}\eta - u\frac{\partial}{\partial x}\eta - v\frac{\partial}{\partial y}\eta = 0, \quad z = \eta, \tag{2.78}$$

or more general

$$(\vec{v} - \vec{v_s}) \cdot \vec{n} = 0, \quad z = \eta, \tag{2.79}$$

where $\vec{v_s}$ denotes the velocity of the moving surface.
    This is an equation of simple shape, but non-linear and difficult to handle. Remember in the complex discussion of the surface boundary condition for wind driven gravity waves.
    A second surface boundary condition applies for the pressure, the pressure at the sea surface is continuous,

$$P = P_A, \quad z = \eta, \tag{2.80}$$

where P_A is the air pressure. P_A is considered to be constant here. Applying again the the operator $\frac{d}{dt}$ and sorting orders of 'primed' terms yields

$$\frac{dP}{dt} \approx \frac{\partial}{\partial t}p' + w\frac{\partial}{\partial z}p_0 = 0, \quad z = \eta, \tag{2.81}$$

and with the hydrostatic equation at rest

$$\frac{\partial}{\partial t}p' = w\rho_0 g \quad z = \eta. \tag{2.82}$$

This is still a nonlinear problem, because the sea level η is unknown and must be determined from the pressure equation. For simplicity small sea level elevations can be assumed and the boundary conditions apply approximately at $z = 0$, the sea level at rest,

$$w \;=\; \frac{\partial}{\partial t}\eta = \frac{\partial}{\partial t}\frac{p'}{g\rho_0} \quad z = 0 \tag{2.83}$$

$$p' \;=\; g\rho_0\eta \quad z = 0 \tag{2.84}$$

Eleminating w with the help of Eq. (2.68) this as a boundary condition for the pressure alone, (remember, $p = p'/\rho_0$)

$$\frac{\partial}{\partial t}\frac{p}{g} = -\frac{1}{N^2}\frac{\partial}{\partial z}\frac{\partial}{\partial t}p \quad z = 0. \tag{2.85}$$

Dynamic boundary conditions

Dynamic boundary conditions specify the momentum transfer (momentum flux) at ocean-land or ocean atmosphere boundaries.

At the ocean-atmosphere as well as at the sea floor turbulent boundary layers develop. The turbulence within these boundary layers determines the vertical momentum flux through the boundary layers. The corresponding theory of the development of these boundary layers in not part of this lecture. Here, only a few statements can be made.

- A boundary layer is neither source or sink of momentum. The vertical flux of horizontal momentum through the boundary layers is continuous.

- The turbulent vertical momentum flux is given by the viscous terms $A_V \partial \vec{u}/\partial z$. At sea sea surface and the bottom this flux equals the surface flux τ^{surf} and the bottom flux τ^{bottom}.

- Both fluxes depend on the turbulence within the boundary layer. Our theory describes the large scale flow, which does not deliver results for the turbulence. This problem is mostly solved by rough parameterisation of the turbulence in terms of the large scale velocity.

2.2. Solution techniques for an ocean with a flat bottom

2.2.1. Separation of coordinates, the vertical eigenvalue problem
The eigenvalue equation

For an ocean with an approximately flat bottom vertical and horizontal coordinates can be factorised, the solution is traced back to a linear eigenvalue problem. This fundamental solution step delivers an essetial part of the dispersion relation of ocean waves.

For an ocean with a flat bottom vertical and horizontal co-ordinates can be separated. There arise some difficulties from vertical friction and diffusion. For the moment we neglect these terms (except the volume force from the wind stress) and discuss a generalised solution technique later.

We assume a solution of the following form,

$$u(xyzt) \;=\; \tilde{u}(xyt)F(z), \tag{2.86}$$

$$v(xyzt) \;=\; \tilde{v}(xyt)F(z), \tag{2.87}$$

$$p(xyzt) \;=\; \tilde{p}(xyt)F(z). \tag{2.88}$$

We seek an expression for the vertical function F and consider the vertical equations. After elimination of the buoyancy b it follows from the equation of continuity

$$\frac{\partial}{\partial t}\tilde{p}\mathcal{Z}F = F\left(\frac{\partial \tilde{u}}{\partial x} + \frac{\partial \tilde{v}}{\partial y}\right),$$ (2.89)

or

$$\frac{\mathcal{Z}F}{F} = \frac{\frac{\partial \tilde{u}}{\partial x} + \frac{\partial \tilde{v}}{\partial y}}{\frac{\partial}{\partial t}\tilde{p}}.$$ (2.90)

The operator $\mathcal{Z}$ is abbreviatory for

$$\mathcal{Z} = \frac{\partial}{\partial z}\frac{1}{N^2(z)}\frac{\partial}{\partial z}.$$ (2.91)

The left hand side depends only on z, the right hand side is a function of the horizontal co-ordinates. This is possible only, if both the right and left hand side are constants. The equation for F reads

$$\mathcal{Z}F(z) + \lambda^2 F(z) = 0,$$ (2.92)

From the pressure surface boundary condtions Eq. (2.85) it follows also

$$F'(0) + \frac{N^2(0)}{g}F(0) = 0$$ (2.93)

$$F'(-H) = 0.$$ (2.94)

Exercise 2.9 Derive these boundary conditions!

This is a so called Sturm - Liouville eigenvalue problem. We know, there exist a countable infinite number of solutions, the eigenfunctions $F_n(z)$ with corresponding eigenvalues λ_n. The mathematical properties of the eigenfunctions are well known. They form a complete orthonormal base of a Hilbert space. This allows us to decompose any steady function into a series of the eigenfunctions F_n. The functions F_n are orthonormal

$$\frac{1}{H}\int_{-H}^{0} dz F_m(z)F_n(z') = \delta_{mn}.$$ (2.95)

Idea for the proof: Subtract the differential equations for F_n and F_m and make use of the boundary conditions.

The decomposition of a function $f(z)$ reads

$$f(z) = \sum_n a_n F_n(z).$$ (2.96)

From orthogonality we find the co-efficients,

$$a_n = \frac{1}{H}\int_{-H}^{0} dz F_n(z)f(z).$$ (2.97)

We may imagine F_n as base vectors, $f(z)$ is projected onto these base vectors, whereupon the coefficients a_n describe the part of $f(z)$ into the direction of F_n. We may write $f(z)$ as

$$f(z) = \int_{-H}^{0} dz' f(z') \left(\frac{1}{H} \sum_n F_n(z) F_n(z') \right). \tag{2.98}$$

For completeness, the sum $\sum_n F_n(z) F_n(z')$ must have properties of a Dirac Delta-distribution:

$$\frac{1}{H} \sum_n F_n(z) F_n(z') = \delta(z - z'). \tag{2.99}$$

Completeness can also be expressed by Parseval's identity,

$$\frac{1}{H} \int_{-H}^{0} dz f^2(z) = \sum_{mn} a_m a_n \frac{1}{H} \int_{-H}^{0} dz F_m(z) F_n(z). \tag{2.100}$$

Because of the orthogonality only term with $m = n$ contribute,

$$\frac{1}{H} \int_{-H}^{0} dz f^2(z) = \sum_n a_n^2. \tag{2.101}$$

Exercise 2.10 Find other examples for complete and orthonormal function systems defined by second order differential equations and appropriate boundary conditions.

Eigenfunctions for a constante Brunt-Väisälä-frequency
For a constant Brunt-Väisälä-frequency an analytical solution for the vertical eigenvalue problem can be found.

We investigate the special case of a constant BVF,

$$N(z) = const, \tag{2.102}$$

which permits an analytical solution of the Sturm - Liouville eigenvalue problem. The general solution of Eq. 2.92 is

$$F(z) = A \sin(\lambda N z) + B \cos(\lambda N z). \tag{2.103}$$

The constants A, B und λ can be determined from the boundary conditions. Inserting F_n in the boundary conditions gives

$$A\lambda N + B \frac{N^2}{g} = 0 \tag{2.104}$$

$$A \cos(\lambda N H) + B \sin(\lambda N H) = 0. \tag{2.105}$$

A non-trivial solution for A and B does exist, but only if the coefficient determinant vanishes, i.e.,

$$\tan(\lambda N H) = \frac{N}{g\lambda}. \tag{2.106}$$

There exist countable infinite solutions of this equation, the so called eigenvalues λ_n.

Approximations:
There exists one solution with $\lambda N H \ll 1$. In this case the tangens is approximately

$$\tan(x) \approx x \tag{2.107}$$

and we get

$$\lambda_0^2 = \frac{1}{gH}. \tag{2.108}$$

This approximation is valid if

$$H \ll \frac{3g}{N^2} \approx 10^5 \text{m}, \tag{2.109}$$

i.e, it is valid (almost) everywhere in the ocean, since the order of magnitude of N is 10^{-3} .. 10^{-2}s^{-1}. On the other hand, if λ very large, the eigenvalue equation reads approximately

$$\tan(\lambda N H) = 0, \tag{2.110}$$

and we find

$$\lambda_n = \frac{n\pi}{NH}. \tag{2.111}$$

This approximation is valid for

$$H \ll \frac{n\pi g}{N^2} \approx n10^5 \text{m}, \tag{2.112}$$

and is compatible with the approximation made for λ_0. With

$$\frac{\lambda_0^2}{\lambda_n^2} = \frac{N^2 H}{n^2 \pi^2 g} \approx 10^{-6} \frac{H}{[m]n^{-2}} \tag{2.113}$$

it follows that λ_0 is one to three orders of magnitude smaller than λ_n.

Now we determine the eigenfunctions by eliminating A or B with help of the boundary conditions. The remaining free constant is defined from the normalisation. (This is not required but helps to simplify the notation.)

The normalised eigenfunctions are

$$F_n(z) = \sqrt{\frac{2}{1 + \frac{\sin(2\lambda_n NH)}{2\lambda_n NH}}} \cos\left(\lambda_n N(z + H)\right). \tag{2.114}$$

The normalisation constant can be simplified with

$$\frac{\sin\left(2\lambda_n NH\right)}{2\lambda_n NH} \approx 1 \quad \text{für} \quad n = 0, \tag{2.115}$$

$$\frac{\sin\left(2\lambda_n NH\right)}{2\lambda_n NH} \approx 0 \quad \text{für} \quad n = 1. \tag{2.116}$$
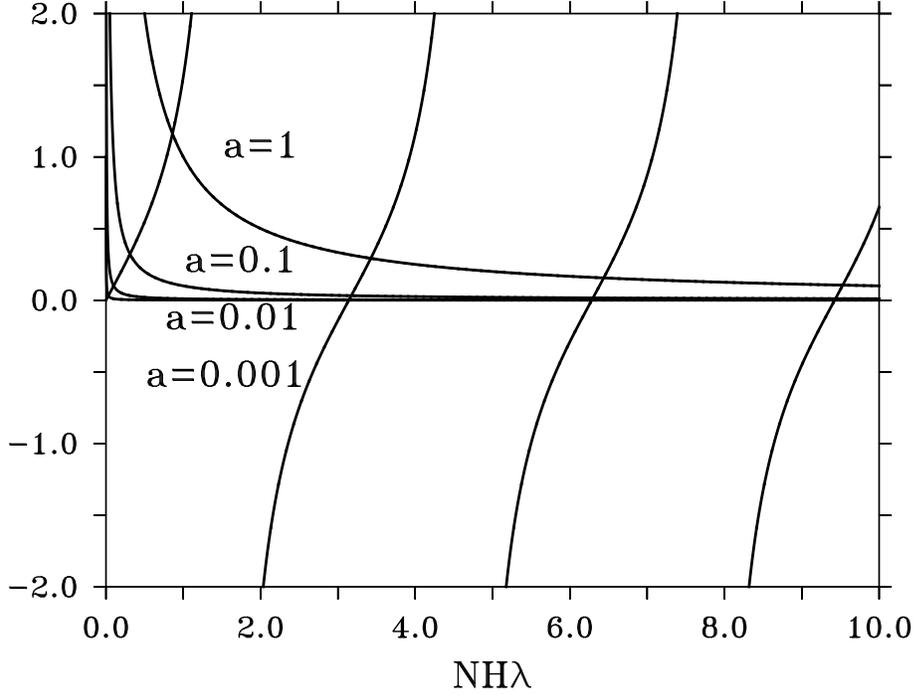
Figure 2.1. Graphical solution of Eq. 2.106. Shown are $\tan(\lambda NH)$ and $a/\lambda NH$. $a = \frac{N^2 H}{g}$ varies over a wide range.

For $n = 0$ the cosin can be also simplified and we get the final result

$$F_0(z) \approx 1 - \frac{N^2 H}{g}\left(\frac{z}{H} + \frac{1}{2}\left(\frac{z}{H}\right)^2\right), \tag{2.117}$$

$$F_n(z) \approx \sqrt{2}(-1)^n \cos\left(n\pi\frac{z}{H}\right). \tag{2.118}$$

F_0 depends only slightly on z and is called barotropic eigenfunktion, F_n varies strongly with z and is called baroclinic eigenfunktion. (A better definition will be given later.)

We will also see later that the inverse eigenvalues $c_n = \lambda_n^{-1}$ play the role of phase velocities. We call the contributions correspondig to the vertical eigenfuctions "vertical modes". Each mode corresponds to wave like processes spreading with a distinct phase velocity. From our example we see that signals in the barotropic mode spread 100 to 1000 times faster than a baroclinic signal. For the Western Baltic Sea typical phase velocites are with $H = 50m$

$$c_0 \approx 20\,\mathrm{ms}^{-1} \tag{2.119}$$

$$c_1 \approx 0.2\,\mathrm{ms}^{-1}. \tag{2.120}$$

This large velocity difference suggests the approximation that barotropic signals spread infinitely fast compared with the baroclinic signals, i.e., $\lambda_0 = 0$. This eigenvalue $\lambda_0 = 0$ is found, if the sea surface is assumed to be like a rigid lid on the ocean and the surface

boundary condition is $w(0) = 0$. This approximation is of great help, if we search for slowly varying or steady solutions. The simplified surface boundary condition is

$$\frac{\partial F}{\partial z} = 0 \quad \text{für} \quad z = 0. \tag{2.121}$$

The barotropic eigenfunktion becomes

$$F_0(z) = 1. \tag{2.122}$$

Quantitative differences are usually small, the gain of simplicity may be considerably.

Finally we test the decomposition of a special function into vertical eigenfunctions. We consider

$$f(z) = \frac{\theta\,(z + H_{mix})}{H_{mix}}. \tag{2.123}$$

We will approximate the divergence of the momentum flux in the mixing surface layer, i.e., the volume force, by such a function. H_{mix} is the mixing layer depth, θ is a step function

$$\theta(x) = \begin{cases} 1 & \text{für} \quad x > 0 \\ 0 & \text{für} \quad x < 0 \end{cases} \tag{2.124}$$

The coefficients a_n are

$$a_n = \frac{1}{H} \int_{-H}^{0} dz \frac{\theta\,(z + H_{mix})}{H_{mix}} F_n(z) = \frac{1}{H} \int_{-H_{mix}}^{0} dz \frac{F_n(z)}{H_{mix}}. \tag{2.125}$$

The integrals are elementary and we find

$$a_0 = \frac{1}{H} \tag{2.126}$$

$$a_n = \frac{\sqrt{2}}{H}(-1)^n \frac{\sin\left(n\pi \frac{H_{mix}}{H}\right)}{n\pi \frac{H_{mix}}{H}}. \tag{2.127}$$

The convergence of this suum can be investigated with Parseval's identity. The Figure shows partial sums of this identity with varying numbers of vertical modes included. It shows that in some cases a few modes are sufficient, in other cases many modes are needed for an accurate representation of the decomposed function. The more details of vertical structures to be resolved, the more modes must be included.

Approximate solution of the vertikal eigenwert problem

A constant BVF is an rough approximation, usually more complex pattern are met, which does not allow for an analytical treatment. In the following we present a systematic analytical approximation method, the Wentzel-Kramers-Brillouin-method, (WKB-method) and a numerical method to determine eigenvalues and eigenfunctions.

The Wentzel-Kramers-Brillouin-Method

The Wentzel-Kramers-Brillouin-method (WKB-method) is developed originally for quantum mechanical scattering problems. It applies well, if the wave properties of the scattered objects become less important, i.e., for high scattering energies. This is also similar to
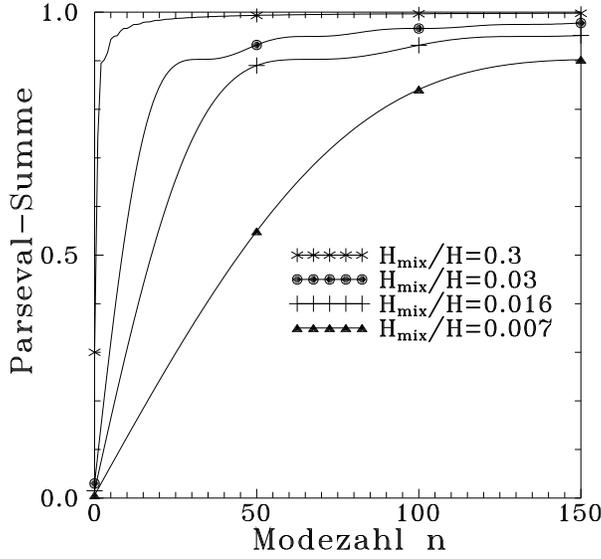
Figure 2.2. Parseval's partial sums for a decomposition of a step functions into vertical eigenfunctions

the transition from wave optics to geometrical optics (Eikonal approximation) which is possible if the influence of refraction is small.

We ask for approximations for eigenfunctions and eigenvalues of the vertical eigenvalue problem. The derivation becomes more clearly if we define a new function

$$Z(z) = \frac{1}{N^2}\frac{\partial F}{\partial z}. \tag{2.128}$$

$F(z)$ is calculated from $Z(z)$ either by integration or by differentiation (employing the eigenvalue equation of F). The equation for Z reads

$$\frac{\partial^2}{\partial z^2}Z + \lambda^2 N^2 Z = 0. \tag{2.129}$$

For $Z(z)$ we make the ansatz

$$Z(z) = A(z)\sin(\lambda S(z)) + B(z)\cos(\lambda S(z)), \tag{2.130}$$

and assume that $S(z)$, $A(z)$ und $B(z)$ are slowly varying functions of z. Inserting this ansatz into the eigenvalue equation for Z gives

$$\begin{aligned} & A'' \sin(\lambda S) + B'' \cos(\lambda S) \\ + \; & \lambda \left(S'' \left(A\cos(\lambda S) - B\sin(\lambda S) \right) + 2S' \left(A'\cos(\lambda S) - B'\sin(\lambda S) \right) \right) \\ - \; & \lambda^2 \left(S'^2 - N^2 \right) \left(A\sin(\lambda S) + B\cos(\lambda S) \right) = 0. \end{aligned} \tag{2.131}$$

For large eigenvalues λ terms with A'' und B'' can be left out. This implies, that the barotropic mode cannot be calculated from the WKB-approximation. Separating terms with different order in λ we find three equations:

$$S'^2 = N^2 \tag{2.132}$$
$$S'' A = -2S' A' \tag{2.133}$$
$$S'' B = -2S' B'. \tag{2.134}$$

These equations can be integrated and give

$$S(z) = \int_H^z dz' N(z') \tag{2.135}$$
$$A(z) = A_0 \sqrt{N}^{-1} \tag{2.136}$$
$$B(z) = B_0 \sqrt{N}^{-1}. \tag{2.137}$$

The corresponding eigenfunctions F are (assuming again large eigenvalues)

$$F(z) = -\frac{\sqrt{N}}{\lambda} \left(A_0 \cos(\lambda S(z)) - B_0 \sin(\lambda S(z)) \right). \tag{2.138}$$

The estimation of the eigenvalues λ follows the case $N = const$. From the boundary conditions we get the transcendental equation

$$\tan\left(\lambda H \bar{N} \right) = \frac{N(0)}{g\lambda}, \tag{2.139}$$

that has the approximate solution

$$\lambda_n = \frac{n\pi}{H\bar{N}}. \tag{2.140}$$

Here $\bar{N}$ is the vertically averaged BVF

$$\bar{N} = \frac{1}{H} \int_{-H}^0 dz N(z). \tag{2.141}$$

For $N = const$ we retain the solutions known from the prevoius section. The approximate baroclinic eigenfunctions are

$$F_n(z) = (-1)^n \left(2\frac{N(z)}{\bar{N}} \right)^{\frac{1}{2}} \cos\left(n\pi \frac{\int_{-H}^z dz' N(z')}{H\bar{N}} \right). \tag{2.142}$$

In summary the WKB-approximation gives results for the bariclinic eigenfunctions and eigenvalue for arbitrarily complex profiles of the BVF. Especially the eigenvalues and eigenfunctions can be calculated corresponding to profiles of the BVF taken from measurements.

Numerical solutions

The WKB-method applies only to some eigenfunctions. It does not permit a systematic enhancement of the accuracy of the solution systematically. Here numerical solution methods can be used. As an example we investigate the eigenvalue problem

$$\frac{d^2 Z}{dz^2} + \lambda^2 N^2 Z = 0 \tag{2.143}$$

with rigid lid boundary conditions

$$Z(z) = 0 \quad \text{für} \quad z = 0, -H. \tag{2.144}$$

We approximate the differential equation by finite differences,   Decomposing a function

$f(z)$ at known at $z = z_n$ into a Taylor at z_{n+1} and z_{n-1}

$$f(z_{n+1}) \approx f(z_n) + f'(z_n)\Delta z_{n+1} + f''(z_n)\frac{\Delta z_{n+1}^2}{2} \tag{2.145}$$

$$f(z_{n-1}) \approx f(z_n) - f'(z_n)\Delta z_n + f''(z_n)\frac{\Delta z_n^2}{2} \tag{2.146}$$

the first derivative can be elimitated, $(f(z_n) = f_n)$

$$f_n'' \approx 2\frac{f_{n+1}\Delta z_n + f_{n-1}\Delta z_{n+1} - f_n(\Delta z_{n+1} + \Delta z_n)}{\Delta z_{n+1}\Delta z_n(\Delta z_{n+1} + \Delta z_n)} \tag{2.147}$$

Hence, we find $n_{max} - 1$ equations. Together with the boundary conditions we $n_{max} + 1$ equations

$$\left(A_{nm} + \lambda^2 \delta_{n,m}\right) Z_m = 0 \quad n = 1..n_{max} - 1 \tag{2.148}$$

$$Z_0 = 0 \tag{2.149}$$

$$Z_{n_{max}} = 0. \tag{2.150}$$

The matirx elements are

$$A_{nm} = \delta_{n+1,m}\frac{2}{N_n^2 \Delta z_{n+1}(\Delta z_{n+1} + \Delta z_n)} \tag{2.151}$$

$$+ \delta_{n-1,m}\frac{2}{N_n^2 \Delta z_n(\Delta z_{n+1} + \Delta z_n)} \tag{2.152}$$

$$- \delta_{n,m}\frac{2}{N_n^2 \Delta z_{n+1}\Delta z_n}. \tag{2.153}$$

This can be implemented easily in FORTRAN or any other language suitable for numerics. Libraries for the eigenvalue calculation should be used. For small sized problems also analytical methods using symbolic algebra (MATHEMATICA) could be used.

We test the numerical method for $N = const$. The table shows known exact results in comparison to numerical results with different numbers of nodes.

n	$n^2\pi^2$	$n_{max} = 3$	$n_{max} = 4$	$n_{max} = 5$	$n_{max} = 6$
1	9.87	9.00	9.30	9.54	9.64
2	39.47	27.00	32.00	34.55	36.00
3	88.83	-	54.62	65.45	72.00
4	157.91	-	-	90.45	108.00
5	246.74	-	-	-	134.35

With a small number of nodes only the lowest eigenvalues can be found with sufficient accuracy, higher eigenvalues have errors up to 50%. The convergence with more nodes is growing only slowly.
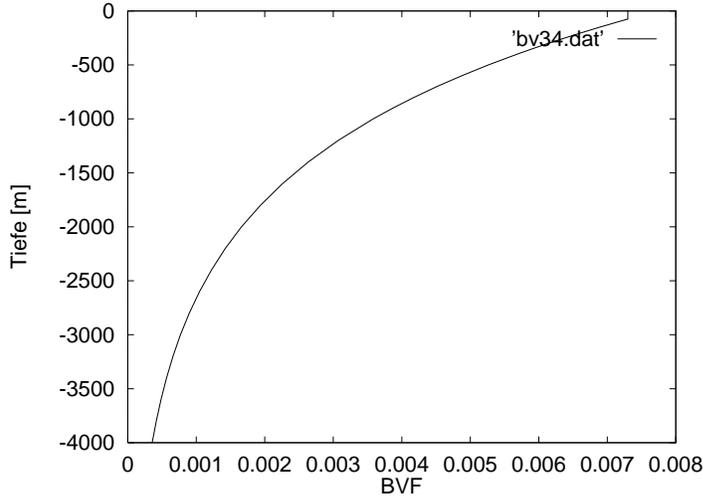

Figure 2.3. Profil der Brunt-Väsiälä-Frequenz

The figure shows the first eigenfunctions calculated for an exponetially shaped BVF.

Separation of the vertical coordinate without vertical friction

Now we are going to separate the vertical coordinate in the system of linearised Boussi-nesq equations. An exact separation is only possible for vanishing vertical frication or for some special vertical profiles of the friction coefficient. We start the discussion with this special case. It is helpful, to eliminate bouyancy and vertical velocity and we investigate the remaining three equations for the horizontal velocity components and the pressure,

$$\frac{\partial}{\partial t}u - fv + \frac{\partial p}{\partial x} = X \tag{2.154}$$

$$\frac{\partial}{\partial t}v + fu + \frac{\partial p}{\partial y} = Y \tag{2.155}$$

$$\frac{\partial u}{\partial x} + \frac{\partial v}{\partial y} - \mathcal{Z}\frac{\partial}{\partial t}p = 0. \tag{2.156}$$
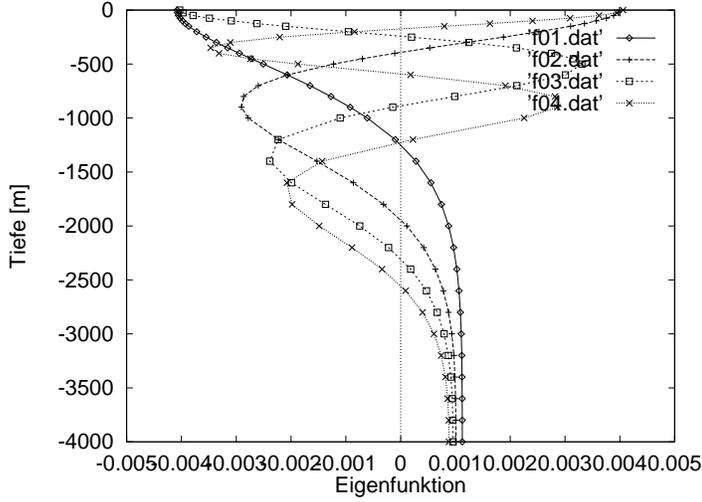
Figure 2.4. The first four baroclinic eigenfunctions $F_n(z)$

Using the hydrostatic approximation, the boundary conditions for the vertical movement are written in terms of the pressure,

$$\frac{\partial}{\partial t}\left(p + \frac{g}{N^2}\frac{\partial p}{\partial z}\right) = 0 \quad \text{für} \quad z = 0, \tag{2.157}$$

$$\frac{\partial}{\partial t}\frac{\partial p}{\partial z} = 0 \quad \text{für} \quad z = -H \tag{2.158}$$

We multiply these equations with an eigenfunktion F_n and integrate over z. For all terms with exception of the continuity equation we find coefficients,

$$C_n = \frac{1}{H}\int_{-H}^{0} dz C(z) F_n(z). \tag{2.159}$$

Recall, the functions F_n are complete and orthonormal, hence

$$C(z) = \sum_n C_n F_n(z). \tag{2.160}$$

For the pressure we integrate twice by parts

$$\frac{\partial}{\partial t}\frac{1}{H}\int_{-H}^{0} dz F_n(z)\mathcal{Z}p = \frac{\partial}{\partial t}\left(F_n(z)\frac{1}{N^2}\frac{\partial p}{\partial z}\Big|_{-H_0}^{0} - \frac{1}{N^2}p\frac{\partial F_n}{\partial z}\Big|_{-H_0}^{0}\right.$$
$$\left. +\frac{1}{H}\int_{-H}^{0} dz p\mathcal{Z}F_n\right). \tag{2.161}$$

Here we see the advantage of the special choice for the boundary conditions for F. With help of the boundary conditions for p and F the first terms vanish. The last one is rewritten using the eigenvalue equation,

$$\frac{1}{H}\int_{-H}^{0} dz p\mathcal{Z}F_n = -\lambda_n^2\frac{1}{H}\int_{-H}^{0} dz P F_n = -\lambda_n^2 p_n. \tag{2.162}$$

The components of the horizontal Boussinesq equations are now

$$\frac{\partial}{\partial t}u_n - fv_n + \frac{\partial p_n}{\partial x} = X_n \tag{2.163}$$

$$\frac{\partial}{\partial t}v_n + fu_n + \frac{\partial p_n}{\partial y} = Y_n \tag{2.164}$$

$$\frac{\partial u_n}{\partial x} + \frac{\partial v_n}{\partial y} + \frac{\partial}{\partial t}\lambda_n^2 p_n = 0. \tag{2.165}$$

Separation of the vertical coordinate with vertical friction

Considering the vertical friction in the horizontal momentum equations

$$\frac{\partial}{\partial z}A_V\frac{\partial}{\partial z}(u, v) \tag{2.166}$$

a separation of the vertical variable in not possible because th application of the operator

$$\frac{\partial}{\partial z}A_V\frac{\partial}{\partial z} \tag{2.167}$$

to eigenfunctions F_n does not reproduce the eigenfunction. Hence, the vertical eigenvalue problem with frictions becomes much more complex.

However, in many cases the details of the vertical shape of the turbulent mixing coefficient $A_V(z)$ are of minor importance. This allows the approximate the vertical profile like

$$A_V(z) \approx A\frac{1}{N^2(z)}. \tag{2.168}$$

In this special case originally proposed by Fjeldstad, we find

$$\frac{\partial}{\partial z}A_V\frac{\partial}{\partial z}F_n(z), = -A\lambda_n^2 F_n(z) \tag{2.169}$$

which allows again the separation of the vertical coordinate. Each vertical mode becomes damped with a friction parameter $A_n = A\lambda_n^2$. Since the eigenvalues are growing with n, the modes with large mode number n experience a stronger vertical friction than the barotropic or the first baroclinic modes..

This concept has a principle shortcoming that needs to be mentioned. Applying the decomposition into vertical modes we get terms of the form

$$\frac{1}{H}\int_{-H}^{0}dzF_n(z)A\mathcal{Z}u = A\left(F_n(z)\frac{1}{N^2}\frac{\partial u}{\partial z}\Big|_{-H_0}^{0} - \frac{1}{N^2}u\frac{\partial F_n}{\partial z}\Big|_{-H_0}^{0}\right.$$
$$\left. +\frac{1}{H}\int_{-H}^{0}dzu\mathcal{Z}F_n\right). \tag{2.170}$$

The vertical boundary condition for u_z is given from the wind stress and frictional bottom stress, but there is no boundary condition for u. The boundary condition for F is taylored for the pressure. Hence terms with u at the surface and the bottom do not vanish. Here the rigid lid approximation helps to find a consistent solution. Since the vertical velocity

at the sea surface becomes small, we may assume that it becomes zero there, i.e., $w(0) = 0$. The corresponding boundary condition for the pressure and F_n read

$$\frac{\partial}{\partial t}\frac{\partial p}{\partial z} = 0 \quad \text{für} \quad z = 0, \tag{2.171}$$

$$\frac{\partial F_n}{\partial z} = 0 \quad \text{für} \quad z = 0. \tag{2.172}$$

Again we find a complete decomposition into vertical modes. The barotropic eigenvalue in rigid lid approximation vanishs, $\lambda_0 = 0$. Hence the barotropic mode is solely damped by bottom friction. A common method to account for the wind stress acting on the ocean surface is the assumption of a volume force drivend by breaking surface waves, $\mathbf{X}$. To avoid double counting of the influence of the wind the vertical shear must vanish at the sea surface $u_z = 0$.

After separation of vertical and horizontal coordinates in Fjeldstad approximation the (Fourier transformed) horizontal equations read

$$-i\bar{\omega}_n u_n - f v_n + \frac{\partial p_n}{\partial x} = X_n \tag{2.173}$$

$$-i\bar{\omega}_n v_n + f u_n + \frac{\partial p_n}{\partial y} = Y_n \tag{2.174}$$

$$\frac{\partial u_n}{\partial x} + \frac{\partial v_n}{\partial y} - i\omega\lambda_n^2 p_n = 0. \tag{2.175}$$

$\bar{\omega}_n$ stands for

$$\bar{\omega}_n = \omega + iA_n. \tag{2.176}$$

Vertical friction results in an imaginary contribution to the frequency which is equivalent to a damped motion.
Finally a more simplified set of equations should be mentioned. considering not only vertical friction but also diffusion of heat and salt, similar terms become part of the bouyancy equation. Taking the same numerical value for friction and diffusion parameters, the equation of continuity becomes

$$\frac{\partial u_n}{\partial x} + \frac{\partial v_n}{\partial y} - i\bar{\omega}\lambda_n^2 p_n = 0. \tag{2.177}$$

As we will see later, this simpliefies the solution of the Boussinesq equations considerably.

The vertical velocity

The decomposition of w with respect to eigenfunctions F_n is possible. However, doing so one faces a so calles Gibbs phenomenon. The point is, that the eigenfuctions do not fulfill the surface and bottom boundary condition for w. This means that a decomposition of w with repect to F_n is badly converging at $z = 0$ and at $z = -H$. To find a solution we return to the eigenvalue problem,

$$\frac{\partial}{\partial z}\frac{1}{N^2}\frac{\partial}{\partial z}F + \lambda^2 F = 0. \tag{2.178}$$

We define a new function

$$Z(z) = \frac{1}{N^2}\frac{\partial}{\partial z}F, \tag{2.179}$$

which is defined from the eigenvalue equation

$$\frac{\partial^2}{\partial z^2}Z + \lambda^2 N^2 Z = 0. \tag{2.180}$$

It has the bottom boundary condition

$$F_z(-H) = N^2 Z(-H) = 0. \tag{2.181}$$

The eigenvalues λ_n are the same like those corresponding to F_n, the eigenfunctions are also orthogonal and complete.

Recall the equation

$$\begin{aligned}\frac{\partial}{\partial z}w &= -\mathcal{Z}p_t\\ &= -\frac{\partial}{\partial z}\frac{1}{N^2}\frac{\partial}{\partial z}p_t.\end{aligned} \tag{2.182}$$

The decomposition of p with respect to F_n

$$p(x,y,z,t) = \sum_n p_n(x,y,t)F_n(z) \tag{2.183}$$

means

$$\begin{aligned}\frac{\partial}{\partial z}w &= -\frac{\partial}{\partial z}\frac{1}{N^2}\frac{\partial}{\partial z}p_t\\ &= -\frac{\partial}{\partial z}\sum_n p_{n,t}(x,y,t)Z_n(z),\end{aligned} \tag{2.184}$$

or

$$\frac{\partial^2}{\partial z^2}w = -\frac{\partial^2}{\partial z^2}\sum_n p_{n,t}(x,y,t)Z_n(z). \tag{2.185}$$

Hence, the natural eigenfunctions for w are the functions Z_n,

$$w = \sum_n w_n(x,y,t)Z_n(z). \tag{2.186}$$

With the eigenvalue equation for Z we find

$$w_n = -p_{n,t}. \tag{2.187}$$

For completeness we give approximations for Z_n for constand N^2

$$Z_0(z) \approx -\frac{1}{g}\left(1 + \frac{z}{H}\right) \tag{2.188}$$

$$Z_n(z) \approx \sqrt{2}(-1)^n\frac{n\pi}{N^2 H}\sin\left(n\pi\frac{z}{H}\right). \tag{2.189}$$

2.2.2. Reduction of the system of equations degree

Systems of partial differential equations are difficult to be solved. By cross-differentiation we derive a singe equation for one variable, but of higher order.

To solve the forced Boussinesq equations we transform the system 2.165 into a single equation for one variable. This could be either the pressure, the vertical velocity or one of the horizontal velocity components.

The v-equation

Aiming an investigation of upwelling, where a coastal boundary condition plays a critical role, we use one of the horizontal velocity components, say v. For a short notation we drop the subscript "n" and use subsrcipts "t", "x" and "y" for partial derivatives,

$$u_t - fv + p_x = X \qquad \text{I} \tag{2.190}$$
$$v_t + fu + p_y = Y \qquad \text{II} \tag{2.191}$$
$$p_t = -\lambda^{-2}(u_x + v_y) \qquad \text{III} \tag{2.192}$$

To eliminate u from Eq. (II) we derive (II) again with respect to time and replace u_t with the help of (I).

$$v_{tt} + f(fv - p_x + X) + p_{ty} = Y_t. \tag{2.193}$$

To eliminate p we use (III). To this end we derive (II) again with respect to time and (III) with respect to x and y,

$$v_{ttt} + f(fv_t - p_{tx} + X_t) + p_{tty} = Y_{tt}, \tag{2.194}$$
$$p_{tx} = -\lambda^{-2}(u_{xx} + v_{xy}), \tag{2.195}$$
$$p_{tty} = -\lambda^{-2}(u_{txy} + v_{tyy}), \tag{2.196}$$
$$\tag{2.197}$$

to get

$$v_{ttt} + f^2 v_t + f(\lambda^{-2}(u_{xx} + v_{xy})) - \lambda^{-2}(u_{txy} + v_{tyy}) = Y_{tt} - fX_t. \tag{2.198}$$
$$\tag{2.199}$$

Cross-differentiating and subtracting (I) and (II) gives

$$u_{ty} - v_{tx} - f(u_x + v_y) - \beta v = X_y - Y_x, \tag{2.200}$$

and again with respect to x

$$u_{txy} - f(u_{xx} + v_{xy}) - \beta v_x = X_{xy} - Y_{xx} + v_{txx}. \tag{2.201}$$

(Remember, β reflects the dependency of the Coriolis-parameter on latitude - see below.) This gives the final equation for v

$$v_{ttt} + f^2 v_t - \lambda^{-2}\Delta_h v_t - \lambda^{-2}\beta v_x = Y_{tt} - fX_t + \lambda^{-2}(X_{xy} - Y_{xx}). \tag{2.202}$$

Assuming that the equation for v is solved, u and p can be calculated,

$$u_{tt} - \lambda^{-2}u_{xx} = fv_t + \lambda^{-2}v_{xy} + X_t, \tag{2.203}$$
$$p_{tt} - \lambda^{-2}p_{xx} = -\lambda^{-2}(fv_x + v_{ty} + X_x). \tag{2.204}$$

Wave equations

The equation for v is a wave equation. Hence, the ocean responds to wind forcing with waves. We will have to investigate the wave spectrum and typical wave pattern. Notably, there is also steady solution corresponding to the terms

$$\beta v_x = (X_{xy} - Y_{xx}). \tag{2.205}$$

This will lead us to the so called Sverdrup balance to be discussed later.

The pressure-equation

Similarly, an equation for the pressure can be derived. Cross differentiation of (I) and (II) gives

$$u_{tx} + v_{ty} - f(v_x - u_y) + \beta u + \Delta_h p = X_x + Y_y, \tag{2.206}$$
$$u_{ty} - v_{tx} - f(u_x + v_y) - \beta v = X_y - Y_x. \tag{2.207}$$

The relative vorticity $v_x - u_y$ can be eliminated,

$$u_{ttx} + v_{tty} + f^2(u_x + v_y) + \Delta_h p_t + \beta(u_t + fv) = X_{tx} + Y_{ty} - f(X_y - Y_x). \tag{2.208}$$

With the help of equation (III) and its second time derivative the horizontal velocity divergency is replced by the pressure,

$$-\lambda^2(p_{ttt} + f^2 p_t) + \Delta_h p_t + \beta(u_t + fv) = X_{tx} + Y_{ty} - f(Y_x - X_y). \tag{2.209}$$

This is not a closed equation in p. such an equation could be gained by cross differencing again. The resulting vorticity equation will be of little use here. Nevertheless, considering small horizontal scales, where the f-plane approximation applies, i.e., $\beta \approx 0$, we find a closed equation in p. Again, assuming p to be known from a solution of the pressure equation, velocities can be calculated,

$$u_{tt} + f^2 u = -fp_y - p_{tx} + X_t + fY, \tag{2.210}$$
$$v_{tt} + f^2 v = fp_x - p_{ty} + Y_t - fX. \tag{2.211}$$

The pressure equation reveals directly, how pressure changes can be induced within the open ocean:

- by a divergent wind field changing with time,

- by a rotational wind.

Otherwise the pressure time tendency remains zero all the time, if the initial pressure perturbation is zero.

2.3. Free waves

Considering fee waves, the spectrum can be derived. We consider the f-plane approximation. From the meridional variability of the Coriolis force there arises a new wave type - the Rossby waves.

2.3.1. Spectrum, phase and group velocity
The f-plane approximation

To sketch the essentials of this section we start with the f-plane approximation, hence, we assume small horizontal excursions of fluid parcels and neglect the meridional variability of the Coriolis force,

$$f \approx f_0. \tag{2.212}$$

This means $\beta \approx 0$, the terms proportional to β are left out in the v-equation or p-equation. Assuming for a moment that the wind forcing (X, Y) is zero, the equations for the velocity and the pressure have the same form. Considering only the x-dimension, the solution is wave like,

$$p(x, t) \quad = \quad p_0(k, \omega) e^{ikx - i\omega t}, \tag{2.213}$$

the total solution is a superposition for all wave numbers k and all frequencies ω. If the ocean is unbounded, k may have any real number, if there are boundaries a discrete spectrum arises from the boundary conditions.

Exercise 2.11 Find the boundary condition for the pressure at a zonally oriented and at a meridionally oriented coastline! Assume a flat bottom, hence, the coast is a vertical wall!

However, ω and k are not independent variables but are linked by a dispersion relation. This is found by inserting the ansatz for p into the pressure equation:

$$-i\omega \left(\lambda^2 (\omega^2 - f_0^2) - k^2 \right) \quad = \quad 0. \tag{2.214}$$

Inserting into the v equation (for $\beta \approx 0$ gives the same result. This equation has the solutions:

$$\omega \quad = \quad 0, \tag{2.215}$$
$$\omega \quad = \quad \pm\sqrt{f_0^2 + k^2 \lambda^{-2}}. \tag{2.216}$$

Hence, there exists either a constant pressure perturbation or there are waves with frequencies above the inertial frequency. Remembering the discrete spectrum of the vertical eigenvalues λ_n, the frequency of waves spreading within a stratified and rotating ocean reads

$$\omega_n \quad = \quad \pm f_0 \sqrt{1 + k^2 R_n^2}. \tag{2.217}$$

The quantity

$$R_n \quad = \quad (\lambda_n f_0)^{-1} \tag{2.218}$$

is called Rossby radius. Phase and group velocity are

$$c_p = \frac{\omega_n}{k} = \frac{1}{\lambda_n}\sqrt{1 - \frac{f_0^2}{\omega_n^2}}^{(-1)} \tag{2.219}$$

$$c_g = \frac{1}{\lambda_n}\sqrt{1 - \frac{f_0^2}{\omega_n^2}} \tag{2.220}$$

For high frequency phase and group velocity become independent of f_0 (hence of rotation) and are constants (non-dipersive). Near the inertial frequency the phase velocity is large, the group velocity tends to zero. Hence, there are only uniform motions (small wave number or large wave length) of the ocean for $\omega = f_0$.

The group velocity c_g is the velocity of signal (energy) propagation by waves. Eq. (2.220) reveals $1/\lambda_n$ as an upper limit for the wave speed.

Exercise 2.12 Find values for the barotropic and baroclinic Rossby radius in the Baltic Sea area. Assume a depth of 100m and $N^2 = 10^{-6}\text{s}^{-2}$! Make a plot of c_p and c_g as function of the wave number. Compare with the non-rotating case! Discuss the role of the Rossby radius as typical horizontal scale of a rotating fluid!

The β-plane approximation

The Coriolis parameter depends on the latitude

$$f = 2\Omega \sin(\phi). \tag{2.221}$$

A Taylor series expansion around a special latitude ϕ_0 gives

$$f \approx 2\Omega\sin(\phi_0) + 2\Omega\cos(\phi_0)\frac{y}{r_{earth}} \tag{2.222}$$

$$\approx f_0 + \beta y. \tag{2.223}$$

We have already used this when deriving the v-equation. To find the spectrum, a simple Fourier-ansatz is not sufficient, since f depends on y. However, the ansatz

$$v(x, y, t) = v_0(k, y, \omega)e^{ik_x x - i\omega t}, \tag{2.224}$$

leads us again to a Sturm-Liouville eigenvale problem. With the correspondence

$$\frac{\partial}{\partial t} \rightarrow -i\omega$$

$$\frac{\partial}{\partial x} \rightarrow ik$$

we find

$$\left(-i\omega\left(-\omega^2 + f^2 + \lambda^{-2}k_x^2\right) - \lambda^{-2}\beta ik_x\right)v_0 + i\omega\lambda^{-2}\frac{\partial^2 v_0}{\partial y^2} = 0. \tag{2.225}$$

Together with the two spatial boundary conditions for v either at some coast ($v = 0$) or at infinity this is a Sturm Liouville eigenvalue problem. Without a proof we note, that the equation

$$\frac{\partial^2 v_0}{\partial y^2} + g(y)v_0 + k_y^2 v_0 \;\; = \;\; 0, \tag{2.226}$$

has a countable infinite number of eigen-values, k_y^2. This gives us the equation

$$-i\omega\left(\left(f^2 - \omega^2\right)\lambda^2 + k_x^2 + k_y^2\right) - i\beta k_x \;\; = \;\; 0. \tag{2.227}$$

For $\beta = 0$ the formula for the f-plane case is retained. However, there are two major differences compared with the dispersion relation for the f-plane,

- the solution $\omega = 0$ does no longer exist, a constant (with time) meridional motion at the rotating earth is not possible. This fact emerges here from the dispersion relation, it the textbooks it is diskussed mostly in relation to the conservation of vorticity.

- the isotropy of space valid in the f-plane approximation is broken.

In other words, we have again three branches of the solutions, but the third one is not a constant flow but is also wave-like. This will be discussed in more detail in a separate section later.

2.3.2. Initial pressure perturbation

Now we consider the spreading of an initial pressure perturbation. We are only interested in the basic principles and consider an ocean uniform in y-direction. This implies the f-plane approximation.

First we consider details of the initial conditions. Assuming an initial pressure gradient in x-direction and zero velocity, from the continuity equation (III) it follows that the initial pressure time derivative also vanishes.

$$p(x,0) \;\; = \;\; p_0(x), \tag{2.228}$$
$$p_t(x,0) \;\; = \;\; 0. \tag{2.229}$$

$$p_{tt} \;\; = \;\; -\lambda^{-2}(u_{tx} + v_{ty}), \tag{2.230}$$
$$\;\; = \;\; -\lambda^{-2}\left(f(v_x - u_y) - p_{xx} - p_{yy}\right). \tag{2.231}$$
$$\tag{2.232}$$

Hence, since the ocean is at rest initially,

$$p_{tt}(x,0) \;\; = \;\; \lambda^{-2} p_{xx}. \tag{2.233}$$

Now we are going to solve the homogeneous pressure equation by means of Fourier transforms. Defining

$$p(x,\omega) \;\; = \;\; \int_0^\infty dt\, e^{i\tilde{\omega} t} p(x,t), \tag{2.234}$$
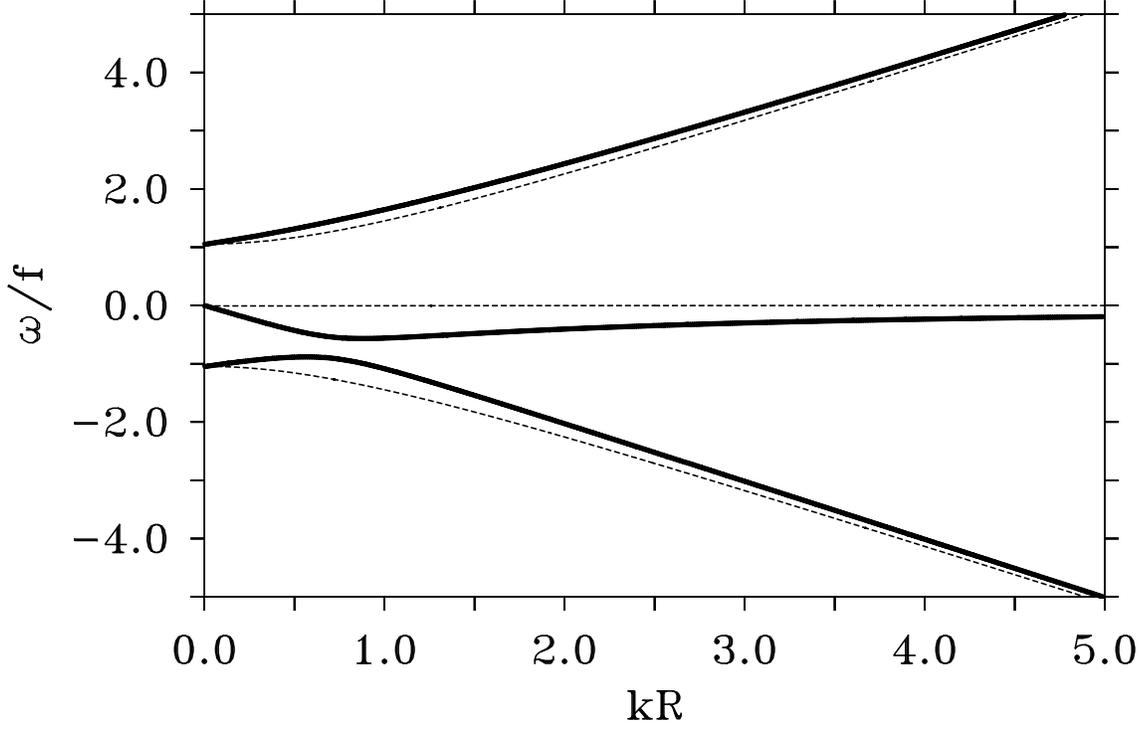$$\tilde{\omega} \;\; = \;\; \omega + i\varepsilon. \tag{2.235}$$

Figure 2.5. The dispersion relation of free waves in the open ocean. The nearly parabolic branches correspond to Poincaré waves, the other branch to Rossby waves. The dashed lines depict the f-plane approximation.

We have added an infinitesimal imaginary part to ω to ensure the convergence of the integral also for a constant pressure.

Applying the Fourier transformation to the pressure equations requires integration by parts (suppress the x argument):

$$\int_0^\infty dt e^{i\tilde{\omega}t} p_t(t) \;=\; -p(0) - \int_0^\infty dt i\tilde{\omega} e^{i\tilde{\omega}t} p(t), \tag{2.236}$$

$$=\; -p(0) - i\tilde{\omega}p(\omega) \tag{2.237}$$

$$\int_0^\infty dt e^{i\tilde{\omega}t} p_{ttt}(t) \;=\; -p_{tt}(0) - \int_0^\infty dt i\tilde{\omega} e^{i\tilde{\omega}t} p_{tt}(t), \tag{2.238}$$

$$=\; -p_{tt}(0) - i\tilde{\omega}\left(-p_t(0) - i\tilde{\omega}\int_0^\infty dt e^{i\tilde{\omega}t} p_t(t)\right), \tag{2.239}$$

$$=\; -p_{tt}(0) - i\tilde{\omega}\left(i\tilde{\omega}p(0) - \tilde{\omega}^2 p(\omega)\right) \tag{2.240}$$

Next we apply a Fourier transformation in space,

$$p(k,\omega) \;=\; \int_{-\infty}^\infty dx e^{-ikx} p(x,\omega). \tag{2.241}$$

$$\tag{2.242}$$

To ensure the convergence of this integral we must require that p vanishs for $x \to \pm\infty$.

Putting all together we end up with a inhomogeneous equation for the pressure,

$$i\tilde{\omega}\left[-\lambda^2(\tilde{\omega}^2 - f^2) + k^2\right]p(k,\omega) = p(0)\lambda^2(\tilde{\omega}^2 - f^2) \tag{2.243}$$

or

$$p(k,\omega) = -\frac{p(0)(\tilde{\omega}^2 - f^2)}{i\tilde{\omega}\left(\tilde{\omega}^2 - f^2 - k^2\lambda^{-2}\right)} \tag{2.244}$$

The denominator is well known. Its zeros define the dispersion relation of waves as given in the previous section.
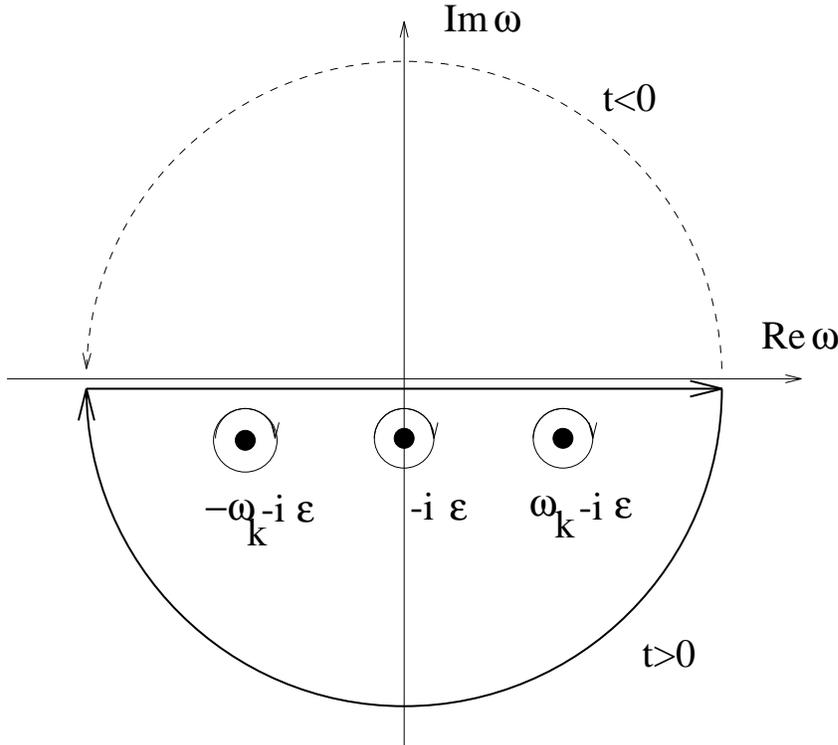

Figure 2.6. The integration path in der complex ω plane. For $t < 0$ the path is closed in the upper half plane and no poles are enclosed, for $t > 0$ the poles in the lower plane are located within the enclosed area.

The solution in the real space requires the inverse Fourier transformation,

$$p(x,t) = \int_{-\infty}^{\infty}\frac{d\omega}{2\pi}\int_{-\infty}^{\infty}\frac{dk}{2\pi}e^{ikx - i\tilde{\omega}t}p(k,\omega). \tag{2.245}$$

This can be done with help of Cauchy's integral theorem,

$$\oint\frac{d\omega}{2\pi i}\frac{f(\omega)}{\omega - \omega_0} = f(\omega_0). \tag{2.246}$$
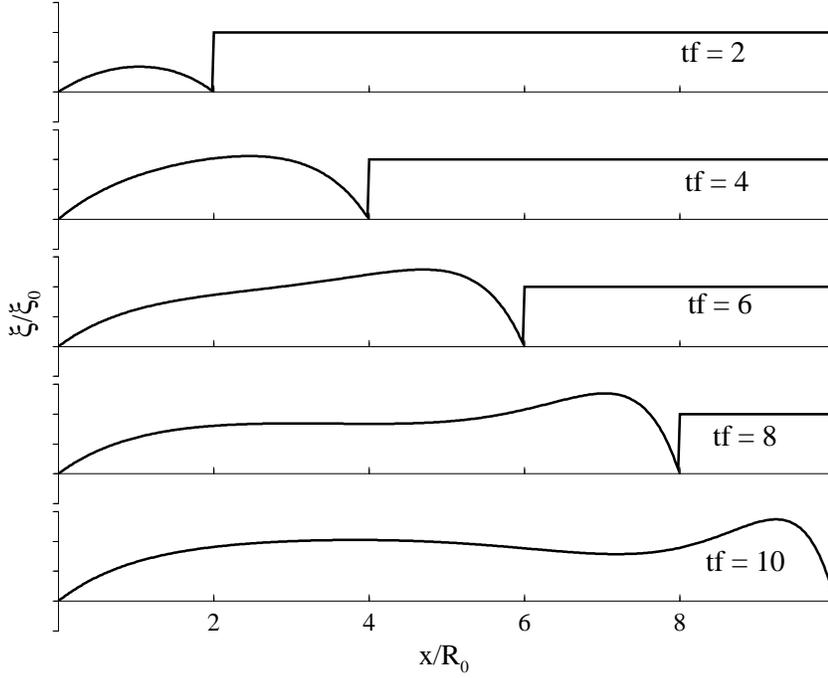
Figure 2.7. Response of the sea level to a step like perturbation at $x = 0$

The integration path in the complex plane is anti-clockwise and must encircle the point $\omega = \omega_0$. It is required, that $f(\omega)$ is an analytical function in the area enclosed by the integration path, singularities outside not enclosed by the integration path do not matter.

The denominator of Eq. (2.244) has the form

$$\frac{1}{i\tilde{\omega}\left(\tilde{\omega}^2 - \omega_k^2\right)} \tag{2.247}$$

$$\omega_k = \sqrt{f^2 + k^2\lambda^{-2}} \tag{2.248}$$

It can be rewritten as follows,

$$\frac{1}{i\tilde{\omega}\left(\tilde{\omega}^2 - \omega_k^2\right)} = \frac{1}{2i\omega_k^2}\left(-\frac{2}{\omega} + \frac{1}{\omega - \omega_k} + \frac{1}{\omega + \omega_k}\right) \tag{2.249}$$

Carrying out the ω integral

$$p(k,t) = \int_{-\infty}^{\infty} \frac{d\omega}{2\pi} e^{-i\tilde{\omega}t} p(k,\omega) \tag{2.250}$$

$$= \int_{-\infty}^{\infty} \frac{d\omega}{2\pi i} \frac{p(0)e^{-i\tilde{\omega}t}(\tilde{\omega}^2 - f^2)}{2\omega_k^2}\left(-\frac{2}{\tilde{\omega}} + \frac{1}{\tilde{\omega} - \omega_k} + \frac{1}{\tilde{\omega} + \omega_k}\right) \tag{2.251}$$

$$= -\theta(t)\oint \frac{d\omega}{2\pi i} \frac{p(0)e^{-i\tilde{\omega}t}(\tilde{\omega}^2 - f^2)}{2\omega_k^2}\left(-\frac{2}{\omega + i\varepsilon} + \frac{1}{\omega - \omega_k + i\varepsilon} + \frac{1}{\omega + \omega_k + i\varepsilon}\right) \tag{2.252}$$
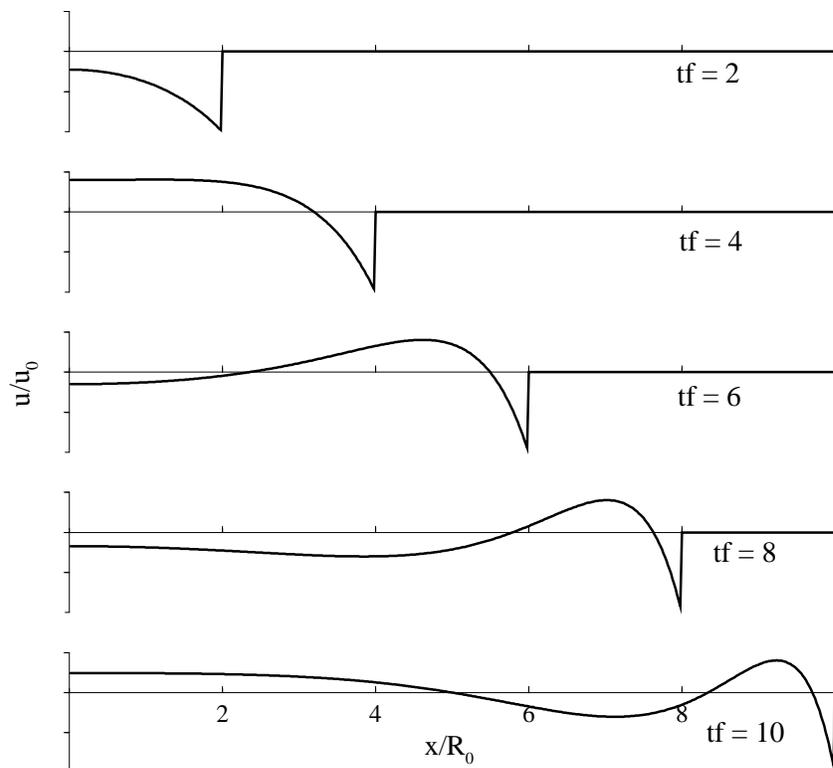
Figure 2.8. u-componente of the response of the sea level to a step like perturbation at $x = 0$

The closed integration path is shown in Fig. 2.6. It shows the importance of accounting ε carefully, to find the correct integration path. Note that for $t > 0$ the exponential diverges for $\omega \to i\infty$ (upper half plane), but tends to zero exponentially for $\omega \to -i\infty$ (lower half plane). The length of the path added by closing it in the lower half plane growth linearly with the radius, but the function tends to zero exponentially. Hence, we may the integration path in the lower half plane for $t > 0$ and in the upper half plane for $t < 0$. Since no singularity is enclosed in the upper half plane, the solution is zero for $t < 0$. This is a satisfying result, there is no action into the past as required by the causality principle. Here we lear, that the infinitesimal ε represents the causality principle in the mathematical treatment of this initial value problem.

$p(k, t)$ reads now

$$p(k,t) \;=\; p_0(k)\theta(t)\left(1 + \frac{k^2}{\lambda^2\omega_k^2}(\cos\omega_k t - 1)\right) \tag{2.253}$$

The k-integral for p cannot be carried out analytically. As an alternative we may consider the continuity equation and find

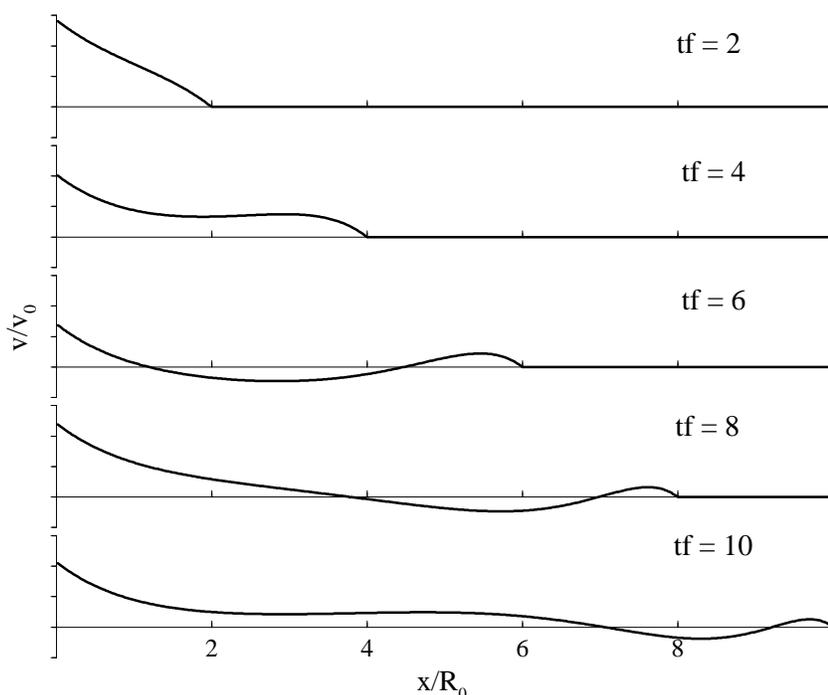$$u(k) \;=\; -\frac{1}{ik}\frac{\partial}{\partial t}p(k) \tag{2.254}$$

Figure 2.9. v-componente of the response of the sea level to a step like perturbation at $x = 0$

$$= \frac{1}{ik} p_0(k) \frac{k^2}{\omega_k} \sin \omega_k t \tag{2.255}$$

Assuming a step like initial pressure perturbation $p_0(x) = p_0 sig(x)$ the Fourier transformed is

$$p_0(k) = \int_{-\infty}^{+\infty} dx e^{ikx} p_0 \mathrm{sgn}(x)$$

$$= -p_0 \frac{2ik}{k^2 + \varepsilon^2}. \tag{2.256}$$

In this case the inverse Fourier transformed for u is

$$u(xt) = \int_{-\infty}^{+\infty} \frac{dk}{2\pi} e^{ikx} \frac{2p_0}{\omega_k} \sin \omega_k t$$

$$= -p_0 \lambda \theta(t - \lambda|x|) J_0 \left(f\sqrt{t^2 - x^2 \lambda^2} \right) \tag{2.257}$$

p can be found from u_x, v by integrating the momentum equation.

Exercise 2.13 The θ-function in Eq. (2.257) reflects causality. Discuss!

For large time, $tf \gg \frac{|x|}{R}$, the asymptotic approximation of the Bessel functionen can be

used. For u it follows

$$u(xt) \approx -\lambda p_0 \sqrt{\frac{2}{\pi f t}} \cos\left(ft - \frac{\pi}{4}\right), \tag{2.258}$$

oscillations take place with the inetrtial frequency f and are decreasing like $\sqrt{(t)}$. The integrals over the Bessel function can be carried out

$$v \quad \rightarrow \quad p_0 \lambda e^{-\frac{|x|}{R}}, \tag{2.259}$$

$$p \quad \rightarrow \quad p_0 \mathrm{sgn}(x)\left(1 - e^{-\frac{|x|}{R}}\right). \tag{2.260}$$

This is a geostrophic balance, which keeps together a part of the initial step like pressure perturbation.

This example reveals a basic difference between adjustment processes in the rotating or non-rotating ocean. In the rotating case there remains a part of the initial perturbation balanced by a geostrophic current.

To be more specific, we consider the case, that only the first vertical mode is excitet. In this case the pressure is $p = g\eta$ and $\lambda^{-1} = \sqrt{gH}$. We have also to multiply with $F_0 \approx 1/\sqrt{H}$. For an initial step of height $\eta(0, x) = \eta_0 sig(x)$ the solution reads

$$v \quad = \quad \frac{\eta_0}{H} c_0 e^{-\frac{|x|}{R}}, \tag{2.261}$$

$$p \quad = \quad p_0 \mathrm{sgn}(x)\left(1 - e^{-\frac{|x|}{R_0}}\right). \tag{2.262}$$

$$c_0 \quad = \quad \lambda_0^{-1} = \sqrt{gH} \tag{2.263}$$

The change of the potential energy between the initial state and the asymptotic state is

$$\Delta E_{pot} \quad = \quad 2\frac{\rho g}{2}\eta_0^2 \int_0^\infty dx\left(1 - \left(1 - e^{-\frac{x}{R_0}}\right)^2\right) \tag{2.264}$$

$$= \quad \frac{3}{2}g\eta_0^2 R_0. \tag{2.265}$$

The final kinetic energy is

$$\Delta E_{kin} \quad = \quad 2\frac{\rho g}{2}\eta_0^2 \int_0^\infty dx e^{-\frac{2x}{R_0}} \tag{2.266}$$

$$= \quad \frac{1}{2}g\eta_0^2 R_0. \tag{2.267}$$

Hence, an important part of the released energy is radiated away with the inertial waves, but 1/3 remains trapped in the geostropic current field near the initial perturbation.

2.4. Forcing an unbounded ocean

For an unbounded, linear, hydrostatic and frictionless (except the wind forcing) ocean a formal solution of the basic equations is derived by Fourier tranformation. Two examples will be discussed, forcing by a uniform and forcing by rotational wind. The examples reveal two basic momentum balances - the Ekman balance and the geostrophic balance.
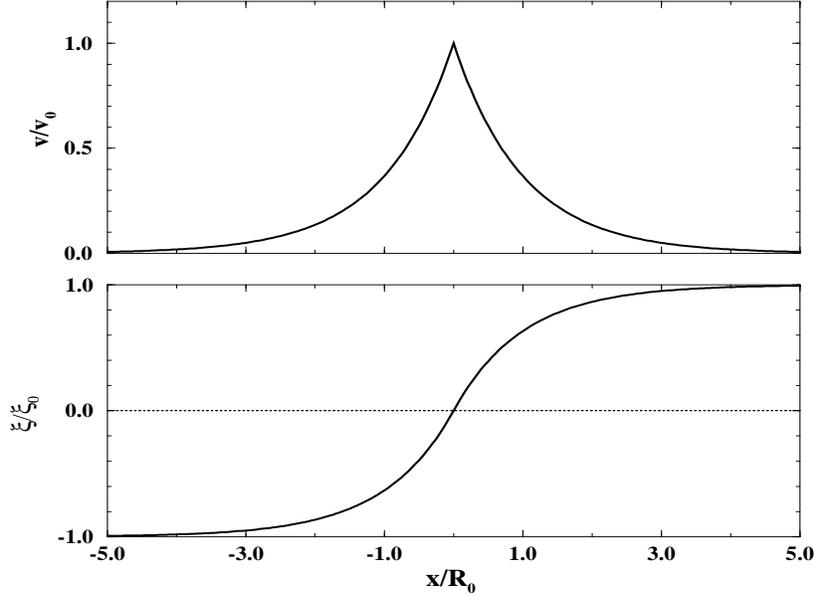
Figure 2.10. Sea level and geostrophically balanced currents for large time.

The formal solution

We return to the pressure equation (2.209) and make the f-plane approximation, $\beta = 0$,

$$-\lambda_n^2(p_{n,ttt} + f^2 p_{n,t}) + \Delta_h p_{n,t} = X_{n,tx} + Y_{n,ty} - f(Y_{n,x} - X_{n,y}). \qquad (2.268)$$

We have added the index of the vertical mode to remember that the mode decomposition is already done. Assuming p_n to be known, velocities can be calculated,

$$u_{n,tt} + f^2 u_n = -f p_{n,y} - p_{n,tx} + X_{n,t} + f Y_n, \qquad (2.269)$$
$$v_{n,tt} + f^2 v_n = f p_{n,x} - p_{n,ty} + Y_{n,t} - f X_n. \qquad (2.270)$$

Pressure changes can only emerge from:

 - a divergent wind field changing with time,

 - a rotational wind.

Otherwise the pressure time tendency remains zero all the time, and we retain the equations for the f-plane Ekman theory from previous lessons.

Now we recall the v-equation in f-plane approximation,

$$v_{ttt} + f^2 v_t - \lambda^{-2}\Delta_h v_t = Y_{tt} - f X_t + \lambda^{-2}(X_{xy} - Y_{xx}). \qquad (2.271)$$

Before we try a solution we need to specify initial conditions. We assume an ocean at rest and a wind suddenly starts blowing at $t = 0$,

$$u(t = 0) = 0, \quad v(t = 0) = 0, \quad p(t = 0) = 0. \qquad (2.272)$$

It is easy to show from the continuity equation and from the momentum equations that this implies also

$$p_t(t=0) \;=\; 0, \quad u_t(t=0)=X, \quad v_t(t=0)=Y, \tag{2.273}$$

and finally deriving the momentum equation for v after t

$$v_{tt}(t=0)+fX(t=0) \;=\; Y_t(t=0) \tag{2.274}$$

We will need these relation below for the Fourier transforms.

Now we define

$$v(\omega) \;=\; \int_0^\infty dt\, e^{i(\omega+i\varepsilon)t} v(t). \tag{2.275}$$

The positive infinitesimal ε ensures convergence of the integral for large time. We will see later that this mathematical operation ensures also causality of the solution, all ocean response will happen ofter the action of a force. Belowe we will write $\omega + i\varepsilon = \tilde{\omega}$.

We find in the same way

$$
\begin{aligned}
\int_0^\infty dt\, e^{i(\omega+i\varepsilon)t}\, v_t(t) &= v(t)e^{i(\omega+i\varepsilon)t}\Big|_0^\infty - \int_0^\infty dt\, i\tilde{\omega}\, e^{i(\omega+i\varepsilon)t}\, v(t) \\
&= -i\tilde{\omega}v(\omega).
\end{aligned}
\tag{2.276}
$$

Note the role of ε especially in the limit $t \to \infty$! The third derivative requires a partial integration three times,

$$
\begin{aligned}
\int_0^\infty dt\, e^{i(\omega+i\varepsilon)t}\, v_{ttt}(t) &= v_{tt}(t)e^{i(\omega+i\varepsilon)t}\Big|_0^\infty - \int_0^\infty dt\, i\tilde{\omega}\, e^{i(\omega+i\varepsilon)t}\, v_{tt}(t) \\
&= -v_{tt}(0) - i\tilde{\omega}\, v_t e^{i(\omega+i\varepsilon)t}\Big|_0^\infty + \int_0^\infty dt\, (i\tilde{\omega})^2\, e^{i(\omega+i\varepsilon)t}\, v_t(t) \\
&= -v_{tt}(0) + i\tilde{\omega}v_t(0) - (i\tilde{\omega})^2 v(0) - \int_0^\infty dt\, (i\tilde{\omega})^3\, e^{i(\omega+i\varepsilon)t}\, v(t) \\
&= -v_{tt}(0) + i\tilde{\omega}v_t(0) - (i\tilde{\omega})^2 v(0) - (i\tilde{\omega})^3 v(\omega) \\
&= -Y_t(0) + fX_t(0) + i\tilde{\omega}Y(0) - (i\tilde{\omega})^3 v(\omega)
\end{aligned}
\tag{2.277}
$$

For the last step we have used the initial conditions. Now we transform the forcing terms at the right hand side,

$$
\begin{aligned}
\int_0^\infty dt\, e^{i(\omega+i\varepsilon)t}\, Y_{tt}(t) &= -Y_t(0) - i\tilde{\omega}\int_0^\infty dt\, e^{i(\omega+i\varepsilon)t}\, Y_t(t) \\
&= -Y_t(0) + i\tilde{\omega}Y(0) + (i\tilde{\omega})^2 Y(\omega),
\end{aligned}
\tag{2.278}
$$

and

$$\int_0^\infty dt\, e^{i(\omega+i\varepsilon)t}\, X_t(t) \;=\; -X(0) - i\tilde{\omega}X(\omega). \tag{2.279}$$

Putting all terms together the forcing at $t=0$ cancels out. This is of great help, since the wind may be "switched on" at $t=0$. The spatial Fourier transformation is defined as

$$v(k,l) \;=\; \int_{-\infty}^\infty dx\, dy\, e^{ikx+ily} v(x,y). \tag{2.280}$$

We require v to be uniform far away from the origin,

$$v(x = \pm\infty) = 0, \quad v(y = \pm\infty) = 0. \tag{2.281}$$

The derivatives must vanish in this case. This means, from far away no wave processes must influence the solution near the origin, at least not at finite time. In this case the derivatives correspond to factors ik or il respectively.

The final result is

$$-i\tilde{\omega}\left(f^2 - \tilde{\omega}^2 + \lambda^{-2}(k^2 + l^2)\right)v(k, l, \omega)$$
$$= -\tilde{\omega}^2 Y(k, l, \omega) + i\tilde{\omega}fX(k, l, \omega) + \lambda^{-2}\left(-klX(k, l, \omega) + k^2Y(k, l, \omega)\right) \tag{2.282}$$

The velocity is now found directly by inversion,

$$v(k, l, \omega) = \frac{-\tilde{\omega}^2 Y(k, l, \omega) + i\tilde{\omega}fX(k, l, \omega) + \lambda^{-2}\left(-klX(k, l, \omega) + k^2Y(k, l, \omega)\right)}{-i\tilde{\omega}\left(f^2 - \tilde{\omega}^2 + \lambda^{-2}(k^2 + l^2)\right)}. \tag{2.283}$$

Remember, most quantities carry also a mode index n. The complete formal solution is

$$v(x, y, z, t) = \sum_n F_n(z) \int_{-\infty}^{\infty} \frac{dk}{2\pi} \int_{-\infty}^{\infty} \frac{dl}{2\pi} \int_{-\infty}^{\infty} \frac{d\omega}{2\pi} \frac{e^{-i(\tilde{\omega}t - kx - ly)}\mathcal{F}_n(k, l, \omega)}{-i\tilde{\omega}\left(f^2 - \tilde{\omega}^2 + \lambda_n^{-2}(k^2 + l^2)\right)}, \tag{2.284}$$

with

$$\mathcal{F}_n(k, l, \omega)$$
$$= -\tilde{\omega}^2 Y_n(k, l, \omega) + i\tilde{\omega}fX_n(k, l, \omega) - \lambda_n^{-2}\left(klX_n(k, l, \omega) - k^2Y_n(k, l, \omega)\right). \tag{2.285}$$

It is valid for any shape of the wind force.

Example - uniform wind

For a uniform wind

$$X(x, y, z, t) = \frac{\tau^x}{\rho_0}\theta(t)\frac{\theta(z + H_{mix})}{H_{mix}} \tag{2.286}$$

we find

$$X_n(k, l, \omega) = \frac{\tau^x}{\rho_0}a_n\frac{i}{\omega + i\varepsilon}2\pi\delta(k)\,2\pi\delta(l). \tag{2.287}$$

The coefficients a_n are give in Eq. 2.127 and are not derived again. The integral over k and l is carried out using the properties of the δ-distribution,

$$v(x, y, z, t) = \sum_n F_n(z)\frac{\tau^x}{\rho_0}a_n\int_{-\infty}^{\infty}\frac{d\omega}{2\pi}\frac{e^{-i\tilde{\omega}t}(-i)f}{\tilde{\omega}\left(f^2 - \tilde{\omega}^2\right)}. \tag{2.288}$$

To perform the ω-integral we transform the integral into a contour integral similar to that show in Figure 2.6. To close the integration path we want to add a zero contribution. With $\tilde{\omega} \to i\bar{\omega}$, where $\bar{\omega}$ is a real number, we get for the exponential

$$e^{-i\tilde{\omega}t} \to e^{\bar{\omega}t}. \tag{2.289}$$

Hence, for $t < 0$ the exponential tends to zero for large $\bar{\omega}$ in the upper half plane and converges to zero for $t > 0$ in lower half plane. The addditional contribution vanishs since the length of the added path growth linearly with the radius, but the function on this path tends to zero exponentially. Only when closing the path in the lower half plane any singularity is enclosed, see Figure 2.6. Here the positive sign of ε decides, where to close the integral for $t > 0$. This ensures causality. Now we use Cauchy's integral theorem,

$$\oint \frac{d\omega}{2\pi i} \frac{f(\omega)}{\omega - \omega_0} = f(\omega_0). \tag{2.290}$$

The integration path in the complex plane is anti-clockwise and must encircle the point $\omega = \omega_0$. We write the singularities explicitly,

$$\frac{1}{\tilde{\omega}\left(f^2 - \tilde{\omega}^2\right)} = f^{-2}\left(\frac{1}{\omega + i\varepsilon} - \frac{1}{2(\omega + i\varepsilon - f)} - \frac{1}{2(\omega + i\varepsilon + f)}\right), \tag{2.291}$$

and find

$$v(x, y, z, t) = -\sum_n F_n(z)\frac{\tau^x}{\rho_0} a_n f^{-1}\theta(t)\left(1 - \cos(ft)\right). \tag{2.292}$$

The mode sum can be carried out and resembles to original vertical structure of X,

$$v(x, y, z, t) = -\frac{\tau^x}{\rho_0}\theta(t)\frac{\theta(z + H_{mix})}{H_{mix}}f^{-1}\left(1 - \cos(ft)\right). \tag{2.293}$$

This is the well know result for inertial oscillations and Ekman transport in the open ocean. The volume force acts within the mixed surface layer. Here exists a constant flow perpendicularly to the wind forcing overlayed with an oscillating flow. The Coriolis force of from the steady flow component balances the wind stress. This is calle **Ekman balance**. Note, the theory neglects friction, except the wind force itself. Nevertheless, the flow does not gain speed over all measures. The reason is the Coriolis force which deflects the flow on circles also against the wind. It is simple to check, that the total kinetic energy is oscillating around an average value but even becomes zero periodically.

Exercise 2.14 Verify the result for u and p:

$$u(x, y, z, t) = \frac{\tau^x}{\rho_0}\theta(t)\frac{\theta(z + H_{mix})}{H_{mix}}f^{-1}\sin(ft). \tag{2.294}$$

$$p(x, y, z, t) = 0. \tag{2.295}$$

Exercise 2.15 Calculate the Ekman transport, i.e. the vertically integrated surface flow. Compare the result with the classical Ekman theory.

Exercise 2.16 Calculate the vertically integrated kinetik energy density! Use the momentum equations to show that the Coriolis force does not provide any mechanical work!

Exercise 2.17 Understand and discuss the example in Appendix E! When using a linux based system try to install ferret. If not - rewrite the script with matlab, R or python.

Forcing by a rotational wind - formal solution

Now we consider an example which is of great importance, forcing of ocean currents by a rotational wind. Figure 2.11 shows an example. Assume a zonal wind, i.e., $Y = 0$, with meridional varibility, suddenly switched on at $t = 0$ but beeing constant thereafter,

$$X(x, y, z, t) = \frac{\tau^x}{\rho_0} \theta(t) \frac{\theta(z + H_{mix})}{H_{mix}} Q(y) \tag{2.296}$$

Such wind fields may emergy in nature near ice edges, but also at fronts between warm and cold water masses. Over the cold water the atmosphere is stable and develops little turbulence for vertical momentum transfer. The opposite holds over warm water. Hence, the wind stress over the warm water becomes larger.

After mode decomposition and Fourier transformation we find

$$X_n(k, l, \omega) = \frac{\tau^x}{\rho_0} a_n \frac{i}{\omega + i\varepsilon} 2\pi\delta(k) Q(l). \tag{2.297}$$

$Q(l)$ is the Fourier transformed

$$Q(l) = \int_{-\infty}^{\infty} dy \, e^{-ily} Q(y). \tag{2.298}$$

With $\delta(k)f(k) = \delta(k)f(0)$ we simplify our v-equation,

$$v(k, l, \omega) = -\frac{\tau^x}{\rho_0} a \frac{if2\pi\delta(k) Q(l)}{\tilde{\omega} (f^2 - \tilde{\omega}^2 + \lambda^{-2}l^2)}. \tag{2.299}$$

The k- integral becomes trival, the remaining expression reads,

$$v(x, y, \omega) = \frac{\tau^x}{\rho_0} a \int_{-\infty}^{\infty} \frac{dl}{2\pi i} e^{ily} \int_{-\infty}^{\infty} dy' e^{-ily'} Q(y') \frac{f}{\tilde{\omega} (f^2 - \tilde{\omega}^2 + \lambda^{-2}l^2)}. \tag{2.300}$$

Now we have the choice how to proceed, either to specify Q, carry out the Fourier transformation in both the directions. This means, to solve two integrals for all choices of Q. Alternatively, we can carry out the l integral first and find a source representation for all Q. Consider the integral

$$\int_{-\infty}^{\infty} \frac{dl}{2\pi i} \frac{e^{il(y-y')}}{(b^2 + l^2)}, \tag{2.301}$$

where b is defined as

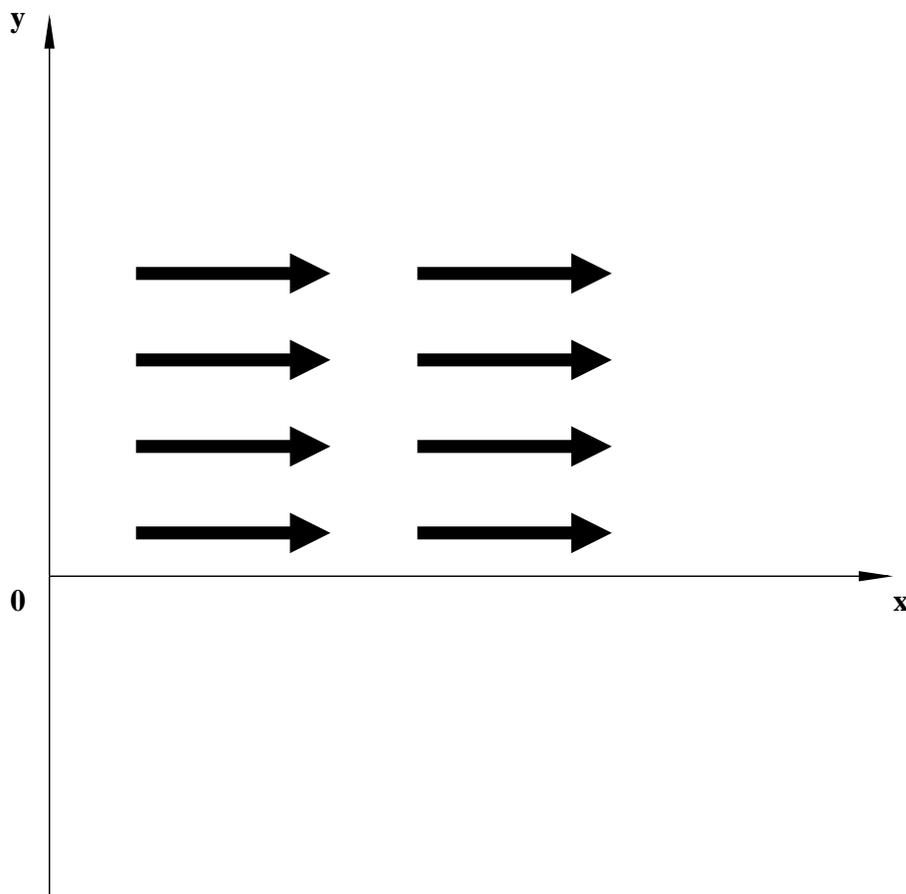$$b^2 = \lambda^2 \left(f^2 - \tilde{\omega}^2 \right). \tag{2.302}$$

Figure 2.11. A rotational wind. The x-component varies in y-direction.

The denominator has two singularities in the complex l-plane,

$$l = \pm ib. \tag{2.303}$$

We promise, never to choose values for ω larger than the inertial frequency f. Here, the small contribution $i\varepsilon$ comes into play that helps to have a finite real part of b for $\omega = f$. In this case we can perform the integral with help of Cauchy's integral theorem. We have to distinguish the case $y > y'$ and $y < y'$ and close the integration path in the upper or lower half plane.

$$\int_{-\infty}^{\infty} \frac{dl}{2\pi i}\, e^{il(y-y')} \frac{1}{(b^2 + l^2)} = \theta(y - y')\frac{e^{-b(y-y')}}{2ib} + \theta(y' - y)\frac{e^{b(y-y')}}{2ib}$$

$$= \frac{e^{-b|y-y'|}}{2ib}. \tag{2.304}$$

As the result we get a convolution integral

$$v(x, y, \omega) = \frac{\tau^x}{\rho_0} a\frac{f}{\tilde{\omega}} \int_{-\infty}^{\infty} dy'\, \frac{e^{-b|y-y'|}}{2ib} Q(y'). \tag{2.305}$$

We will see later, that the exponential is a so called Green's function.

As the next step we consider a specific example, a zonal wind blowing in one half plane,

$$Q(y) = \theta(y). \tag{2.306}$$

The y'- integral can be carried out and we find

$$
\begin{aligned}
v(x,y,\omega) &= \frac{\tau^x}{\rho_0} a \frac{f}{2i\tilde{\omega}\left(f^2 - \tilde{\omega}^2\right)} \left(\theta(-y)e^{by} + \theta(y)\left(2 - e^{-by}\right)\right) \\
&= -\frac{\tau^x}{\rho_0} a \frac{f}{2i\tilde{\omega}\left(\tilde{\omega}^2 - f^2\right)} \left[2\theta(y) - sig(y)e^{i\lambda\sqrt{\omega^2 - f^2}|y|}\right].
\end{aligned} \tag{2.307}
$$

Note,

$$i\lambda\sqrt{\omega^2 - f^2} = \lambda\sqrt{f^2 - \omega^2} = b. \tag{2.308}$$

From the momentum equation and $p_x = 0$ we find

$$
\begin{aligned}
u(x,y,\omega) &= -\frac{if}{\tilde{\omega}}v + \frac{i}{\tilde{\omega}}X(y,\omega) \\
&= -\frac{\tau^x}{\rho_0} a \left[\frac{\theta(y)}{(\tilde{\omega}^2 - f^2)} - \frac{sig(y)f^2 e^{i\lambda\sqrt{\omega^2 - f^2}|y|}}{2\tilde{\omega}^2\left(\tilde{\omega}^2 - f^2\right)}\right].
\end{aligned} \tag{2.309}
$$

$$
\begin{aligned}
p(x,y,\omega) &= \frac{1}{\lambda^2 i\tilde{\omega}}v_y \\
&= -\frac{\tau^x}{\rho_0} a \frac{if}{2\lambda} \frac{e^{i\lambda\sqrt{\omega^2 - f^2}|y|}}{\tilde{\omega}^2\sqrt{\omega^2 - f^2}}.
\end{aligned} \tag{2.310}
$$

Forcing by a rotational wind - low frequency limit

The Fourier transformation back into the time domain is not as simple as for the previous example. The reason is the square root in the exponential that is not unique in the lower and upper complex half-plane and the application of Cauchy's integral theorem is not possible. Nevertheless, in the limit $\omega \to 0$, i.e., for the limit of large time after the onset of the wind a simple expression can be found. This helps to understand the difference to the flow generated by uniform wind and we discuss this limit shortly. For $|\omega| \ll f$ we get

$$v(x,y,\omega) \approx \frac{\tau^x}{\rho_0} a_n \frac{1}{2i\tilde{\omega}f} \left[2\theta(y) - sig(y)e^{-|y|/R_n}\right] \tag{2.311}$$

$$u(x,y,\omega) \approx \frac{\tau^x}{\rho_0} a_n \left[\frac{\theta(y)}{f^2} - \frac{sig(y)e^{-|y|/R_n}}{2\tilde{\omega}^2}\right] \tag{2.312}$$

$$p(x,y,\omega) \approx -\frac{\tau^x}{\rho_0} a_n \frac{R_n f}{2} \frac{e^{-|y|/R_n}}{\tilde{\omega}^2}. \tag{2.313}$$

The quantity

$$R_n = \frac{1}{\lambda_n f} \tag{2.314}$$

(We have reintroduced the vertical mode index n.) has the dimension of a length and is called Rossby radius. The only remaining singularity is the single pole in the expression for v and the double pole in the expressions for u and p. The other terms do not contribute. Using the Cauchy integrals

$$\oint \frac{d\omega}{2\pi i} \frac{e^{-i\omega t}}{\omega + i\varepsilon} = -\theta(t) \tag{2.315}$$

$$\oint \frac{d\omega}{2\pi} \frac{e^{-i\omega t}}{(\omega + i\varepsilon)^2} = -t\theta(t) \tag{2.316}$$

we find

$$v_n(x, y, t) \approx -\frac{\tau^x}{\rho_0} a_n \frac{\theta(t)}{2f} \left[2\theta(y) - sig(y) e^{-|y|/R_n} \right] \tag{2.317}$$

$$u_n(x, y, t) \approx \frac{\tau^x}{\rho_0} a_n \left[\theta(t) t \frac{sig(y) e^{-|y|/R_n}}{2} \right] \tag{2.318}$$

$$p_n(x, y, t) \approx \frac{\tau^x}{\rho_0} a_n \theta(t) t \frac{R_n f}{2} e^{-|y|/R_n}. \tag{2.319}$$

Let us test the consistency of the approximation. We verify for each vertical mode

$$u_t - fv = X \tag{2.320}$$

$$fu + p_y = 0 \tag{2.321}$$

$$p_t = -\lambda^{-2} v_y. \tag{2.322}$$

The asymptotic expression is solution of the equations of motion.
We recognise the first term in v as the Ekman transport. Far away from the wind edge for $y \to \infty$, v it is the undisturbed Ekman transport. The inertial oscillations are missing in our result. This is quite clear, we did not include the poles at $\omega = \pm f$ into the contour integrals. The Ekman transport is confined to that area, where the wind force is acting. It cannot cross the line $y = 0$, since the wind force vanishs there. Indeed for $y \to -\infty$ the meridional flow v vanishs. In summary, distant from the wind edge the steady meridional flow is the Ekman transport, near the wind edge there is a limited transition area.

Zonal flow u and pressure perturbation are confined to a narrow band around the wind edge. We find the Rossby radius as the characteristic horizontal scale for this flow band. At $y = 0$, v and p are a steady function of y, the velocity along the wind edge is not steady. Pressure perturbation and zonal flow are in geostrophic balance - as it is expected for a flow pattern for large time.

Zonal flow and pressure perturbation are accelerating linearly with time. Hence, the solution becomes unrealistic after some time. Some basic mechanism to balance the flow is missing. We have shown previously that Newtonian friction (velocity loss proportionly to the velocity itself) can be treated by replacing our infinitesimal imaginary part of ω by a finite value r. This leaves the derivation unchanged, only in the last Fourier integral we end up with

$$\oint \frac{d\omega}{2\pi} \frac{e^{-i(\omega)t}}{(\omega + ir)^2} = -\theta(t) \frac{1 - e^{-rt}}{r}. \tag{2.323}$$
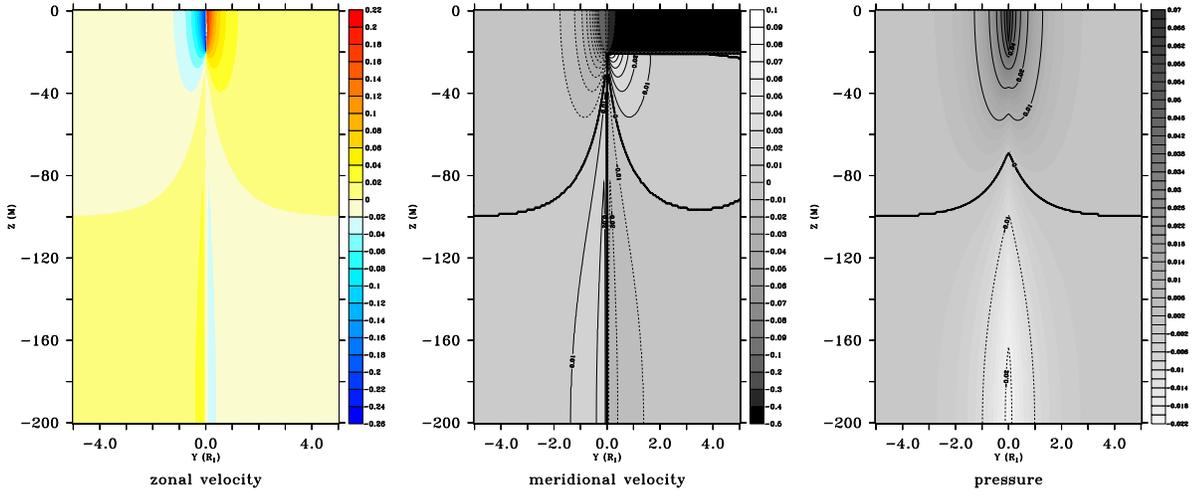
Figure 2.12. Zonal and meridional velocity and pressure perturbation near a wind edge. Pressure and zonal velocity are shown for $t = 1/f$. The mixing depth is 20 m, the baroclinic Rossby radius is about 6.4 km.

For the example of a constant N^2 the sum over the vertical eigenfunctions can be carried out analytically. This needs some efforts as outlined when discussing the coastal upwelling. In Figure 2.12 the results are shown. Here, the sum over the vertical eigenfunctions is carried out numerically. Vertical sections of the flow pattern are shown for a mixing depth of 20 m. The wind stress was set to 1 Pa, the baroclinic Rossby radius is about 6.4 km.

Forcing by a rotational wind - upwelling from a rotational wind
To discuss the upwelling we remember in

$$w(x, x, z, t) = \sum_n w_n(x, y, t) Z_n(z) \tag{2.324}$$

$$w_n = -p_{n,t}. \tag{2.325}$$

Any vertical velocity is coupled with a pressure perturbation. More specific, the pressure perturbation is the result of the linearly growing excursion of isopycnals. Remember, that we employ the hydrostatic approximation. Hence, out theory does not say anything about the reason of the vertical flow. It is simply diagnosed from the divergence of the horizontal flow, in our example this is the meridional variation of v near the wind edge. Figure 2.13 shows the vertical velocity for the example of a wind edge. At the northern hemisphere the east-ward wind generates south-ward Ekman flow that is stopped at the wind edge. Accordingly, downwelling is generated there. The maximum vertical velocity is located near the wind edge and in mixed layer depth. Since the curl of the wind stress is singular directly at the wind edge, our theory has a singularity there, the vertical velocity diverges at $z = -H_{mix}$ and $y = 0$.
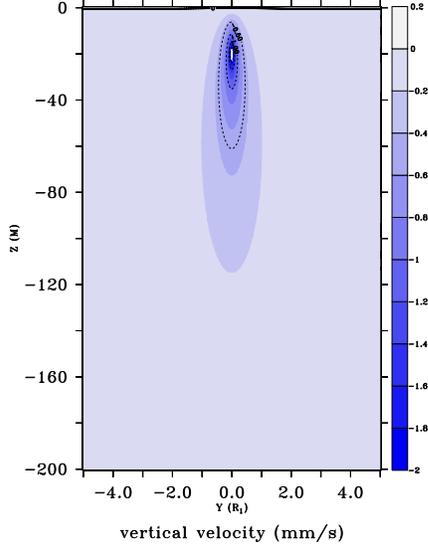
Figure 2.13. Downwelling near the wind edge. The mixing depth is 20 m, the baroclinic Rossby radius is about 6.4 km.

Forcing by a rotational wind - the role of inertial waves

We recall Equations 2.307, 2.309 and 2.310.

$$v(x,y,\omega) \;=\; -\frac{\tau^x}{\rho_0} a \frac{f}{2i\tilde{\omega}\left(\tilde{\omega}^2-f^2\right)} \left[2\theta(y)-sig(y)e^{i\lambda\sqrt{\omega^2-f^2}|y|}\right], \tag{2.326}$$

$$u(x,y,\omega) \;=\; -\frac{\tau^x}{\rho_0} a \left[\frac{\theta(y)}{\left(\tilde{\omega}^2-f^2\right)} - \frac{sig(y)f^2 e^{i\lambda\sqrt{\omega^2-f^2}|y|}}{2\tilde{\omega}^2\left(\tilde{\omega}^2-f^2\right)}\right], \tag{2.327}$$

$$p(x,y,\omega) \;=\; \frac{1}{\lambda^2 i\tilde{\omega}} v_y$$

$$\;=\; -\frac{\tau^x}{\rho_0} a \frac{if}{2\lambda} \frac{e^{i\lambda\sqrt{\omega^2-f^2}|y|}}{\tilde{\omega}^2\sqrt{\omega^2-f^2}}. \tag{2.328}$$

The first contribution is known from the previous example - forcing by a uniform wind. Inverse Fourier transformation gives the Ekman flow as found for a uniform wind, inertial oscillations and a constant transport perpendicularly to the wind.

The second term arises from the spatial wind stress variability. The inverse Fourier integral to be carried out are of the type

$$C^{(1)}(|y|,t) \;=\; \int_{-\infty}^{\infty} \frac{d\omega}{2\pi i} \frac{e^{i|y|\lambda\sqrt{\tilde{\omega}^2-f^2}-i\tilde{\omega}t}}{\tilde{\omega}^2\sqrt{\omega^2-f^2}}, \tag{2.329}$$

$$C^{(2)}(|y|,t) \;=\; \int_{-\infty}^{\infty} \frac{d\omega}{2\pi} \frac{f^2 e^{i|y|\lambda\sqrt{\tilde{\omega}^2-f^2}-i\tilde{\omega}t}}{\tilde{\omega}^2\left(\omega^2-f^2\right)}, \tag{2.330}$$

$$\tag{2.331}$$

Let us first discuss the integration path. We complete it again by a semicircle in the lower or upper complex half plane. This is possible, since the length of the path growth like ω, but the function decreases exponentially when

closing in the upper half plane for $t < \lambda|y|$,

closing in the lower half plane for $t > \lambda|y|$.

In the first case the resulting contour integral encloses no singulatities and vanishs. Hence, we have to close the contour in the lower half plane and the result carries a factor $\theta(t - \lambda|y|)$. Away from the cut the integrand is an analytical function and we can contract the integration path around the singularities. Figure 2.14 depicts the contour of the integration path. The fact, that a time $t > \lambda|y|$ is needed until the perturbation (perssure
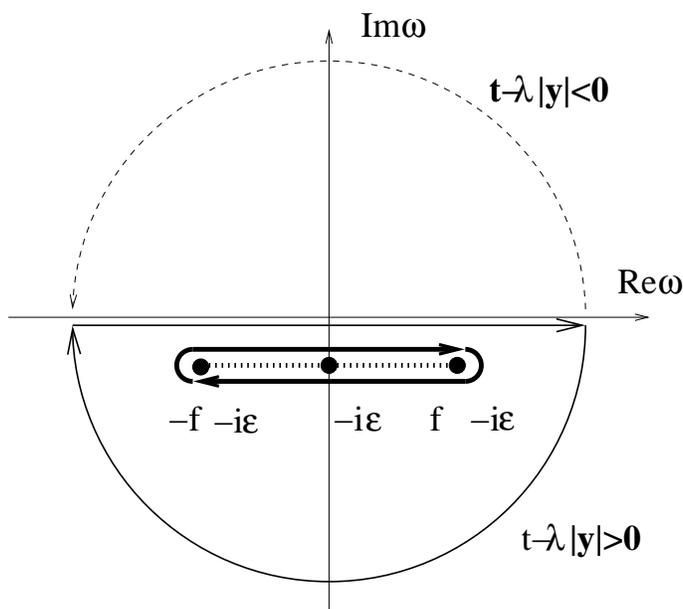

Figure 2.14. Choice of the integration path for the general integrals $C^{(1)}$ and $C^{(2)}$. A separate integration around the singularities is not possible, since the real part of the square root changes sign when crossong the cut in the complex plane (dashed line).

or velocity) differs from the Ekman solution is very important. It shows that the signal carrying the information on the existence of the wind edge spreads with waves. The maximum phase velocity is λ^{-1}. The response is zero, until a wave from the wind edge has arrived. Causality is ensured!

The expressions for u, v and p are

$$v(x,y,t) = -\frac{\tau^x}{\rho_0 f} a \left[\theta(t)\theta(y)\left(1 - \cos(ft)\right) - \frac{sig(y)}{2}\theta(t - \lambda|y|)C_t^{(2)}(|y|,t) \right] \qquad (2.332)$$

$$u(x, y, t) = \frac{\tau^x}{\rho_0} a \left[\theta(t)\theta(y)\frac{\sin(ft)}{f} + \frac{sig(y)}{2}\theta(t - \lambda|y|)C^{(2)}(|y|, t) \right], \tag{2.333}$$

$$p(x, y, t) = \frac{\tau^x}{\rho_0} a\frac{f}{2\lambda}\theta(t - \lambda|y|)C^{(1)}(|y|, t) \tag{2.334}$$

Details on approximations for the integrals is given in Appendix D. For large time we get

$$v(x, y, t) = -\frac{\tau^x}{\rho_0 f} a \left[\theta(t)\theta(y)\left(1 - \cos(ft)\right) - \frac{sig(y)}{2}\theta(t - \lambda|y|) \right.$$
$$\left. \left(e^{-\frac{|y|}{R}} - \cos ft + \frac{|y|}{R}\sqrt{\frac{2}{f\pi t}}\cos\left(f\sqrt{t^2 - \lambda^2 y^2} + \frac{\pi}{4}\right) \right) \right] \tag{2.335}$$

$$u(x, y, t) = \frac{\tau^x}{\rho_0} a \left[\theta(t)\theta(y)\frac{\sin(ft)}{f} + \frac{sig(y)}{2}\theta(t - \lambda|y|) \right.$$
$$\left. \left(te^{-\frac{|y|}{R}} - \frac{\sin ft}{f} + \frac{|y|}{Rf}\sqrt{\frac{2}{f\pi t}}\sin\left(f\sqrt{t^2 - \lambda^2 y^2} + \frac{\pi}{4}\right) \right) \right], \tag{2.336}$$

$$p(x, y, t) = \frac{\tau^x}{\rho_0} a\frac{R}{2}\theta(t - \lambda|y|)\left(tfe^{-\frac{|y|}{R}} - \sqrt{\frac{2}{f\pi t}}\sin\left(f\sqrt{t^2 - \lambda^2 y^2} + \frac{\pi}{4}\right) \right). \tag{2.337}$$

A detailed discussion demonstrates the role of inertial waves for establishing a flow balance. The waves start at $y = 0$ and the wave fronts are spreading meridionally with a wave speed λ^{-1}. Information on the wind edge needs time to spread to a latitude y. Before the waves have not passed through some latitude y, the momentum balance is a pure Ekman balance in the area influenced by the wind. The ocean stays at rest otherwise. For $t \gg \lambda y$ this becomes changed. The Ekman transport is modified near the wind edge,

$$v_E(x, y, t) = -\frac{\tau^x}{\rho_0 f} a \left(\theta(y)\left(1 - \frac{1}{2}e^{-\frac{|y|}{R}}\right) + \theta(-y)\frac{1}{2}e^{-\frac{|y|}{R}} \right) \tag{2.338}$$

and penetrates slightly into the windless domain. The typical length scale of the perturbation is the Rossby radius R. Note, this quantity is continuous at $y = 0$.

The inertial oscillations within the wind domain become reduced, but are exported into the windless domain,

$$v_i(x, y, t) = \frac{\tau^x}{\rho_0 f} a\frac{1}{2}\cos ft,$$

$$u_i(x, y, t) = \frac{\tau^x}{\rho_0 f} a\frac{1}{2}\sin ft. \tag{2.339}$$

The ocean surface oscillates uniformly again but with reduced amplitude.

The jets developing at the wind edge are in geostrophic balance with the pressure perturbation,

$$fu_g + p_{g,y} = 0. \tag{2.340}$$

They are also confined to a stripe with a width of the Rossby radius. Remarkably, the zonal momentum balance is not closed any more, since the Ekman transport at the wind edge is disturbed. In more detail, within the wind driven area the zonal wind is not fully balanced by the Coriolis acceleration and the jet gains speed. Within the windless domain the Coriolis acceleration from meridional flow into this area drives a jet in opposite direction to the wind.

The theory as developped here is missing a process to limit the acceleration. Vertical and horizontal friction may limit the growth of the speed over all limits. In nature a meandring flow should be expected. With Newtonian damping, the linear speed gain would be replaced by

$$t \quad \rightarrow \quad \frac{1 - e^{-rt}}{r}. \tag{2.341}$$

The inertial waves are the key to understand, how the flow regime near the wind edge is established and how even areas away from the wind edge are influenced.

Exercise 2.18 Find the solution for a wind band! Remember, the governing differential equations are linear! What about Ekman transport and the inertial oscillations after long time?

2.5. The influence of a coast - coastal upwelling

We consider a fundamental process of the ocean dynamics near a coast - wind driven coastal upwelling as a basic mechanism of the ocean surface layer with the deeper ocean. We use a linear theory and find as a first step a general formal solution for any wind field. We discuss the upwelling as a result of the off-shore Ekman transport distorted by the coast. We show that upwelling is related to a longshore coastal jet. If the wind field has a long-shore structure, Kelvin waves are modify the upwelling strength and generate a pole-ward undercurrent. We will learn the Yoshida balance as a new balance priciple between wind stress and ocean currents.

2.5.1. Inhomogeneous boundary value problems - Green's functions
We use a Green's function as a formal inverse operator of linear partial differential equations to solve the linearised hydrodynamic equations for arbitrary wind forcing. We consider the example of a f-plane ocean, which is initially at rest and forced by a wind field starting at $t = 0$. The ocean is bounded by a coastline which orients zonally. The we transform the equation for v into the Fourier space. The transformation with respect to the time is simple, because all variables are zero initially. Also the transformation of the zonal variable x is simple because the v is assumed to be finite for $x \rightarrow \pm\infty$,

$$v(x, y, t) \quad = \quad \int_{-\infty}^{\infty} \frac{d\omega}{2\pi} \int_{-\infty}^{\infty} \frac{dk}{2\pi} e^{ikx - i\tilde{\omega}t} v(k, y, \omega). \tag{2.342}$$

Our start equation reads

$$-i\tilde{\omega} \left(f^2 - \tilde{\omega}^2 + \lambda^{-2} \left(k^2 - \frac{\partial^2}{\partial y^2} \right) \right) v \quad = \quad -\tilde{\omega}^2 Y + i\tilde{\omega} f X + \lambda^{-2} \left(ikX_y + k^2 Y \right). \tag{2.343}$$

Remember, that v, λ, X and Y have an index n from the decomposition into vertical modes. A more suitable form for a solution is

$$\left(\frac{\partial^2}{\partial y^2} + \alpha^2\right) v = \mathcal{F}, \tag{2.344}$$

$$\mathcal{F} = \left(\lambda^2 f + \frac{k}{\tilde{\omega}}\frac{\partial}{\partial y}\right) X + \frac{i\left(\lambda^2\tilde{\omega}^2 - k^2\right)}{\tilde{\omega}}Y, \tag{2.345}$$

$$\alpha^2 = \lambda^2\left(\tilde{\omega}^2 - f^2\right) - k^2 \tag{2.346}$$

The boundary value for v reads simply

$$v = 0 \quad \text{for} \quad y = 0, \tag{2.347}$$
$$v = 0 \quad \text{for} \quad y \to \infty, \tag{2.348}$$

there is no flow through the coastline and no flow is excited far away from the coast.

The general solution of this boundary value problem problem is a linear superposition of a solution of the homogeneous equation and a particular solution of the inhomogeneous equation, which conform with the boundary conditions.

We will use a systematic method to derive an expression for an arbitrary forcing function $\mathcal{F}$. To this end we consider a function $G(y, y')$ defined by the equation

$$\left(\frac{\partial^2}{\partial y'^2} + \alpha^2\right) G(y, y') = \delta(y - y'). \tag{2.349}$$

Renaming the coordinate in the v-equation y by y' and multiplying this equation by G and the equation for G by v gives

$$G(y, y')\frac{\partial^2}{\partial y'^2}v(y') - v(y')\frac{\partial^2}{\partial y'^2}G(y, y') = \mathcal{F}(y')G(y, y') - \delta(y - y')v(y'). \tag{2.350}$$

As the next step we integrate over y' and use the property of the δ-distribution

$$\int_0^\infty dy'\, v(y')\delta(y - y') = v(y). \tag{2.351}$$

We restrict the domain of y to the ocean area, $y \geq 0$ and get

$$v(y) = \int_0^\infty dy'\, \mathcal{F}(y')G(y, y') - \int_0^\infty dy'\, G(y, y')\frac{\partial^2}{\partial y'^2}v(y') + v(y')\frac{\partial^2}{\partial y'^2}G(y, y'). \tag{2.352}$$

The expression with the second order derivatives can be simplified by partial integration

$$\int_0^\infty dy' \left(G(y, y')\frac{\partial^2}{\partial y'^2}v(y') - v(y')\frac{\partial^2}{\partial y'^2}G(y, y')\right) \tag{2.353}$$

$$= G(y, y')\frac{\partial}{\partial y'}v(y') - v(y')\frac{\partial}{\partial y'}G(y, y')\Big|_0^\infty. \tag{2.354}$$

To specify this term, four boundary values for v and four boundary conditions for G are needed. We are free to chose the boundary conditions for the Green's functions G as

$$G(y, y') = 0 \quad \text{for} \quad y' = 0, \tag{2.355}$$
$$G(y, y') = 0 \quad \text{for} \quad y \to \infty. \tag{2.356}$$

With this choice all terms in Eq. (2.354) vanish and the formal solution for v reads,

$$v(y) \;=\; \int_0^\infty dy' \mathcal{F}(y') G(y, y') = \mathcal{F} * G. \tag{2.357}$$

What is the purpose of this mathematical manipulations? The task of solving an inhomogeneous differential equation is traced back to the task of solving a homogeneous equation. This is a great simplification. Instead of dealing with a large variety of inhomogeneous equations for various forms of wind fields we have to solve a single homogeneous problem instead. A similar treatment is known classical electrodynamics, quantumstatistics or also from engeneering, where a so called "step function response" is considered to analyse the properties of electronic circuits or mechanical constructs.

2.5.2. Estimation of the Green's function

We estimate the Green's function for an f-plane ocean bounded by a straight coastline. It is build from solutions of the homogeneous equations applying appropriate boundary conditions. The Wronskian determinant is introduced as basic ingredient reflecting the analytical properties of the Green's function. The differential equation of the Green's function has a δ-like right hand side. Hence, to construct G we try the ansatz

$$G(y, y') \;=\; \theta(y - y') g^>(y, y') + \theta(y' - y) g^<(y, y'). \tag{2.358}$$

The first derivative reads

$$\frac{\partial}{\partial y'} G(y, y') \;=\; -\delta(y - y') \left(g^>(y, y') - g^<(y, y') \right) \tag{2.359}$$

$$+ \;\; \theta(y - y') \frac{\partial}{\partial y'} g^>(y, y') + \theta(y' - y) \frac{\partial}{\partial y'} g^<(y, y'), \tag{2.360}$$

$$= \;\; -\delta(y - y') \left(g^>(y, y) - g^<(y, y) \right) \tag{2.361}$$

$$+ \;\; \theta(y - y') \frac{\partial}{\partial y'} g^>(y, y') + \theta(y' - y) \frac{\partial}{\partial y'} g^<(y, y') \tag{2.362}$$

$$. \tag{2.363}$$

Note, that the term $g^>(y, y) - g^<(y, y)$ is independent of y'. The second derivative is

$$\frac{\partial^2}{\partial y'^2} G(y, y') \;=\; -\left(g^>(y, y') - g^<(y, y') \right) \frac{\partial}{\partial y'} \delta(y - y') \tag{2.364}$$

$$- \;\; \delta(y - y') \left(\frac{\partial}{\partial y'} g^>(y, y') - \frac{\partial}{\partial y'} g^<(y, y') \right) \tag{2.365}$$

$$+ \;\; \theta(y - y') \frac{\partial^2}{\partial y'^2} g^>(y, y') + \theta(y' - y) \frac{\partial^2}{\partial y'^2} g^<(y, y') \tag{2.366}$$

Inserting into the differential equation for the Green's function gives the boundary conditions for $g^>$ and $g^<$ at $y = y'$,

$$g^>(y, y') - g^<(y, y') \;=\; 0 \qquad y = y', \tag{2.367}$$

$$g^>_{y'}(y, y') - g^<_{y'}(y, y') \;=\; -1 \qquad y = y'. \tag{2.368}$$

Finally, $g^>$ and $g^<$ are solutions of the homogeneous equation,

$$\left(\frac{\partial^2}{\partial y'^2} + \alpha^2\right) g^>(y, y') = 0 \qquad y > y', \tag{2.369}$$

$$\left(\frac{\partial^2}{\partial y'^2} + \alpha^2\right) g^<(y, y') = 0 \qquad y < y'. \tag{2.370}$$

These equations have an oscillating solution $\alpha^2 > 0$ and an exponential solution for $\alpha^2 < 0$.
We make now the ansatz

$$g^<(y, y') = A(y)e^{i\alpha y'}, \tag{2.371}$$
$$g^>(y, y') = B(y)\sin \alpha y'. \tag{2.372}$$

$g^>(y, y')$ fulfills the boundary condition for $y' = 0$, $g^>(y, 0) = 0$, $g^<(y, y')$ is finite for $y' \to \infty$ and vanishs exponentially for small frequency values, where $\alpha^2 < 0$. Now we apply the boundary conditions at $y = y'$,

$$A(y)e^{i\alpha y} - B(y)\sin \alpha y = 0, \tag{2.373}$$
$$-i\alpha A(y)e^{i\alpha y} + \alpha B(y)\cos \alpha y = 1, \tag{2.374}$$
$$\tag{2.375}$$

$$\begin{pmatrix} e^{i\alpha y} & -\sin \alpha y \\ -i\alpha e^{i\alpha y} & \alpha \cos \alpha y \end{pmatrix} \begin{pmatrix} A(y) \\ B(y) \end{pmatrix} = \begin{pmatrix} 0 \\ -1 \end{pmatrix} \tag{2.376}$$

The determinant is

$$det = \alpha e^{i\alpha y}(\cos \alpha y - i \sin \alpha y) = \alpha. \tag{2.377}$$

It is called Wronskian-determinant. Remarkably this quantity is independent of y. This general property will not be discussed in detail here. For A and B we find

$$A(y) = \alpha^{-1} \begin{vmatrix} 0 & -\sin \alpha y \\ -1 & \alpha \cos \alpha y \end{vmatrix} = -\alpha^{-1}\sin \alpha y \tag{2.378}$$

$$B(y) = \alpha^{-1} \begin{vmatrix} e^{i\alpha y} & 0 \\ -i\alpha e^{i\alpha y} & -1 \end{vmatrix} = -\alpha^{-1}\alpha e^{i\alpha y} \tag{2.379}$$

This gives our finar result for the Green's function,

$$G(y, y') = -\frac{1}{\alpha}\left(\theta(y - y')e^{i\alpha y}\sin \alpha y' + \theta(y' - y)\sin \alpha y e^{i\alpha y'}\right) \tag{2.380}$$

or equivalently

$$G(y, y') = \frac{1}{2i\alpha}\left(e^{i\alpha|y-y'|} - e^{i\alpha(y+y')}\right) \tag{2.381}$$

Note the symmetry of the Green's function in y and y'. On the other hand, it does not depend on $y - y'$ alone. Hence, the homegenity of space is broken by the existence of the coast.
    A more formal method to find the Green's function is the following:

- find two linearly independent solutions $u^{(1)}$ and $u^{(2)}$ of the homogeneous equation 2.370. One should fulfill the boundary condition for $y = \infty$ the other one $y = -\infty$. To achieve this, linear combinations of $u^{(1)}$ and $u^{(2)}$ can be used instead. Normalisation of $u^{(i)}$ is not necessary.

- Define

$$
\begin{aligned}
g^{>}(y, y') &= \frac{u^{(1)}(y)u^{(2)}(y')}{W} \\
g^{<}(y, y') &= \frac{u^{(1)}(y')u^{(2)}(y)}{W}
\end{aligned}
\tag{2.382}
$$

With this choice the condition

$$
g^{>}(y, y') - g^{<}(y, y') = 0 \qquad y = y'
\tag{2.383}
$$

is satisfied.

- From the second boundary condition

$$
g^{>}_{y'}(y, y') - g^{<}_{y'}(y, y') = -1 \qquad y = y',
\tag{2.384}
$$

we find W,

$$
W(y) = u^{(2)}(y)u^{(1)}_{y}(y) - u^{(1)}(y)u^{(2)}_{y}(y).
\tag{2.385}
$$

W is called the Wronskian of the functions $u^{(1)}$ and $u^{(2)}$. Using the homegeneous differential equation, it can be shown that

$$
\frac{\partial}{\partial y}W(y) = 0,
\tag{2.386}
$$

hence, $W(y)$ does not depend on y.

For our example the Wronskian is easily found. However, for other differential equations, like for the equatorial ocean, where the solutions of the homogeneous equation are parabolic cylinder functions, it requires extended knowledge on the analytical theory of special functions. (See Miller or Abramowitz and Stegun)

Exercise 2.19 Repeat the estimation of the Green function for an ocean bounded by a single straight coastline using the more formal method.

2.5.3. The formal solution

We summarise and find velocities and pressure in Fourier space. Keeping in mind the meaning of the convolution integral

$$v(y) \;=\; G * \mathcal{F} = \int_0^\infty dy' G(y, y') \mathcal{F}(y'), \tag{2.387}$$

the formal solution for v reads

$$v(y) \;=\; G * \mathcal{F} \tag{2.388}$$

$$=\; \lambda^2 f G * X + \frac{k}{\tilde{\omega}} G * X_{y'} + \frac{i\left(\lambda^2 \tilde{\omega}^2 - k^2\right)}{\tilde{\omega}} G * Y. \tag{2.389}$$

The form of the Green's function assures that v fulfills the boundary condition at $y = 0$ and $y = \infty$. To find u, p and w we return to Eqs 2.204, here in as Fourier transformed equations

$$-(\omega^2 - \lambda^{-2} k^2) u \;=\; -i\tilde{\omega} f v + ik\lambda^{-2} v_y - i\tilde{\omega} X, \tag{2.390}$$

$$-(\omega^2 - \lambda^{-2} k^2) p \;=\; -\lambda^{-2}(ik f v - i\tilde{\omega} v_y + ik X). \tag{2.391}$$

or

$$u \;=\; \frac{i\tilde{\omega}(f v + X) - ik\lambda^{-2} v_y}{\omega^2 - \lambda^{-2} k^2}, \tag{2.392}$$

$$p \;=\; \frac{\lambda^{-2}\left(ik(f v + X) - i\tilde{\omega} v_y\right)}{\omega^2 - \lambda^{-2} k^2}. \tag{2.393}$$

Inserting v and v_y we find

$$u(k, y, \omega) \;=\; -f\lambda^2 G * Y + \frac{k}{\tilde{\omega}} G_y * Y + \frac{i}{\omega^2 - \lambda^{-2} k^2}$$

$$\left(\tilde{\omega} X + \lambda^2 f^2 \tilde{\omega} G * X + k f G * X_{y'} - k G_y * \left(f X + \frac{k}{\tilde{\omega}} \lambda^{-2} X_{y'}\right)\right)$$

$$\tag{2.394}$$

$$p(k, y, \omega) \;=\; -f\frac{k}{\tilde{\omega}} G * Y + G_y * Y + \frac{i\lambda^{-2}}{\tilde{\omega}^2 - \lambda^{-2} k^2}$$

$$\left(k X + k\lambda^2 f^2 G * X + \frac{k^2}{\tilde{\omega}} f G * X_{y'} - \tilde{\omega} G_y * \left(\lambda^2 f X + \frac{k}{\tilde{\omega}} X_{y'}\right)\right)$$

$$\tag{2.395}$$

2.5.4. A first look at the spectrum

From our previous studies we know singularities as essential for the Fourier transformation back to the time domain. There are poles at

- $\tilde{\omega} = 0$, i.e., $\omega = -i\varepsilon$. For this pole the Fourier factor is constant and this part of the solution corresponds to a non-oscillating current field.

- $\tilde{\omega} = \pm k\lambda^{-1}$. In this case we have $\alpha_n^2 = -1/R_n^2$ (remember, $R_n = 1/(\lambda f)$) and the Green's functions reads

$$G(y, y')|_{\omega^2 = \lambda^{-2}k^2} = -\frac{R}{2}\left(e^{-\frac{|y-y'|}{R}} - e^{-\frac{y+y'}{R}}\right). \tag{2.396}$$

- a branch point at $\alpha = 0$. For a given value of ω there are two values for the square root of α^2, $\alpha = \pm\sqrt{\lambda^2(\tilde{\omega}^2 - f^2) - k^2}$. Both solutions coincide at a single point $\alpha = 0$. This point acts as a branch point, i.e., when varying ω away from this point one has to decide which one of the two leafs in the complex α-plane is used. This has to be considered when carrying out contour integrals in the complex ω-plane.

As it will be shown in more detail below, the localised Green's function results in wave pattern trapped at the coast. Only the zonal wind X (parallel to the coast) contributes to terms with poles at $\tilde{\omega} = \pm k\lambda^{-1}$, a wind field perpendicularly to the coast drives other flow pattern. In order to discuss the role of the Kelvin waves in more detail we assume $Y = 0$ for the moment.

To find the residues decomposition into partial fractions is needed:

$$\frac{k}{\tilde{\omega}^2 - \lambda^{-2}k^2} = \frac{\lambda}{2}\left(\frac{1}{\tilde{\omega} - \frac{k}{\lambda}} - \frac{1}{\tilde{\omega} + \frac{k}{\lambda}}\right) \tag{2.397}$$

$$\frac{\tilde{\omega}}{\tilde{\omega}^2 - \lambda^{-2}k^2} = \frac{1}{2}\left(\frac{1}{\tilde{\omega} - \frac{k}{\lambda}} + \frac{1}{\tilde{\omega} + \frac{k}{\lambda}}\right) \tag{2.398}$$

$$\frac{1}{\tilde{\omega}(\tilde{\omega}^2 - \lambda^{-2}k^2)} = -\frac{\lambda^2}{k^2}\left(\frac{1}{\tilde{\omega}} - \frac{1}{2}\left(\frac{1}{\tilde{\omega} - \frac{k}{\lambda}} + \frac{1}{\tilde{\omega} + \frac{k}{\lambda}}\right)\right). \tag{2.399}$$

The result for u is

$$u = \frac{i}{\tilde{\omega}}G_y * X_{y'}$$

$$+\frac{i}{2\left(\tilde{\omega} - \frac{k}{\lambda}\right)}\left(X + \lambda^2 f^2 G * X + \lambda f G * X_{y'} - \lambda f G_y * X - G_y * X_{y'}\right)$$

$$+\frac{i}{2\left(\tilde{\omega} + \frac{k}{\lambda}\right)}\left(X + \lambda^2 f^2 G * X - \lambda f G * X_{y'} + \lambda f G_y * X - G_y * X_{y'}\right) \tag{2.400}$$

In the next step we write the expression in the form $u = X * ()$, which allows to discuss the terms with the Green's function separately. With the relations

$$X = X * \delta(y - y') \tag{2.401}$$

$$G * X_{y'} = -G_{y'} * X \tag{2.402}$$

one finds

$$u = \frac{i}{\tilde{\omega}}G_y * X_{y'}$$

$$+\frac{iX}{2\left(\tilde{\omega} - \frac{k}{\lambda}\right)} * \left(\delta(y - y') + \lambda^2 f^2 G - \lambda f(G_{y'} + G_y) + G_{y,y'}\right)$$

$$+\frac{iX}{2\left(\tilde{\omega} + \frac{k}{\lambda}\right)} * \left(\delta(y - y') + \lambda^2 f^2 G + \lambda f(G_{y'} + G_y) + G_{y,y'}\right) \tag{2.403}$$

For $\tilde{\omega} = \pm\frac{k}{\lambda}$ we have $\alpha^2 = -\frac{1}{R^2}$. (Remember, $\lambda|f| = \frac{1}{R}$, R is also positive at the southern hemispere, where f is negative.) For this special value for ω, the Green's function equation reads

$$G_{yy} = \delta(y - y') + \frac{G}{R^2}. \tag{2.404}$$

Other useful relations are

$$G = -\frac{R}{2}\left(e^{-\frac{|y-y'|}{R}} - e^{-\frac{y+y'}{R}}\right)$$

$$G_y = sig(y - y')\frac{e^{-\frac{|y-y'|}{R}}}{2} - \frac{e^{-\frac{y+y'}{R}}}{2}$$

$$G_{y'} = -sig(y - y')\frac{e^{-\frac{|y-y'|}{R}}}{2} - \frac{e^{-\frac{y+y'}{R}}}{2}$$

$$G_{y,y'} = -\delta(y - y') + \frac{e^{-\frac{|y-y'|}{R}}}{2R} + \frac{e^{-\frac{y+y'}{R}}}{2R}$$

$$G_y + G_{y'} = -e^{-\frac{y+y'}{R}} \tag{2.405}$$

Hence, for $\tilde{\omega} = \frac{k}{\lambda}$ we find

$$
\begin{aligned}
\delta(y - y') + \lambda^2 f^2 G - \lambda f\left(G_{y'} + G_y\right) + G_{y,y'} &= -\frac{e^{-\frac{|y-y'|}{R}}}{2R} + \frac{e^{-\frac{y+y'}{R}}}{2R} \\
&\quad + sig(f)\frac{e^{-\frac{y+y'}{R}}}{R} + \frac{e^{-\frac{|y-y'|}{R}}}{2R} + \frac{e^{-\frac{y+y'}{R}}}{2R}, \\
&= \theta(f)\frac{2}{R}e^{-\frac{y+y'}{R}}. \tag{2.406}
\end{aligned}
$$

For the second term $\tilde{\omega} = -\frac{k}{\lambda}$ we get

$$
\begin{aligned}
\delta(y - y') + \lambda^2 f^2 G + \lambda f\left(G_{y'} + G_y\right) + G_{y,y'} &= -\frac{e^{-\frac{|y-y'|}{R}}}{2R} + \frac{e^{-\frac{y+y'}{R}}}{2R} \\
&\quad - sig(f)\frac{e^{-\frac{y+y'}{R}}}{R} + \frac{e^{-\frac{|y-y'|}{R}}}{2R} + \frac{e^{-\frac{y+y'}{R}}}{2R}, \\
&= \theta(-f)\frac{1}{R}e^{-\frac{y+y'}{R}}. \tag{2.407}
\end{aligned}
$$

Hence, at the northern hemisphere, $(f > 0)$, only a Kelvin wave with $\tilde{\omega} = \frac{k}{\lambda}$ can propagate, at the southern hemisphere we get a non-vanishing residuum for $\tilde{\omega} = -\frac{k}{\lambda}$.

2.5.5. Adjustment to homogeneous wind forcing - coastal jets, upwelling and intertial waves

Now we consider a special example and assume a uniform wind field switched on at $t = 0$,

$$X(xyzt) = \frac{u_*^2}{H_{mix}}\theta(z + H_{mix})\theta(t). \tag{2.408}$$

Fourier transformation and decomposition into vertical modes gives

$$X_n(kyz\omega) \;=\; u_*^2 a_n 2\pi\delta(k)\frac{i}{\omega + i\varepsilon}. \tag{2.409}$$

Subsequently we drop the mode index "n" again.

Using the property of the δ-distribution, $\delta(k)f(k) = \delta(k)f(0)$, the expressions for u, v and p become much simpler,

$$u(k, y, \omega) \;=\; \frac{i}{\tilde\omega}\left(X + \lambda^2 f^2 G * X\right) \tag{2.410}$$

$$v(k, y, \omega) \;=\; \lambda^2 f G * X, \tag{2.411}$$

$$p(k, y, \omega) \;=\; -\frac{i}{\tilde\omega}G_y * fX, \tag{2.412}$$

and

$$\alpha^2 \;=\; \lambda^2\left(\tilde\omega^2 - f^2\right) \tag{2.413}$$

To transform these expression back into the space-time domain we perform first the convolution integrals. Since X is independent of y, the convolution integrals are simple integrals over the Green's function. Remember,

$$G(y, y') \;=\; -\frac{1}{\alpha}\left(\theta(y - y')e^{i\alpha y}\sin\alpha y' + \theta(y' - y)\sin\alpha y\, e^{i\alpha y'}\right). \tag{2.414}$$

$$\int_0^\infty dy' G(y, y') \;=\; -\frac{1}{\alpha}\left(e^{i\alpha y}\int_0^y dy'\sin\alpha y' + \sin\alpha y\int_y^\infty dy' e^{i\alpha y'}\right)$$
$$=\; \frac{1}{\alpha^2}\left(1 - e^{i\alpha y}\right) \tag{2.415}$$

The y-derivative needed for the pressure reads

$$\int_0^\infty dy' G_y(y, y') \;=\; -\frac{i}{\alpha}e^{i\alpha y}. \tag{2.416}$$

Hence, we find expressions for pressure and currents in dependence on k, y and ω,

$$u(k, y, \omega) \;=\; u_*^2 a_n 2\pi\delta(k)\frac{-1}{\tilde\omega^2}\left(1 + \lambda^2 f^2\frac{1}{\lambda^2\left(\tilde\omega^2 - f^2\right)}\left(1 - e^{i\alpha y}\right)\right)$$
$$=\; \frac{u_*^2}{h_n}2\pi\delta(k)\left(\frac{-1}{\tilde\omega^2 - f^2} + \frac{f^2 e^{i\alpha y}}{\tilde\omega^2\left(\tilde\omega^2 - f^2\right)}\right)$$
$$=\; \frac{u_*^2}{h_n}2\pi\delta(k)\left(\frac{-1}{\tilde\omega^2 - f^2} - e^{i\alpha y}\left(\frac{1}{\tilde\omega^2} - \frac{1}{\tilde\omega^2 - f^2}\right)\right) \tag{2.417}$$

$$v(k, y, \omega) \;=\; u_*^2 a_n 2\pi\delta(k)\frac{if}{\tilde\omega\left(\tilde\omega^2 - f^2\right)}\left(1 - e^{i\alpha y}\right)$$
$$=\; u_*^2 a_n 2\pi\delta(k)\frac{(-1)}{f}\left(\frac{i}{\tilde\omega} - \frac{i\tilde\omega}{\tilde\omega^2 - f^2}\right)\left(1 - e^{i\alpha y}\right) \tag{2.418}$$

$$p(k, y, \omega) \;=\; u_*^2 a_n 2\pi \delta(k) \frac{f}{\tilde{\omega}^2 i \lambda \sqrt{\tilde{\omega}^2 - f^2}} e^{i\alpha y}. \tag{2.419}$$

To find the inverse Fourier transforms the singularities of the integrand must be considered.

- $\omega = -i\varepsilon$. The residuum can be calculated using Cauchy's theorem. Here we use the following results:

$$\int_{-\infty}^{\infty} \frac{d\omega}{2\pi} e^{-i\omega t} \frac{i}{\omega + i\varepsilon} \;=\; \theta(t), \tag{2.420}$$

$$\int_{-\infty}^{\infty} \frac{d\omega}{2\pi} e^{-i\omega t} \frac{(-1)}{(\omega + i\varepsilon)^2} \;=\; \int_{-\infty}^{\infty} \frac{d\omega}{2\pi} e^{-i\omega t} \frac{\partial}{\partial \omega} \frac{1}{(\omega + \varepsilon)} = t \int_{-\infty}^{\infty} \frac{d\omega}{2\pi} e^{-i\omega t} \frac{i}{\omega + \varepsilon} \tag{2.421}$$

$$= t\theta(t). \tag{2.422}$$

Hence, these poles correspond to constant (switched on) or linearly growing flow amplitudes. We get

$$u_n(y, t) \;=\; u_*^2 a_n \theta(t) t e^{-\frac{y}{R_n}} \tag{2.423}$$

$$v_n(y, t) \;=\; -\frac{u_*^2 a_n}{f} \theta(t) \left(1 - e^{-\frac{y}{R_n}}\right) \tag{2.424}$$

$$p_n(y, t) \;=\; u_*^2 a_n R_n f \theta(t) t e^{-\frac{y}{R_n}} \tag{2.425}$$

Note that we have recovered the vertical mode index and will carry out the sum over vertical modes now. We have, as derived previously,

$$R_n \;=\; \frac{R_1}{n}, \qquad \lambda_n = \frac{n\pi}{NH} = \frac{1}{f R_n} \tag{2.426}$$

$$F_0 \;=\; \frac{1}{\sqrt{H}}, \qquad F_n = \sqrt{\frac{2}{H}} (-1)^n \cos \frac{\pi z}{H}. \tag{2.427}$$

The coefficients h_n for the z-dependency of the volume force are

$$a_0 \;=\; \sqrt{\frac{1}{H}}, \qquad a_n = \sqrt{\frac{2}{H}} (-1)^n \frac{\sin\left(\frac{n\pi H_{mix}}{H}\right)}{\frac{n\pi H_{mix}}{H}}. \tag{2.428}$$

Hence, we find

$$u(y, z, t) \;=\; u_*^2 t \sum_{n=0}^{\infty} F_n a_n e^{-\frac{y}{R_n}} = \frac{u_*^2 t}{H_{mix}} \left(\frac{H_{mix} e^{-\frac{y}{R_0}}}{H} + S^1(y, z) \right), \tag{2.429}$$

$$v(y, z, t) \;=\; -\frac{X}{f} + \frac{u_*^2}{f H_{mix}} \left(\frac{H_{mix} e^{-\frac{y}{R_0}}}{H} + S^1(y, z) \right), \tag{2.430}$$

$$w(y, z, t) \;=\; -\frac{u_*^2}{N^2} \sum_{n=1}^{\infty} \frac{F_n' a_n}{\lambda_n} e^{-\frac{y}{R_n}} = \frac{u_*^2}{N H_{mix}} S^2(y, z) \tag{2.431}$$

The last equation is gained from

$$w = -\frac{1}{N^2} p_{zt}. \tag{2.432}$$

This sums could be carried out numerically, especially, when the eigenfunctions F_n are calculated numerically. To find an analytical result for the constant N^2 case the formula

$$\sum_{n=1}^{\infty} \frac{\chi^n}{n} = -\ln(1-\chi) = -\ln|1-\chi| - i \arg(1-\chi)$$

$$= -\ln\sqrt{1-\chi-\chi^*+\chi\chi^*} - i\arctan\frac{Im(1-\chi)}{Re(1-\chi)} \tag{2.433}$$

will be used. This motivates the subsequent operations to bring the summands into an appropriate form. We have to calculate both the sums

$$S^1 = H_{mix} \sum_{n=1}^{\infty} F_n a_n e^{-\frac{y}{R_n}} \tag{2.434}$$

$$S^2 = -\frac{H_{mix}}{N} \sum_{n=1}^{\infty} \frac{F_n' a_n}{\lambda_n} e^{-\frac{y}{R_n}}. \tag{2.435}$$

With

$$F_n a_n = \frac{2}{H} \cos\left(\frac{n\pi z}{H}\right) \frac{H}{n\pi H_{mix}} \sin\left(\frac{n\pi H_{mix}}{H}\right) \tag{2.436}$$

$$= \frac{2}{n\pi H_{mix}} \cos\left(\frac{n\pi z}{H}\right) \sin\left(\frac{n\pi H_{mix}}{H}\right), \tag{2.437}$$

and

$$-\frac{1}{N} \frac{F_n' a_n}{\lambda_n} = \frac{2}{H} \frac{n\pi}{H} \sin\left(\frac{n\pi z}{H}\right) \frac{HN}{Nn\pi} \frac{H}{n\pi H_{mix}} \sin\left(\frac{n\pi H_{mix}}{H}\right) \tag{2.438}$$

$$= \frac{2}{n\pi H_{mix}} \sin\left(\frac{n\pi z}{H}\right) \sin\left(\frac{n\pi H_{mix}}{H}\right), \tag{2.439}$$

Writing the trigonometric functions in exponential form we find,

$$H_{mix} F_n a_n = \frac{1}{n\pi} Im\left(e^{in\phi_+} + e^{in\phi_-}\right) \tag{2.440}$$

$$-\frac{H_{mix}}{N} F_n a_n = -\frac{1}{n\pi} Re\left(e^{in\phi_+} - e^{in\phi_-}\right), \tag{2.441}$$

with the abbreviations

$$\phi_+ = \frac{\pi}{H}\left(H_{mix} + z\right), \tag{2.442}$$

$$\phi_- = \frac{\pi}{H}\left(H_{mix} - z\right). \tag{2.443}$$

Hence, we have to calculate sums of the form

$$S \;=\; \frac{1}{\pi} \sum_{n=1}^{\infty} \frac{e^{-\frac{y}{R_n}}}{n} e^{in\phi} = \frac{1}{\pi} \sum_{n=1}^{\infty} \frac{\chi^n}{n}, \tag{2.444}$$

which is exactly the form Eq. 2.433. Hence, since S^1 is related to the argument of the sum (imaginary part)

$$S^1 \;=\; -\frac{1}{\pi} \left(\arctan -\frac{e^{-\frac{y}{R_1}} \sin \phi_+}{1 - e^{-\frac{y}{R_1}} \cos \phi_+} + \arctan -\frac{e^{-\frac{y}{R_1}} \sin \phi_-}{1 - e^{-\frac{y}{R_1}} \cos \phi_-} \right) \tag{2.445}$$

$$\;=\; \frac{1}{\pi} \left(\arctan \frac{\sin \phi_+}{e^{\frac{y}{R_1}} - \cos \phi_+} + \arctan \frac{\sin \phi_-}{e^{\frac{y}{R_1}} - \cos \phi_-} \right). \tag{2.446}$$

S^2 is related to the difference of the two real parts (modulus) and reads

$$1 - \chi - \chi^* + \chi\chi^* \;=\; 1 - e^{-\frac{y}{R_1}} \left(e^{i\phi} - e^{-i\phi} \right) + e^{-\frac{2y}{R_1}} \tag{2.447}$$

$$\;=\; 2 e^{-\frac{y}{R_1}} \left(\cosh \left(\frac{y}{R_1} \right) - \cos \phi \right), \tag{2.448}$$

and S^2 becomes

$$S^2 \;=\; \frac{1}{2\pi} \ln \frac{\cosh \left(\frac{y}{R_1} \right) - \cos \phi_+}{\cosh \left(\frac{y}{R_1} \right) - \cos \phi_-} \tag{2.449}$$

Now we collect all terms to the final result for the non-oscillating contributions,

$$u(y, z, t) \;=\; \frac{u_*^2 t}{\pi H_{mix}}$$
$$\left(\frac{\pi H_{mix} e^{-\frac{y}{R_0}}}{H} + \arctan \frac{\sin \phi_+}{e^{\frac{y}{R_1}} - \cos \phi_+} + \arctan \frac{\sin \phi_-}{e^{\frac{y}{R_1}} - \cos \phi_-} \right), \tag{2.450}$$

$$v(y, z, t) \;=\; -\frac{X}{f} + \frac{u_*^2}{f \pi H_{mix}}$$
$$\left(\frac{\pi H_{mix} e^{-\frac{y}{R_0}}}{H} + \arctan \frac{\sin \phi_+}{e^{\frac{y}{R_1}} - \cos \phi_+} + \arctan \frac{\sin \phi_-}{e^{\frac{y}{R_1}} - \cos \phi_-} \right), \tag{2.451}$$

$$w(y, z, t) \;=\; \frac{u_*^2}{N H_{mix} 2\pi} \ln \frac{\cosh \left(\frac{y}{R_1} \right) - \cos \phi_+}{\cosh \left(\frac{y}{R_1} \right) - \cos \phi_-} \tag{2.452}$$

This is a rather complex result. It needs some efforts to show that the coastal boundary condition is fulfilled. The best way to study the shape of these flow
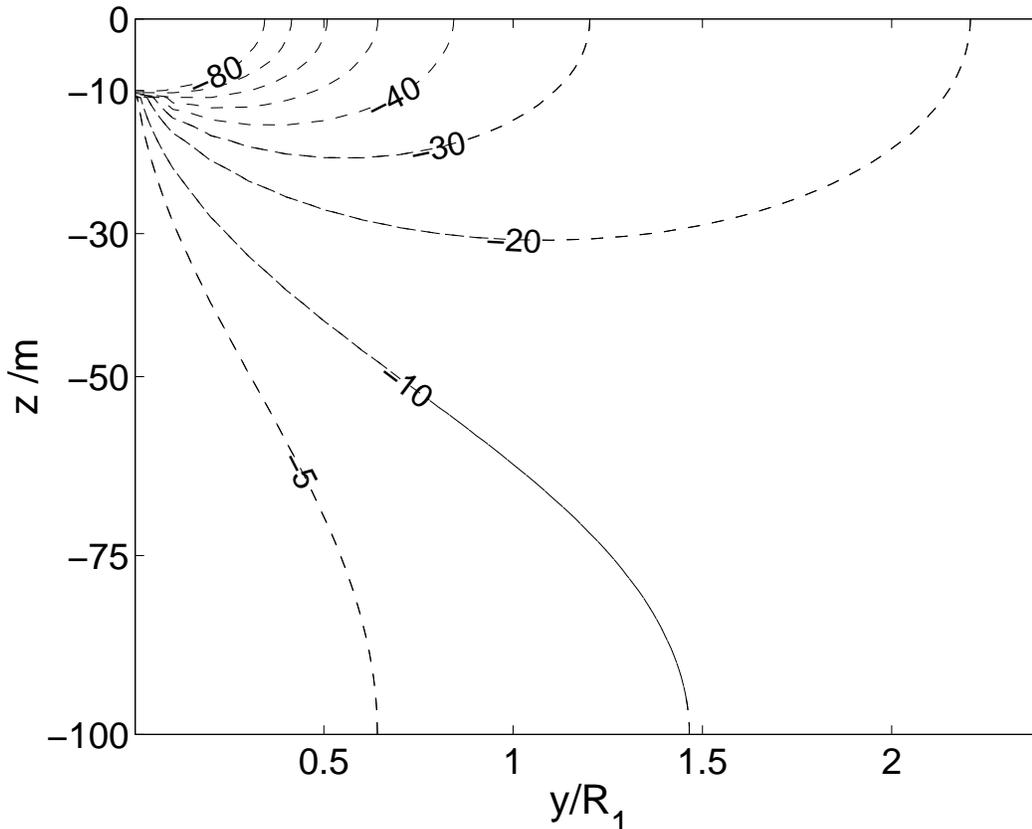
Figure 2.15. The coastal jet

pattern is to write a short program for visualisation. This can be done with matlab or ferret or similar tools. Because the solution does not depend on x and has a simple time dependency, sections in the y-z plane are possibly the best choice.

For the visualisation we choose an easterly wind, hence, blowing in negative zonal direction. X carries a minus sign. As a result the zonal flow is driven westward too. Maximum speed is found at the surface and near the coast, it decreases downward and in off shore direction. This is the reason for the name "coastal jet".

- $\omega = \pm f - i\varepsilon$. Distant from the coast, $y \to \infty$ the exponentials tend to zero. This is so because of the small imaginary part of $\tilde{\omega}$. In this case we find

$$u_n(y, \omega) = u_*^2 a_n \frac{-1}{\tilde{\omega}^2 - f^2} \tag{2.453}$$

$$v_n(y, \omega) = u_*^2 a_n \frac{(-1)}{f} \left(\frac{i}{\tilde{\omega}} - \frac{i\tilde{\omega}}{\tilde{\omega}^2 - f^2} \right) \tag{2.454}$$

$$p_n(y, \omega) = 0 \tag{2.455}$$

The pressure perturbation vanishs. This is not surprising, far offshore a homgeneous wind drives only Ekman transport and inertial oscillations in the surface layer.
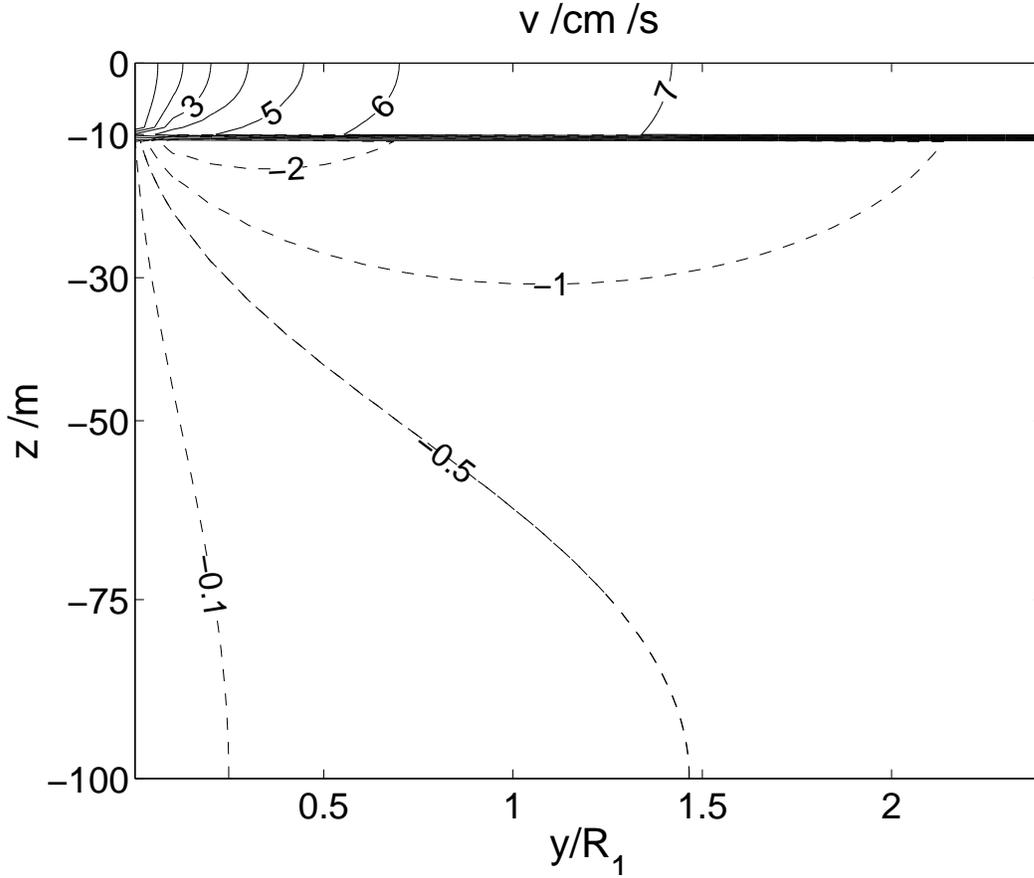
Figure 2.16. The cross shore current

Again with Cauchy's integral theorem we can solve the follwoing integrals,

$$\int_{-\infty}^{\infty} \frac{d\omega}{2\pi} e^{-i\omega t} \frac{-f}{\tilde{\omega}^2 - f^2} \;=\; \theta(t)\sin ft, \tag{2.456}$$

$$\int_{-\infty}^{\infty} \frac{d\omega}{2\pi} e^{-i\omega t} \frac{i\tilde{\omega}}{\tilde{\omega}^2 - f^2} \;=\; \theta(t)\cos ft. \tag{2.457}$$

$$u_n(y,t) \;=\; u_*^2 a_n \frac{1}{f}\theta(t)\sin ft \tag{2.458}$$

$$v_n(y,t) \;=\; u_*^2 a_n \frac{(-1)}{f}\theta(t)\left(1 - \cos ft\right) \tag{2.459}$$

$$p_n(y,t) \;=\; 0 \tag{2.460}$$

The sum over the vertical eigenfunctions $\sum_{n=0}^{\infty} F_n(z)(u_n, v_n, p_n)$ just reconstructs the volume force X
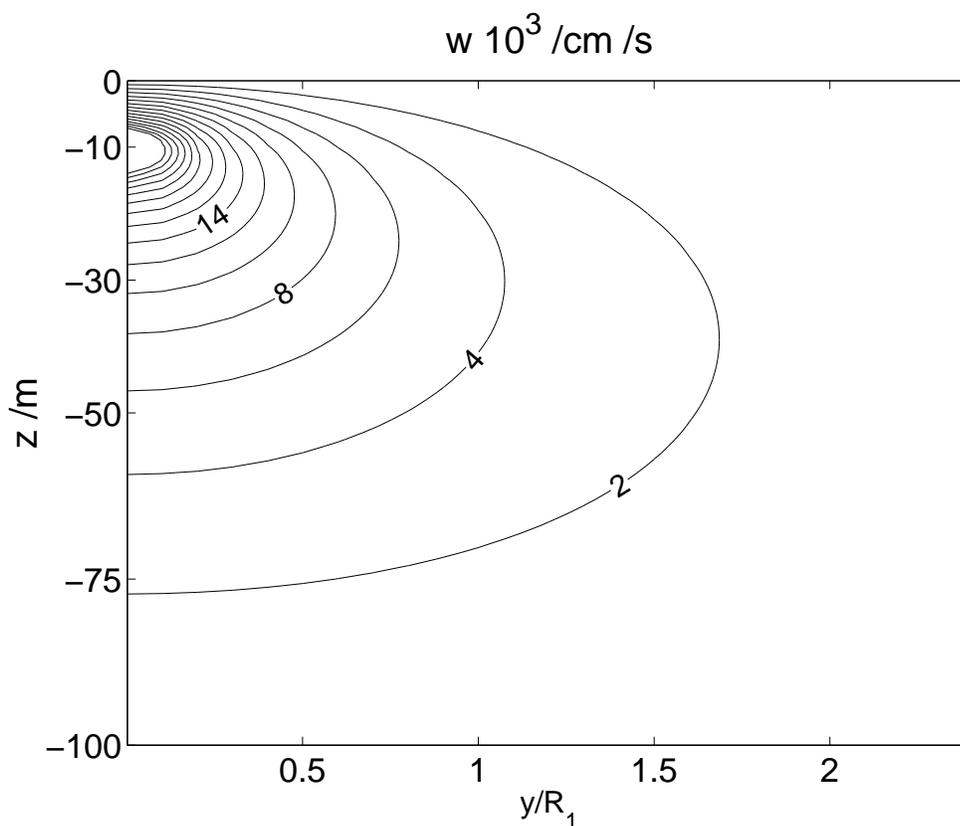
$$u(y,z,t) \;=\; \frac{1}{f}X\sin ft, \tag{2.461}$$

Figure 2.17. The vertical velocity

$$v(y, z, t) = \frac{(-1)}{f} X (1 - \cos ft), \tag{2.462}$$

$$p(y, z, t) = 0, \tag{2.463}$$

which is the well known solution for an f-plane ocean forced by a homoheneous wind. The balance of forces (accelerations) is

$$\frac{\partial}{\partial t} u_n - f v_n = X_n, \tag{2.464}$$

$$\frac{\partial}{\partial t} v_n + f u_n = 0. \tag{2.465}$$

Hence, far off shore there remains only the Ekman balance. Inertial oscillations will be discussed below. The accelerating current is confined to the coast, therefor it is called coastal jet. Each vertical mode has the baroclinic Rossby radius R_n as its characteristic length scale. The coastal jet is in geostrophic balance with a cross shore pressure gradient.

Note, this part of the solution does not explain how the cross shore current v is driven!

- Branch points at $\alpha = 0$. A separate calculation of the contribution of the branch points at $\alpha = 0$ is not possible, but is partly coupled with the asymptotic express-sions discussed previously.
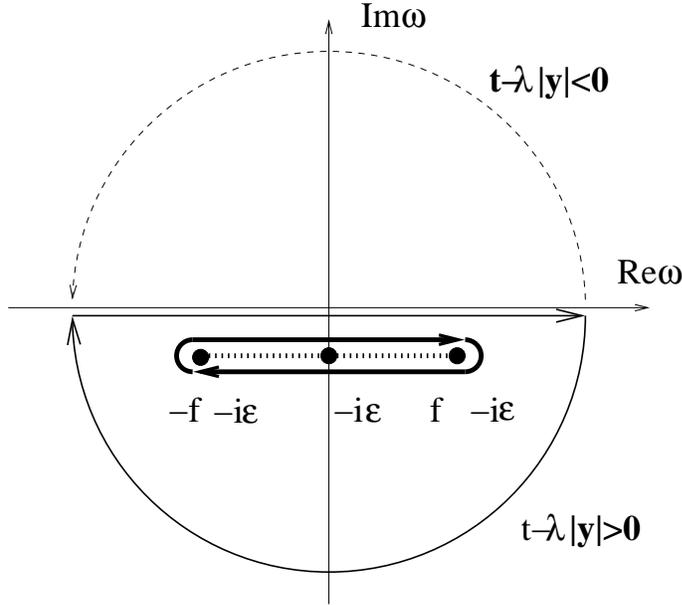

Figure 2.18. Choice of the integration path for the general integrals $C^{(1)}$ and $C^{(2)}$. A separate integration around the singularities is not possible, since α changes sign when crossong the cut in the complex plane (dashed line).

We return to equations 2.417, 2.418 and 2.419, perform the backward Fourier integral with respect to k. Now we transform back into the time domain. Some expression have been discussed before and we use the results.

$$u(x,y,t) \;=\; u_*^2 a \left(\theta(t) \frac{\sin ft}{f} + C^{(2)}(y,t) \right) \tag{2.466}$$

$$v(x,y,t) \;=\; u_*^2 a \left(\frac{\theta(t)}{f} \left(\cos ft - 1 \right) + \frac{1}{f} C_t^{(2)}(y,t) \right) \tag{2.467}$$

$$p(x,y,t) \;=\; u_*^2 a \frac{f}{\lambda} C^{(1)}(y,t) \tag{2.468}$$

The two integrals $C^{(1)}$ and $C^{(2)}$ are

$$C^{(1)} \;=\; \int_{-\infty}^{\infty} \frac{d\omega}{2\pi i} \frac{e^{i\sqrt{\tilde\omega^2 - f^2}\lambda y - i\omega t}}{\tilde\omega^2 \sqrt{\tilde\omega^2 - f^2}}, \tag{2.469}$$

$$C^{(2)} = \int_{-\infty}^{\infty} \frac{d\omega}{2\pi} \frac{f^2 e^{i\sqrt{\tilde{\omega}^2 - f^2}y - i\omega t}}{\tilde{\omega}^2 (\tilde{\omega}^2 - f^2)}. \tag{2.470}$$

Approximations for $C^{(1)}$ and $C^{(2)}$

Approximations for the the integrals $C^{(1)}$ and $C^{(2)}$ are derived in Appendix D. The asymptotic result for large time reads,

$$C^{(1)} \approx \theta(t - \lambda y) \left(\frac{t}{f} e^{-f\lambda y} - \frac{1}{f^2} \sqrt{\frac{2}{f\pi t}} \sin\left(f\sqrt{t^2 - \lambda^2 y^2} + \frac{\pi}{4} \right) \right), \tag{2.471}$$

$$C^{(2)} \approx \theta(t - \lambda y) \left(t e^{-\frac{y}{R}} - \frac{\sin ft}{f} + \frac{y}{R} \sqrt{\frac{2}{f\pi t}} \sin\left(f\sqrt{t^2 - \lambda^2 y^2} + \frac{\pi}{4} \right) \right), \tag{2.472}$$

$$C_t^{(2)} \approx \theta(t - \lambda y) \left(e^{-\frac{y}{R}} - \cos ft + \frac{y}{Rf} \sqrt{\frac{2}{f\pi t}} \cos\left(f\sqrt{t^2 - \lambda^2 y^2} + \frac{\pi}{4} \right) \right) \tag{2.473}$$

Note that these terms have wave-like character, λ^{-1} plays the role as a maximum phase speed.
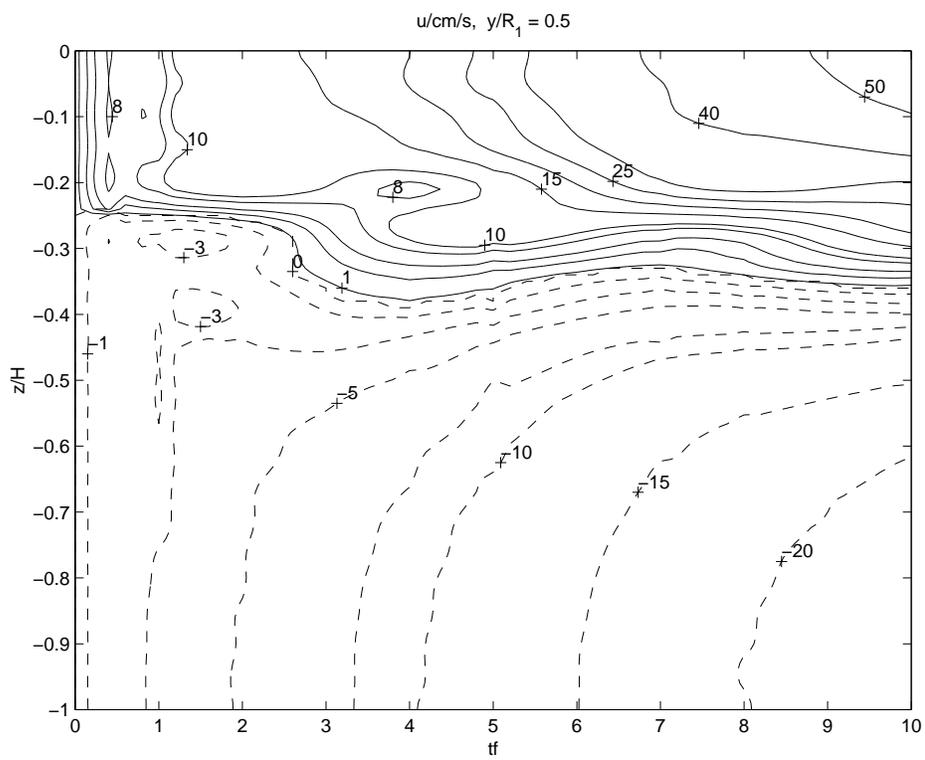
Switch from Ekman balance to Yoshida balance

Figure 2.19. Long shore current at $y/R_1 = .5$. After passing through of the first baroclinic mode there develops a coastal jet.
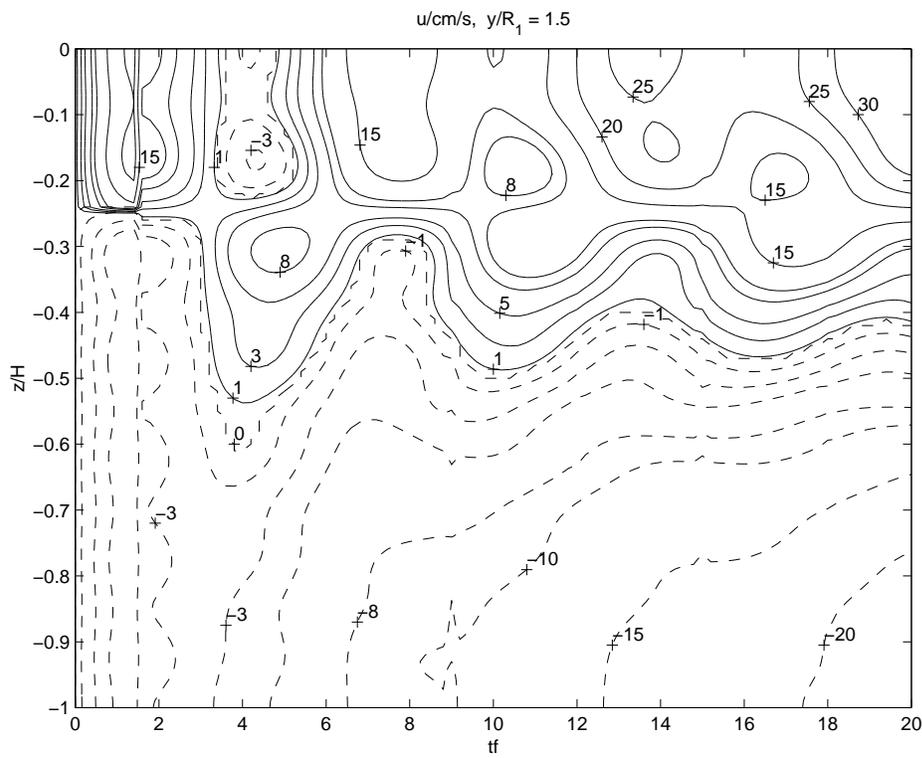
Figure 2.20. Long shore current at $y/R_1 = 1.5$. After passing through of the first baroclinic mode there develops a coastal jet modulated by inertial waves.
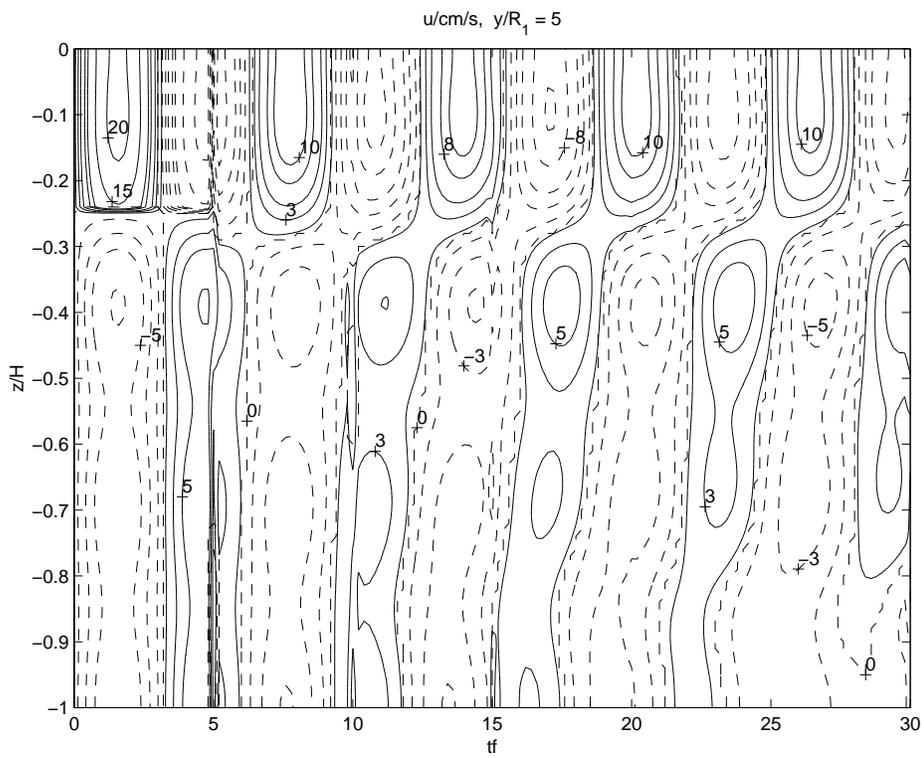
Figure 2.21. Long shore current at $y/R_1 = 5$. Inertial oscillations are modified after passage of the first baroclinic wave but remain still visible.

We summarize the result in the asymptotic form:

$$
\begin{aligned}
u(x, y, t) &= u_*^2 a \left(\theta(t) \frac{\sin ft}{f} \right. \\
&\left. + \theta(t - \lambda y) \left(te^{-\frac{y}{R}} - \frac{\sin ft}{f} + \frac{y}{R}\sqrt{\frac{2}{f\pi t}} \sin\left(f\sqrt{t^2 - \lambda^2 y^2} + \frac{\pi}{4}\right) \right) \right) \quad (2.474)
\end{aligned}
$$

$$
\begin{aligned}
v(x, y, t) &= u_*^2 a \left(\frac{\theta(t)}{f} (\cos ft - 1) \right. \\
&\left. + \frac{\theta(t - \lambda y)}{f} \left(e^{-\frac{y}{R}} - \cos ft + \frac{y}{Rf}\sqrt{\frac{2}{f\pi t}} \cos\left(f\sqrt{t^2 - \lambda^2 y^2} + \frac{\pi}{4}\right) \right) \right) \quad (2.475)
\end{aligned}
$$

$$
p(x, y, t) = u_*^2 a \frac{f}{\lambda} \theta(t - \lambda y) \left(\frac{t}{f} e^{-\frac{y}{R}} - \frac{1}{f^2}\sqrt{\frac{2}{f\pi t}} \sin\left(f\sqrt{t^2 - \lambda^2 y^2} + \frac{\pi}{4}\right) \right) \quad (2.476)
$$

$$
w(x, y, t) = u_*^2 a \frac{f}{\lambda} \theta(t - \lambda y) \left(\frac{1}{f} e^{-\frac{y}{R}} - \frac{1}{f}\sqrt{\frac{2}{f\pi t}} \cos\left(f\sqrt{t^2 - \lambda^2 y^2} + \frac{\pi}{4}\right) \right) \quad (2.477)
$$

The vertical velocity is diagnosed from the equation of continuity.

This representation of the solution highlights the role of waves. Assume to be an observer at a fixed position with distance y from the coast. The wind starts blowing and intertial oscillations in the mixed surface layer in combination with Ekman transport can be observed with a current meter. Analysing the balance of forces (accelerations) an Ekman balance is found.

After the time $t_0 = \lambda_0 y$ the current field changes. The oscillations in the surface layer become weaker, instead some oscillation in depth with opposite phase can be observed.

Near the coast the Ekman transport becomes rapidly diminished and the sea level in falling. Vertical movement rises deeper water, which upwells to the surface even seen from space as a band of cold water.

For small time we have an Ekman balance,

$$
\begin{aligned}
u_t - fv &= X \\
v_t + fu &= 0 \\
p &= 0.
\end{aligned}
$$

For large times when the inertial waves radiated away a geostrophically balanced pressure perturbation develops and the balance is called a Yoshida balance,

$$
\begin{aligned}
u_t - fv &= X \\
fu + p_y &= 0 \\
\lambda^2 p_t + v_y &= 0.
\end{aligned}
$$

Note, in some text books there are statements like "The pressure gradient drives a geostrophic current.". In this chapter it is shown that in the sense of physical causality such statements are completely wrong. The categories "balance" and "reason" are mixed but should be distinguished carefully. It is an adjustment process governed by inertial waves that establishes the geostrophically balanced flow!
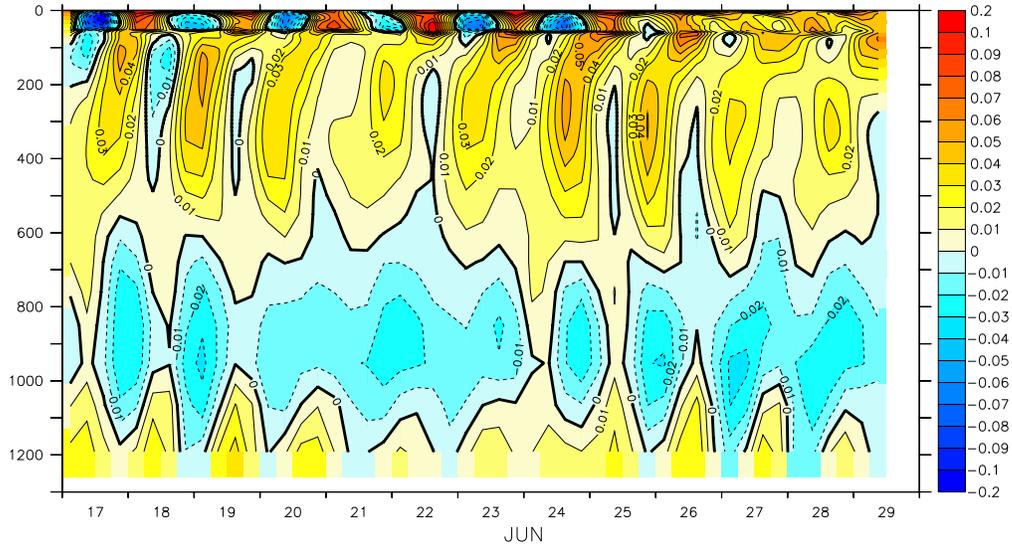
Figure 2.22. Inertial waves in the cross shore current off Namibia seen in model results. Note the phase jump at mixed layer depth.

2.5.6. A note on the accellerating coastal jet

Near the coast the Ekman balance ist disturbed and a Yoshida balance develops. This implies that the Coriolis force does not balance the acceleration in the direction of the wind stress. Hence, the along-shore current u accelerates linearly. The permanent radiation of inertial waves from the coast establishes a growing pressure gradient in geostrophic balance with the coastal jet. This is not a satisfying result so far. The reason seem to be simple - friction is missing completely. Bottom friction could be considered by an additional stress term. However, experiments show that this term must be proportional to the square of the bottom velocity. Inclusion into our Green's function approach is difficult. In Section 10 the decomposition into vertical eigenfunction for a special form of vertical vertical friction is described. The result was, that the time derivatives of the velocity are replaced by terms of the form

$$\frac{\partial}{\partial t}u_n \quad \rightarrow \quad \frac{\partial}{\partial t}u_n + A_n u_n, \tag{2.478}$$

or after Fourier transformation

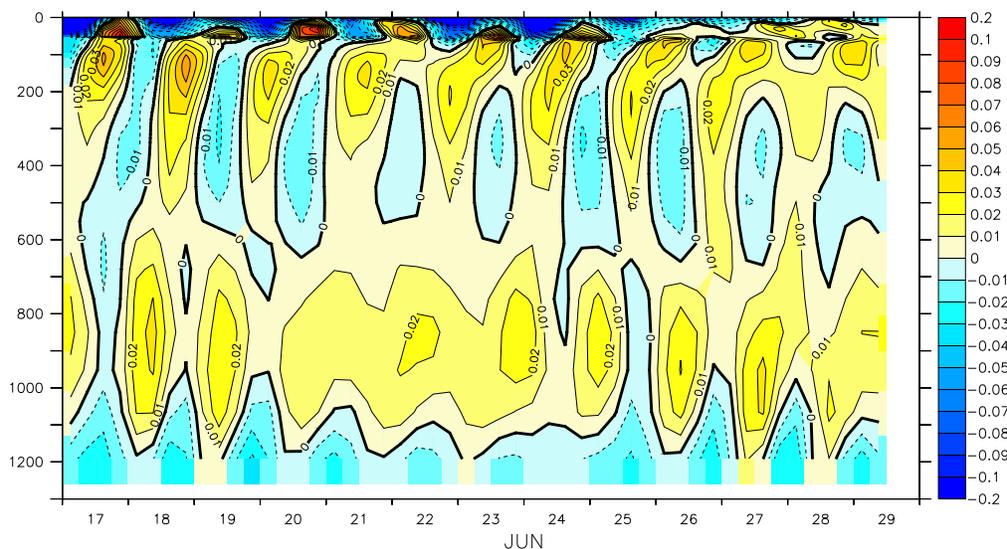$$i\omega u_n \quad \rightarrow \quad i(\omega + iA_n)u_n, \tag{2.479}$$

Figure 2.23. Inertial waves in the long shore current off Namibia seen in model results. Note the phase jump at mixed layer depth.

Hence, we can replace ω everywhere by $\omega + iA$, except the forcing term X. The linear growth of u and p is replaced by

$$t \rightarrow \frac{1 - e^{-At}}{A}. \tag{2.480}$$

For small times, $At \ll 1$ the linear accelleration is retained.

Another limitation of the linearly growing coastal jet is shown in the next section. The f-plane approximation, hence the assumption of an infinitely extended ocean driven by a uniform wind field is clearly unrealistic. Laterally limited winds lead to the generation of Kelvin waves propagating along the coast. Behind these wave fronts the linear acceleration of the coastal jet will be stopped and a limited solution can be found even for the frictionless case.

2.5.7. Adjustment to inhomogeneous forcing - coastal jets, undercurrents and Kelvin waves

We consider now an alongshore wind field over a half plane. We have seen that coastally trapped waves can only propagate with the coast to the right hand side of the propagation direction (northern hemisphere). Hence, we have to consider two cases,

$$X(xyzt) = \frac{u_*^2}{H_{mix}} \theta(z + H_{mix}) \theta(t) \theta(\pm x). \tag{2.481}$$
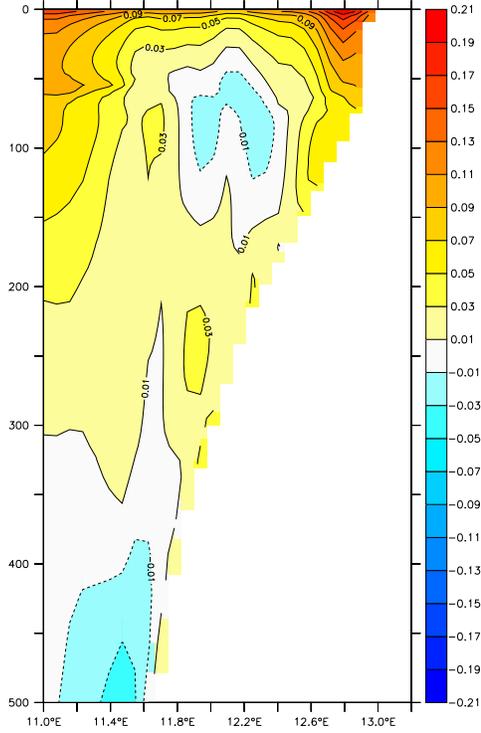
Figure 2.24. Example for a coastal jet seen in model results at 20°S

Fourier transformation of $\theta(x)$ needs a short discussion. It reads

$$\int_{-\infty}^{\infty} dx\, \theta(\pm x) e^{-i\tilde{k}x} \;=\; \frac{i}{\tilde{k}} \left\{ \begin{array}{lll} e^{-i\tilde{k}x} - 1, & x \to \infty & : \quad + \\ 1 - e^{-i\tilde{k}x}, & x \to -\infty & : \quad - \end{array} \right. \tag{2.482}$$

Hence, $\tilde{k}$ needs to be defined differently in both cases to let the exponential expression vanish,

$$\int_{-\infty}^{\infty} dx\, \theta(\pm x) e^{-i(k \mp i\varepsilon)x} \;=\; \frac{\mp i}{k \mp i\varepsilon} \tag{2.483}$$

Fourier transformation of X and decomposition into vertical eigenfunctions gives

$$X_n(k\omega) \;=\; u_*^2 a \frac{i}{\omega + i\varepsilon} \frac{\mp i}{k \mp i\varepsilon}. \tag{2.484}$$

We return to the formal solution and skip all terms with Y and X_y,

$$u(k,y,\omega) \;=\; u_*^2 a \frac{i}{\omega + i\varepsilon} \frac{\mp i}{k \mp i\varepsilon} \frac{i}{\omega^2 - \lambda^{-2}k^2} \left(\tilde{\omega} + \lambda^2 f^2 \tilde{\omega} G * 1 - k f G_y * 1 \right) \tag{2.485}$$

$$v(k,y,\omega) \;=\; u_*^2 a \frac{i}{\omega + i\varepsilon} \frac{\mp i}{k \mp i\varepsilon} \lambda^2 f G * 1 \tag{2.486}$$

$$p(k,y,\omega) \;=\; u_*^2 a \frac{i}{\omega + i\varepsilon} \frac{\mp i}{\omega \mp i\varepsilon} \frac{i\lambda^{-2}}{\tilde{\omega}^2 - \lambda^{-2}k^2} \left(k + k\lambda^2 f^2 G * 1 - \tilde{\omega}\lambda^2 f G_y * 1 \right) \tag{2.487}$$

The spectrum has been considered previously, poles at $\tilde{\omega} = 0$, $\tilde{\omega} = \pm k/\lambda$ and a branche point at $\alpha = 0$. We have seen, that the residuum at $\tilde{\omega} = -k/\lambda$ vanishs (at the northern hemishere for $f > 0$). We have also shown, that the branch point corresponds to inertial waves. Here we consider all contributions except inertial waves and have to find the residuum at $\tilde{\omega} = 0$ and $\tilde{\omega} = k/\lambda$. Repeating the considerations made for the spectrum we find

$$u(k,y,\omega) \;=\; u_*^2 a \frac{\pm i}{k \mp i\varepsilon} \frac{\lambda}{k} \left(\frac{e^{-\frac{y}{R}}}{\tilde{\omega} - \frac{k}{\lambda}} - \frac{1}{\omega} \frac{e^{-\sqrt{1+k^2 R^2}\frac{y}{R}}}{\sqrt{1+k^2 R^2}} \right) \tag{2.488}$$

$$v(k,y,\omega) \;=\; u_*^2 a \frac{\mp 1}{k \mp i\varepsilon} \frac{i}{\tilde{\omega}} \left(\frac{1 - e^{-\sqrt{1+k^2 R^2}\frac{y}{R}}}{f\left(1 + k^2 R^2\right)} \right) \tag{2.489}$$

$$p(k,y,\omega) \;=\; u_*^2 a \frac{\mp i}{k \mp i\varepsilon} \frac{1}{k} \left(\frac{e^{-\frac{y}{R}}}{\tilde{\omega} - \frac{k}{\lambda}} - \left(\frac{k^2 R^2 + e^{-\sqrt{1+k^2 R^2}\frac{y}{R}}}{\tilde{\omega}\left(1 + k^2 R^2\right)} \right) \right) \tag{2.490}$$

We apply Cauchy's theorem and find for the inverse Fourier transformed with respect to time

$$u(k,y,t) \;=\; u_*^2 a \frac{\mp i}{k \mp i\varepsilon} \frac{i\lambda}{k} \left(e^{-\frac{y}{R}} \left(e^{-\frac{itk}{\lambda}} - 1 \right) - \left(\frac{e^{-\sqrt{1+k^2 R^2}\frac{y}{R}}}{\sqrt{1+k^2 R^2}} - e^{-\frac{y}{R}} \right) \right) \tag{2.491}$$

$$v(k,y,t) \;=\; u_*^2 a \frac{\mp i}{k \mp i\varepsilon} \frac{1}{f} \left(\left(e^{-\frac{y}{R}} - 1 \right) + \frac{k^2 R^2}{1 + k^2 R^2} + \left(\frac{e^{-\sqrt{1+k^2 R^2}\frac{y}{R}}}{1 + k^2 R^2} - e^{-\frac{y}{R}} \right) \right) \tag{2.492}$$

$$p(k,y,t) \;=\; u_*^2 a \frac{\mp i}{k \mp i\varepsilon} \frac{i}{k} \left(e^{-\frac{y}{R}} \left(e^{-\frac{itk}{\lambda}} - 1 \right) - \frac{k^2 R^2}{1 + k^2 R^2} - \left(\frac{e^{-\sqrt{1+k^2 R^2}\frac{y}{R}}}{1 + k^2 R^2} - e^{-\frac{y}{R}} \right) \right) \tag{2.493}$$

Now we have to be specific with the meaning of k. The Fourier transormation needs an infinitesimal imaginary part. For a uniform wind field this needs no specification, since only wave processes with wave number $k = 0$ can be excited. Here we make the same choice as for the wind forcing and replace k with $k \mp i\varepsilon$. This guaranties that all Fourier integrals exist where integrands are finite for $x \to \pm\infty$.

Performing the inverse Fourier integral over k we consider only the residuum of $k = 0$. For this pole the expression in the last paranthesis has a vanishing contribution. This can be shown by a Taylor series with repect to k where the zero'th order vanishs and the next term is of order k^2. Using the integrals:

$$\int_{-\infty}^{\infty} \frac{dk}{2\pi} \frac{\mp i e^{ikx}}{(k \mp i\varepsilon)} \;=\; \theta(\pm x) \tag{2.494}$$

$$\int_{-\infty}^{\infty} \frac{dk}{2\pi} \frac{-e^{ikx}}{(k \mp i\varepsilon)^2} \;=\; \pm x\theta(\pm x) \tag{2.495}$$
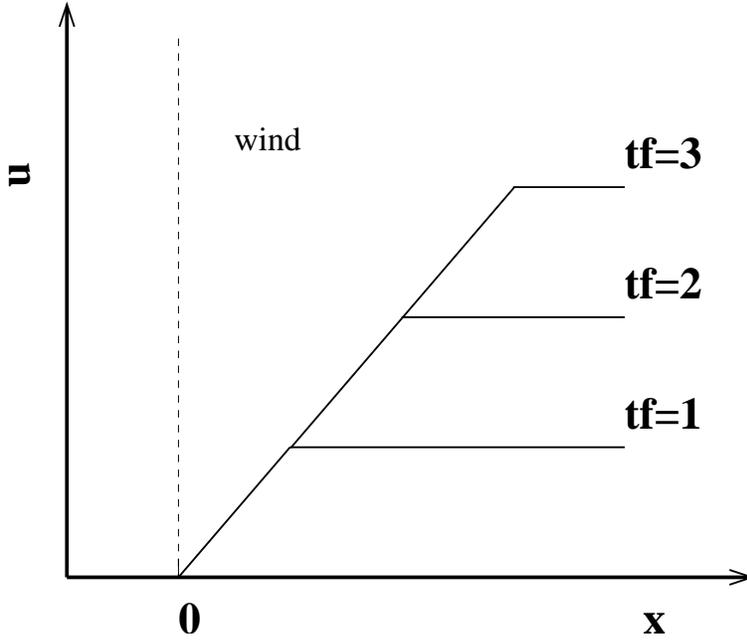
Figure 2.25. Kelvin waves arresting the coastal jet. Distant from the origin, the jet accelerates linearly with time and is independent of the coordinate x. When a wave front has passed through, u remains constant with time. The value depends on the time of arrest and is growing linearly with the distance of the origin.

the result is

$$u(x,y,t) \quad = \quad u_*^2 a e^{-\frac{y}{R}} \left[(t - \lambda x)\theta(\pm(\lambda x - t)) + \lambda x \theta(\pm x) \right] \tag{2.496}$$

$$v(x,y,t) \quad = \quad u_*^2 a \frac{e^{-\frac{y}{R}} - 1}{f} \theta(\pm x) \tag{2.497}$$

$$p(x,y,t) \quad = \quad u_*^2 a \frac{1}{\lambda} e^{-\frac{y}{R}} \left[(t - \lambda x)\theta(\pm(\lambda x - t)) + \lambda x \theta(\pm x) \right] \tag{2.498}$$

Upwelling velocity itself is given by the time derivative of the pressure perturbation, $w_n = -p_{n,t}$,

$$w(k,y,t) \quad = \quad -u_*^2 a \frac{1}{\lambda} e^{-\frac{y}{R}} \theta(\pm(\lambda x - t)). \tag{2.499}$$

 Comparing with the case of a uniform wind forcing, for small time and within those regions where the wind is non-zero, there is again the linearly growing coastal jet. New is that the solution includes a signal propagating with the phase speed λ_n^{-1}. In any case independent of the wind forcing the propagation is directed eastward leaving the coast to the right.
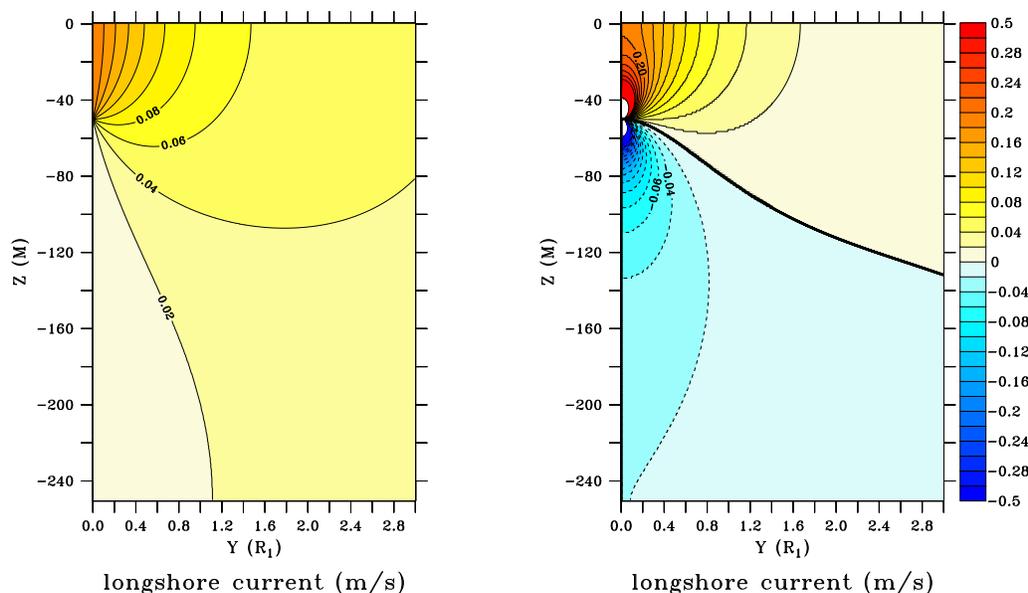
Figure 2.26. The coastal jet distant from the wind edge (left) and after all vertical model passed through. Note the undercurrent below the coastal jet.

Wind in the right half-plane

If the wind blows in the right half-plane, the cross-shore velocity v is non-zero only in this area. Neither $\theta((\lambda x - t))$ nor $\theta(x)$ become non-zero for negative x. Hence, the ocean remains totally quiescent in the left half-plane. (Inertial waves may propagate into the left half-plane, but are not considered in the approximation $k = 0$.) In the right half plane both θ-functions are switched on for small times. The solution is the same like for uniform forcing. Coastal jet and pressure perturbation are growing linearly with time, the cross-shore velocity is zero at the coast and growth towards the open ocean. The vertical structure of the flow is discussed in the previous section. However, after a period $t = \lambda_n x$ a wave originating from the wind edge at $x = 0$ arives. The speed of the n-th mode of the coastal jet stays constant now. With increasing time more vertical modes become "arrested" in ascending order of the vertical index n.

Consider the case that the first mode (the barotropic mode) has passed through. Hence, u reads

$$u(k, y, t) = \sum_n F_n(z) u_*^2 a_n e^{-\frac{y}{R_n}} t + (\lambda_0 x - t) F_0(z) u_*^2 a_0 e^{-\frac{y}{R_0}}. \qquad (2.500)$$

Since $t > \lambda_0 x$, the second term is negative and implies a small negative velocity below the coastal jet. After first mode has passed through this current directed against the wind is
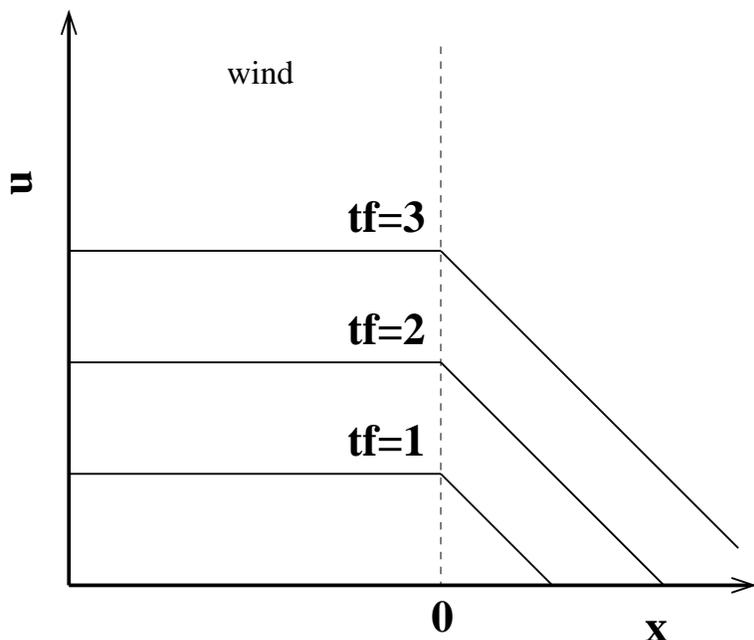
Figure 2.27. Kelvin waves exporting the coastal jet. In the wind forced area the coastal jet is linearly growing with time. The jet is exported to the area without wind. The wave arrives $t = \lambda x$ and the jet is growing linearly after the front has passed through.

growing,

$$
\begin{aligned}
u(k, y, t) \quad = \quad & \sum_n F_n(z) u_*^2 a_n e^{-\frac{y}{R_n}} t \\
& + (\lambda_0 x - t) \, F_0(z) u_*^2 a_0 e^{-\frac{y}{R_0}} + (\lambda_1 x - t) \, F_1(z) u_*^2 a_1 e^{-\frac{y}{R_1}}
\end{aligned}
\tag{2.501}
$$

When a wave front corresponding to a vertical mode passes through a similar term arises. Hence, the coastal jet as shown in Fig. 2.15 is replaced step by step by a different pattern as shown in Figure 2.26. There develops an undercurrent flowing into the opposite direction of the coastal jet. Such an undercurrent is observed often in upwelling areas.

The upwelling velocity of the n-th's mode is switched to zero by a passing Kelvin wave front,

$$
w(k, y, t) \quad = \quad -u_*^2 a \frac{1}{\lambda} e^{-\frac{y}{R}} \theta(\lambda x - t).
\tag{2.502}
$$

This is a very important result. Upwelling does not only depend on the local winds but is strongly influenced by remote inhomogeneities of the wind field. The action is mediated by coastally trapped waves - here Kelvin waves. (If the coast has a shelf and cannot be approximated by perpendicular walls, the wave dispersion relation is more complex, but the basic idea of remotely forced or suppressed upwelling is the same.)

Wind in the left half-plane

In the left half plane both step functions are always "switched on". There is simply a linearly growing coastal jet in geostrophic balance with the growing pressure perturbation. Hence, in this case the solution in the left half plane is the same like for a uniform wind field. This is a consequence of the fact, that Kelvin waves cannot propagate with the coast at the left hand side. The wind edge does not influence the ocean in the left half plane.

In the right half plane the cross-shore velocity is always zero, but both, the coastal jet and the up- or downwelling are exported from the wind driven half plane. Again, Kelvin waves mediate the remotly forced ocean response. Figure 2.27 shows the extension of the coastal jet into the right half plane. Its velocity is linearly growing with time but it starts the later the longer a Kelvin wave needs to propagate to a given position x. Upwelling velocity,

$$w(k, y, t) \quad = \quad -u_*^2 a \frac{1}{\lambda} e^{-\frac{y}{R}} \theta(t - \lambda x), \tag{2.503}$$

remains zero until the wave front comes through.

The scenario developed here is highly idealised. It neglects turbulence and friction (except the volume force!), more complex winds and the existence of a shelf instead of a perpendicular coastal wall. However, it comprises the basic ideas how coastal flow pattern and upwelling in inhomogeneous wind fields can be understood. It elucidates the role of remote forcing mediated by Kelvin waves. Although known since decades this is not commonly used in the discussion of field experiments. There are many scientific papers discussing upwelling only as the result of local winds. This chapters shows that this is not a sufficient approach.

Chapter 3

Quasi-geostrophic theory for ocean processes

3.1. The quasi-geostrophic approximation

We have seen in several examples that the ocean response to wind forcing develops from an initial Ekman balance to some other dynamic regime governed by a geostrophic balance. Such a balance is commonly found in field data if they cover areas exceeding the baroclinic Rossby radius. In many cases the adjustment process itself is of minor interest, but the final geostrophically balanced state shall be investigated. This rises the question for a simplified set of dynamic equation that excludes the adjustment process from the solution. Using the f-plane approximation, the set of geostrophic equations,

$$-fv + p_x = 0, \tag{3.1}$$
$$fu + p_y = 0, \tag{3.2}$$

is of little help, since the geostrophically balanced field is non-divergent,

$$u_x + v_y = f^{-1}(p_{yx} - p_{xy}) = 0, \tag{3.3}$$

and the related vertical velocity vanishes. Another point is, that the two geostrophic equations are not sufficient to define the three variables u, v and p.

Here a systematic method is shown to find the asymptotic geostrophic solution but without the detailed calculation of the transient states. We start with the non-linear Boussinesq equations 2.19, but in hydrostatic approximation

$$\frac{d}{dt}u - fv + \frac{\partial}{\partial x}p = F_u + F_x^{ext}, \tag{3.4}$$
$$\frac{d}{dt}v + fu + \frac{\partial}{\partial y}p = F_v + F_y^{ext}, \tag{3.5}$$
$$\frac{\partial}{\partial z}p - b = F_w + F_z^{ext}, \tag{3.6}$$
$$\frac{d}{dt}b + wN^2 = 0. \tag{3.7}$$
$$\nabla \cdot \vec{v} = 0. \tag{3.8}$$

We have already discussed, that the order of the different terms can be estimated by scale parameters, namely the Rossby number, Burger number and Ekman number (see Pedlosky). Here we line out the principle and do not discuss the detailed form of these scale parameters. We assume, that all dynamic quantities q have the form

$$q = q^{(0)} + \epsilon q^{(1)}, \tag{3.9}$$

where ϵ is a dimensionless small number $\epsilon \ll 1$. We have

$$u = u^{(0)} + \epsilon u^{(1)}..., \tag{3.10}$$
$$v = v^{(0)} + \epsilon v^{(1)}..., \tag{3.11}$$
$$p = p^{(0)} + \epsilon p^{(1)}..., \tag{3.12}$$
$$w = w^{(0)} + \epsilon w^{(1)}..., \tag{3.13}$$
$$b = b^{(0)} + \epsilon b^{(1)}.... \tag{3.14}$$

The superscript (0) should mark the geostrophic solution. For this reason we decompose also the Coriolis parameter f,

$$f = 2\Omega \sin\varphi = 2\Omega \sin\varphi_0 + \beta y = f_0 + \beta y. \tag{3.15}$$

For the earth the value of β is:

$$\beta = \frac{2\Omega}{a}\cos\varphi_0 \approx 2.287\,10^{-11}\,(\text{ms})^{-1}\cos\varphi_0. \tag{3.16}$$

So we start with the statement: **A frictionless ocean on a rotating planet without external forces is in geostrophic and hydrostatic balance.**

$$-f_0 v^{(0)} + p_x^{(0)} = 0, \tag{3.17}$$
$$f_0 u^{(0)} + p_y^{(0)} = 0, \tag{3.18}$$
$$\frac{\partial}{\partial z}p^{(0)} - b^{(0)} = 0. \tag{3.19}$$

For a known density distribution, the hydrostatic pressure and the geostrophic velocity can be calculated. However, there is no way to find the density distribution (except measuring it) in terms of the zero order velocities. The reason is, that $w^{(0)}$ is zero. Hence, the system of geostrophic and hydrostatic equations is incomplete and does not provide enough information on ocean dynamics. Considering the next order of equations in the limit $\epsilon \to 0$ under the assumption the friction and external forces are of order ϵ, we get

$$\frac{d^{(0)}}{dt}u^{(0)} - f_0 v^{(1)} - \beta y v^{(0)} + \frac{\partial}{\partial x}p^{(1)} = F_u + F_x^{ext}, \tag{3.20}$$
$$\frac{d^{(0)}}{dt}v^{(0)} + f_0 u^{(1)} + \beta y u^{(0)} + \frac{\partial}{\partial y}p^{(1)} = F_v + F_y^{ext}, \tag{3.21}$$
$$\frac{\partial}{\partial z}p^{(1)} - b^{(1)} = F_w + F_z^{ext}, \tag{3.22}$$
$$\frac{d^{(0)}}{dt}b^{(0)} + w^{(1)}N^2 = 0. \tag{3.23}$$
$$\nabla \cdot \overrightarrow{v^{(1)}} = 0. \tag{3.24}$$

The buoyancy equation relates a first order quantity $w^{(1)}$ to a zero order quantity. Hence, we try to eliminate first order quantities to get a closed system for zero order quantities. Knowing that geostrophic adjustment conserves potential vorticity, we consider the curl of the first two equations,

$$\frac{d^{(0)}}{dt}\chi^{(0)} + \beta v^{(0)} = f_0 w_z^{(1)} + curl\mathcal{F}, \tag{3.25}$$

$$\chi^{(0)} = \frac{\partial}{\partial x}v^{(0)} - \frac{\partial}{\partial y}u^{(0)} \tag{3.26}$$

With

$$\frac{d^{(0)}}{dt}\beta y = \beta v^{(0)} \tag{3.27}$$

this reads

$$\frac{d^{(0)}}{dt}\left(\chi^{(0)} + \beta y\right) = f_0 w_z^{(1)} + curl\mathcal{F}. \tag{3.28}$$

$w^{(1)}$ is the only quantity of first order in this equation. $w^{(1)}$ can be substitute by $\frac{d^{(0)}}{dt}b^{(0)}$,

$$w^{(1)} = -\frac{1}{N^2}\frac{d^{(0)}}{dt}b^{(0)} = -\frac{1}{N^2}\frac{d^{(0)}}{dt}\frac{\partial}{\partial z}p^{(0)}. \tag{3.29}$$

We need the vertical derivative,

$$\frac{\partial}{\partial z}w^{(1)} = -\frac{d^{(0)}}{dt}\frac{\partial}{\partial z}\frac{1}{N^2}\frac{\partial}{\partial z}p^{(0)}. \tag{3.30}$$

(Show that $\frac{d^{(0)}}{dt}$ commutes with $\frac{\partial}{\partial z}$.

Exercise 3.20 Show that $\frac{d^{(0)}}{dt}$ commutes with $\frac{\partial}{\partial z}$!

Hence, we have got an equation in terms of zero order quantities.

$$\frac{d^{(0)}}{dt}\left(\chi^{(0)} + \beta y + \frac{\partial}{\partial z}\frac{f_0}{N^2}\frac{\partial}{\partial z}p^{(0)}\right) = curl\mathcal{F}. \tag{3.31}$$

Finally we introduce the *quasi-geostrophic stream function* Ψ,

$$v^{(0)} = \Psi_x, \tag{3.32}$$

$$u^{(0)} = -\Psi_y \tag{3.33}$$

$$\Psi = \frac{p}{f_0}, \tag{3.34}$$

and end up with a single equation for the quasi-geostrophic stream function,

$$\frac{d^{(0)}}{dt}\left(\Delta_h\Psi + \beta y + \frac{\partial}{\partial z}\frac{f_0^2}{N^2}\frac{\partial}{\partial z}\Psi\right) = curl\mathcal{F}. \tag{3.35}$$

This is the equation of motion for the *quasi-geostrophic potential vorticity* Q_{qg},

$$Q_{qg} = \Delta_h \Psi + \beta y + \frac{\partial}{\partial z} \frac{f_0^2}{N^2} \frac{\partial}{\partial z} \Psi, \tag{3.36}$$

$$\frac{d^{(0)}}{dt} Q_{qg} = \text{curl} \mathcal{F}. \tag{3.37}$$

Hence, the asymptotic state developing for large time scales is governed by a conservative quantity quasi-geostrophic potential vorticity Q_{qg}. The source and sink of this quantity is the curl of the external force (wind stress and bottom friction) accelerating the horizontal flow velocity and the curl of the internal frictional forces. If the quasi-geostrophic potential vorticity is known, a stream function can be diagnosed to deliver velocity and density distribution. (It should be mentioned, that diabatic effects (compressibility, steric effects) contribute to the quasi-geostrophic potential vorticity with a force term. This is important for the long development of global circulation, by is not considered here.)

3.2. Planetary geostrophic motion

A more general geostrophic approximation considers the zonal variability of f as well as friction and external drivers

$$-fv + p_x = \mathcal{F}_u, \tag{3.38}$$
$$fu + p_y = \mathcal{F}_v. \tag{3.39}$$

Neglecting friction for the moment, the divergence of (fu, fv) gives

$$f(u_x + v_y) + \beta v = 0. \tag{3.40}$$

Together with the continuity equation this gives the so called **Sverdrup balance**,

$$f \frac{\partial}{\partial z} w = \beta v. \tag{3.41}$$

It is valid for the frictionless ocean interior and relates the meridional movement of water with a vertical velocity. The background is again conservation of potential vorticity and the change of relative vorticity from changing planetary vorticity. This equation in principle permits the estimate of vertical motion from measured density fields - v is diagnosed with the geostrophic method and w from the vertical integral of βv.

3.3. Planetary waves

In this section we introduce a wave type governed by the meridional variability of the Coriolis force. To find the dispersion relation of these waves we consider the linearized frictionless equation for the quasi-geostrophic stream function,

$$\frac{\partial}{\partial t} \left(\Delta_h \Psi + \frac{\partial}{\partial z} \frac{f_0^2}{N^2} \frac{\partial}{\partial z} \Psi \right) + \beta \frac{\partial}{\partial x} \Psi = 0. \tag{3.42}$$

3.3.1. The basic restoring mechanism

To understand the restoring force we consider an idealized case of the conservation of angular momentum on the rotating earth, no forcing, no zonal flow, no vertical advection, linearized equations (Olbers et al. (2012), p 227)

$$\frac{\partial}{\partial t}\chi^{(0)} + \beta v^{(0)} = 0, \tag{3.43}$$

$$\chi^{(0)} = \frac{\partial}{\partial x}v^{(0)} - \frac{\partial}{\partial y}u^{(0)} \tag{3.44}$$

Northward moving water means increasing planetary vorticity f. Conservation of vorticity implies decreasing relative vorticity χ. Hence the flow shear v_x must be decreasing. The faster the northward flow the stronger its reduction. We consider an initial flow field directed northward with

$$v_0(x) = V\sin(x/L), \qquad \chi_0(x) = \frac{V}{L}\cos(x/L). \tag{3.45}$$

Integrating over time gives

$$\chi = \chi_0(x) - t\beta v_0(x) = \frac{V}{L}\cos(x/L) - t\beta V\sin(x/L) \approx \frac{V}{L}\cos\left(\frac{x}{L} + \beta Lt\right) \tag{3.46}$$

Integrating over x gives v oscillating with a sin-function.

$$v \approx V\sin\left(\frac{x}{L} + \beta Lt\right) \tag{3.47}$$

Remarkably the wave has the shape of the initial disturbance spreading westward, since $\beta L > 0$. It moves faster near the equator and slowly at high latitudes. Any initial rotational flow, for example a coastal jet or an undercurrent within the eastern boundary current system has the tendency to decay slowly by radiation of planetary waves. The phase speed depends on the horizontal scale L of the flow pattern, the planetary waves are dispersive.

3.3.2. The dispersion relation

As in the previous sections we decompose into vertical modes F_n and apply a Fourier transformation with respect to time and horizontal coordinates:

$$\Psi_n = \Psi_{n0}e^{ik_1x+k_2y-\omega t}. \tag{3.48}$$

This gives the dispersion relation

$$\omega = -\frac{\beta k_1}{k_1^2 + k_2^2 + R^{-2}}. \tag{3.49}$$

Remarkably, these waves can especially exist near the equator but are of minor importance at high latitudes where β becomes small.

The **phase velocity** is always negative, hence, the phase propagates westward and southward.
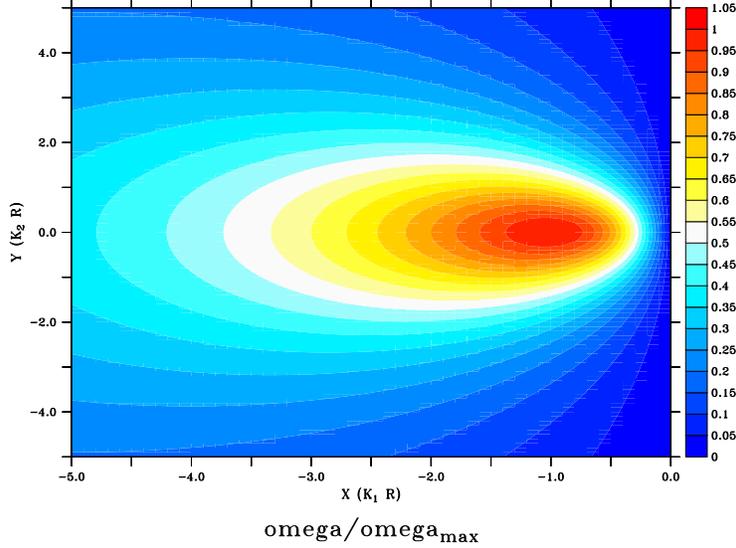
Figure 3.1. The frequency, scaled with the maximum frequency in dependency on the wave numbers.

We investigate the analytical properties of the group velocity. Considering a fixed k_2 there is a maximum of ω from

$$\frac{\partial \omega}{\partial k_1} = -\frac{\beta}{k_1^2 + k_2^2 + R^{-2}} + \frac{2k_1^2 \beta}{(k_1^2 + k_2^2 + R^{-2})^2} = 0. \quad k_1 = -\sqrt{k_2^2 + R^{-2}}. \tag{3.50}$$

The maximum frequency is

$$\omega_m = +\frac{\beta}{2\sqrt{k_2^2 + R^{-2}}}. \tag{3.51}$$

The global maximum is found for $k_2 = 0$,

$$\omega_{max} = +\frac{\beta R}{2}. \tag{3.52}$$

If there is a maximum frequency in dependency on k_1 the group velocity changes its sign here. The group velocity vector is,

$$c_g = \begin{pmatrix} c_g^x \\ c_g^y \end{pmatrix} = \begin{pmatrix} \frac{\beta(k_1^2 - k_2^2 - R^{-2})}{(k_1^2 + k_2^2 + R^{-2})^2} \\ \frac{2\beta k_1 k_2}{(k_1^2 + k_2^2 + R^{-2})^2} \end{pmatrix} \tag{3.53}$$

Hence, short waves ($k_1 R \gg 1$), propagate eastward, but long waves ($k_1 R \ll 1$) always propagate westward. Remarkably, for short waves phases and energy spread into the opposite direction. Long waves $k_1 R \ll 1, k_2 R \ll 1$ obey the asymptotic dispersion relation
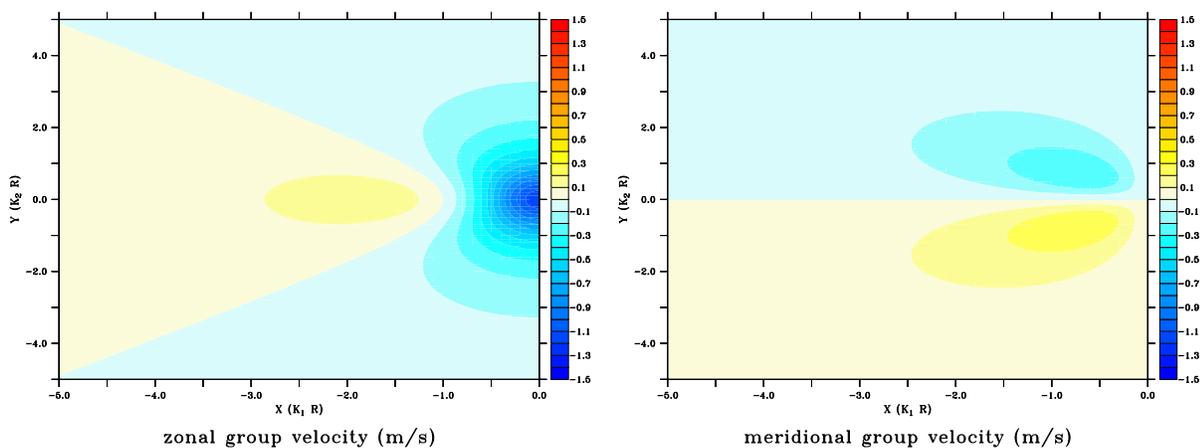
$$\omega = -\beta k_1 R^2. \tag{3.54}$$

Figure 3.2. Zonal and meridional group velocity. Blue means westward (southward) propagation.

R_n	c_g	time (5000 km)
1000 km	10 m/s	5.8 d
30 km	$9 \cdot 10^{-3}$ m/s	17.6 y
15 km	$2 \cdot 10^{-3}$ m/s	70.6 y
10 km	$1 \cdot 10^{-3}$ m/s	158.5 y

Table 3.1
Maximum group speed of planetary Rossby waves and time to spread of 5000 km distance for different values of the Rossby radius

Long waves have the largest group velocity and are approximately non-dispersive.
Exercise
Consider the spreading of a wave packet, defined by the superposition of waves with different wave number and frequency,

$$\Psi(x,t) \quad = \quad \int \frac{dk}{2\pi} \int \frac{d\omega}{2\pi} a_k e^{ikx-\omega t} f(k,\omega) \tag{3.55}$$

a_k is the amplitude of partial waves with wave number k, $f(k,\omega)$ describes the spectral density of the partial waves. It reads for for Poincaré waves

$$\begin{aligned} f(k,\omega) &= 2\pi\delta(\omega-\omega_k), \\ \omega_k^2 &= f^2(1+k^2R^2). \end{aligned} \tag{3.56}$$

- How should the spectral density look like for planetary Rossby waves?

Consider spreading of a wave packet starting from an initial condition that looks like

$$\Psi_0(x,t) \quad = \quad \sin(k_0 x)e^{-x^2/x_0^2} \tag{3.57}$$

To this end, the amplitudes a_k must be found by Fourier analysis.

- Use the matlab script to perform the Fourier analysis and make a plot of a_k as function of k.

- If the a_k are known, $\Psi(x, t)$ can be calculated for a sequence of time steps. Use the given matlab-script as a template to generate an AVI-movie that illustrates the wave spreading. Investigate the wave spreading for typical wave numbers k_0 for Rossby waves with eastward and westward group velocity. Investigate the special case of zero group velocity, $k_0^2 = R^{-2}$.

- Consider also a superposition like

$$\Psi_0(x, t) = \left(\sin(k_1 x) + \sin(k_2 x)\right) e^{-x^2/x_0^2} \tag{3.58}$$

  where k_1 and k_2 are below and above the wave number R^{-2} corresponding to zero group velocity.

3.4. Planetary circulation adjustment to large scale winds

If a wind field acts on the ocean surface a local balance is rapidly established. Within the open ocean it consists of inertial oscillations. The subtropical gyres are established by Ekman pumping in relation to the wind stress curl. At the coasts up- or down welling is established by radiation of inertial waves, Kelvin waves tend to modify this flow pattern arresting the coastal jets and generating undercurrents. All these wave and flow pattern can be understood with a f-plane theory. However, considering the meridional variability of f, these flow pattern cannot be stable but are source of Rossby waves starting an adjustment to the external forcing on a planetary scale by planetary Rossby waves.

Here we try to understand this adjustment process without considering the waves on frequencies $\omega > f$. We assume a pure zonal wind field (again a volume force)

$$X(y, t) = -X_0 \cos \frac{\pi y}{L} \theta(t) \tag{3.59}$$

which reflects roughly the band of the westward directed trade winds and the westerlies at higher latitudes. The ocean is a rectangular basin $0 < x < B$, the wind band is non-zero at $0 < y < L$. Assuming a flat bottom, we may decompose into vertical eigenfunctions and find for the components of the stream function

$$\frac{\partial}{\partial t}\left(\Delta_h \Psi - \frac{1}{R^2}\Psi\right) + \beta \frac{\partial}{\partial x}\Psi = -\frac{\partial}{\partial y}X. \tag{3.60}$$

With the Ansatz

$$\Psi(x, y, t) = -\Phi(x, t)u_*^2 a_n l \sin(ly), \quad l = \frac{\pi}{L}, \tag{3.61}$$

we find an equation for Φ,

$$\frac{\partial}{\partial t}\left(\frac{\partial^2 \Phi}{\partial x^2} - \left(l^2 + \frac{1}{R^2}\right)\Phi\right) + \beta \frac{\partial}{\partial x}\Phi = \theta(t). \tag{3.62}$$

The forcing is independent of x, hence, away from the coast Φ should be also independent of x,

$$\Phi \;\; \hat{=} \;\; \Phi_{loc} = -\frac{\theta(t)t}{l^2 + \frac{1}{R^2}} = \frac{\theta(t)tc_g}{\beta}. \tag{3.63}$$

c_g is the zonal group velocity of Rossby waves for $k_1 = 0$,

$$c_g \;\; = \;\; -\frac{\beta}{l^2 + \frac{1}{R^2}}. \tag{3.64}$$

Starting at $t = 0$ the response is a linearly growing stream function with time. The horizontal velocities are

$$
\begin{aligned}
v_{loc} \;\; &= \;\; \Psi_x = 0, \\
u_{loc} \;\; &= \;\; -\Psi_y = u_*^2 a l^2 \cos(ly)\frac{tc_g}{\beta},
\end{aligned}
\tag{3.65}
$$

the current follows the wind and its amplitude is linearly growing. (Remember, $c_g < 0$!) The Ekman transport is not part of this solution, it is not in geostrophic balance and must be considered separately.
At the coasts this solution is not valid, since $u(x = 0, B) = 0$.

Eastern coast
At the east coast waves must propagate westward, hence they must be long planetary waves. The total solution has the form

$$\Phi^E \;\; = \;\; \Phi_{loc} + \Phi^E_{wave} \tag{3.66}$$

For theses waves we neglect the second derivative (long waves) and find

$$-\left(l^2 + \frac{1}{R^2}\right)\frac{\partial}{\partial t}\Phi^E_{wave} + \beta\frac{\partial}{\partial x}\Phi^E_{wave} \;\; = \;\; 0. \tag{3.67}$$

The solution is a wave front,

$$\Phi^E_{wave}(x,t) \;\; = \;\; F(x - c_g t). \tag{3.68}$$

At the coast $x = B$, for the boundary condition $u(B) = 0$, the total stream function must always vanish, and we get

$$\Phi^E_{wave}(B,t) \;\; = \;\; -\frac{tc_g}{\beta}, \tag{3.69}$$

and

$$\Phi^E_{wave}(x,t) \;\; = \;\; -\frac{B - x + tc_g}{\beta}, \tag{3.70}$$

The time a wave front needs to move from the coast B to a position x is

$$t_f \;\; = \;\; \frac{B - x}{c_g}. \tag{3.71}$$

If a wave front arrives at position x, a contribution Φ_{wave}^E is added to the linearly growing part Φ_{loc},

$$\Phi^E(x,t) \;=\; \Phi_{loc} + \Phi_{wave}^E = \begin{cases} \frac{tc_g}{\beta} & t < t_f \\ -\frac{B-x}{\beta} & t > t_f \end{cases} \tag{3.72}$$

(Note, $c_g < 0$!) From the first point of view this is a very satisfying result. For large time, when all wave fronts have passed, Φ is independent of the mode index. This will take centuries since the group velocity for higher vertical modes becomes very small, see Table 3.1. The vertical mode sum can be carried out and the meridional current is simply

$$\beta v \;=\; \beta\Psi_x = curlX. \tag{3.73}$$

This is the well known Sverdrup balance, which is believed (and validated for some cases) to be valid in the mid-latitude ocean. Here we can understand the Sverdrup balance as the result of an adjustment process of the ocean to the large scale wind field by planetary Rossby waves radiating away from the eastern boundary. Again, waves are the key to understand the origin of steady flow pattern. Notably, the adjustment takes place without any friction (except in the surface, where small scale turbulence establishs the volumn force).

A closer look on the result reveals a serios problem. $curlX$ is confined to the surface layer and the ocean interior is at rest (Sverdrup catastrophy). This is not observed and the theory needs extension and refinement.

Western coast

Waves generated at the west coast may spread only eastward. Hence these waves must be Rossby waves with short wave length (high wave number). The east-ward group velocity is very slow which justifies to neglect these waves considering the boundary condition at the east coast. The influence of these waves must be confined to a boundary layer at the west.

$$\Phi^W \;=\; \Phi_{loc} + \Phi_{wave}^E + \Phi_{wave}^W \tag{3.74}$$

Inserting into Eq. 3.62 the equation for Φ_{wave}^W reads

$$\frac{\partial}{\partial t}\frac{\partial^2\Phi_{wave}^W}{\partial x^2} + \beta\frac{\partial}{\partial x}\Phi_{wave}^W \;=\; 0. \tag{3.75}$$

Integrating once gives

$$\frac{\partial}{\partial t}\frac{\partial}{\partial x}\Phi_{wave}^W + \beta\Phi_{wave}^W \;=\; c(t). \tag{3.76}$$

However, since Φ_{wave}^W (and the derivatives) is confined to a boundary layer at the west and vanishs outside, $c(t)$ must be zero. Analysing this equation it turns out that the assumption

$$\Phi_{wave}^W \;=\; A\left(\frac{t\beta B^2}{x}\right)^{m/2} G\left(2\sqrt{xt\beta}\right) \tag{3.77}$$

results in a differential equation for G

$$z^2 G'' + z G' + (z^2 - m^2) G = 0. \tag{3.78}$$

This is Bessel's differential equation, the solutions are Bessel functions of the first (J_m) and second kind (Y_m). The Bessel functions of second kind diverge at $z \to 0$, Bessel functions of first kind have the form

$$J_m(z) = \frac{1}{m!} \left(\frac{z}{m}\right)^m \quad \text{for} \quad z \to 0. \tag{3.79}$$

Hence, Φ_{wave}^W has the form

$$\Phi_{wave}^W = A \left(\frac{t\beta B^2}{x}\right)^{m/2} J_m \left(2\sqrt{xt\beta}\right) \tag{3.80}$$

Now we can use the boundary condition

$$\Phi^W(x = 0) = 0, \tag{3.81}$$

to specify the amplitude A and the unknown index m. For $t < t_f$ the local solution is linearly growing with time and Φ_{wave}^W must be,

$$\Phi_{wave}^W = A \left(\frac{t\beta B^2}{x}\right)^{m/2} J_m \left(2\sqrt{xt\beta}\right) = -\frac{tc_g}{\beta} \quad \text{for} \quad x \to 0. \tag{3.82}$$

This can be satisfied only for $m = 1$ and gives

$$A = -\frac{c_g}{\beta^2 B} \quad \text{for} \quad t < t_f. \tag{3.83}$$

For $t > t_f$ the long wave have passed and the boundary condition is

$$\Phi_{wave}^W = A \left(\frac{t\beta B^2}{x}\right)^{m/2} J_m \left(2\sqrt{xt\beta}\right) = \frac{B - x}{\beta} \quad \text{for} \quad x \to 0. \tag{3.84}$$

Here the choice $m = 0$ and

$$A = \frac{B}{\beta} \quad \text{for} \quad t > t_f \tag{3.85}$$

satisfies the western boundary condition. The final result is

$$\Phi^W(x,t) = \Phi_{loc} + \Phi_{wave}^E + \Phi_{wave}^W = \begin{cases} \frac{tc_g}{\beta} - c_g \left(\frac{t}{x\beta^3}\right)^{1/2} J_1 \left(2\sqrt{xt\beta}\right) & t < t_f \\ -\frac{B-x}{\beta} + \frac{B}{\beta} J_0 \left(2\sqrt{xt\beta}\right) & t > t_f. \end{cases} \tag{3.86}$$

For large arguments the Bessel function oscillates with decreasing amplitude,

$$J_m(z) = \sqrt{2/(\pi z)} \cos(z - m\pi/2 - \pi/4) \quad \text{for} \quad z \to \infty. \tag{3.87}$$

Hence, for large time the oscillating solution near the western boundary becomes more and more trapped to the coast (within $1/\beta t$) but changes rapidly in sign. It's derivative (velocity) is growing in time and friction needs to be included to avoid a divergence. This is subject of Stommel's theory of western boundary currents.

3.5. The elementary current system

This Section follows the ideas of Chapter 14 in [6]. Now it is time to combine two ingredients to understand wind driven large scale current systems, the Ekman theory and quasigeostrophic theory. Both solutions exclude each other, the flow in the Ekman surface layer is not in geostrophic balance and the quasigeostrophic theory does not include the Ekman transport. Here we ask again if a steady state solution exists. Until now we know the steady Ekman transport balanced by the wind field and the steady Sverdrup regime. Now we investigate the interplay between the flow governed by thew Ekman balance and the geostrophic flow on the β-plane.

Both flow regimes are related to the Coriolis acceleration, which is linked with angular momentum. For a short notation we introduce a new symbol that acts on horizontally 2-dimensional fields:

$$\hat{\mathbf{u}} \;=\; (-v, u), \qquad \text{where} \quad \mathbf{u} = (u, v). \tag{3.88}$$

A vector $\hat{\mathbf{u}}$ has the same modulus like the original vector $\mathbf{u}$ but is turned anticlockwise by an angle of $\pi/2$. Similarly divergence and curl read

$$\nabla_h \cdot \mathbf{u} \;=\; \frac{\partial}{\partial x}u + \frac{\partial}{\partial y}v, \tag{3.89}$$

$$curl\,\mathbf{u} \;=\; -\frac{\partial}{\partial y}u + \frac{\partial}{\partial x}v = \hat{\nabla}_h\mathbf{u}. \tag{3.90}$$

Note,

$$\hat{\hat{\mathbf{u}}} \;=\; -\mathbf{u}. \tag{3.91}$$

To keep the consideration simple, we assume week stratification. The hydrostatic pressure becomes simply

$$p(z) \;=\; p_{atm} - g\rho(z - \eta(x,y,t)). \tag{3.92}$$

Assuming constant air pressure, all horizontal pressure variability is related to a sea level elevation η. We remember - horizontal flow driven by these surface elevation gradients is depth independent. Behind the scene acts the conservation of angular momentum on a rotating planet as stated by the Taylor-Proudman theorem. This comprises the frame for the subsequent discussion - slow and large scale fluid motion dominated by the Coriolis force.

With these approximations we summarise the equations describing a steady state ocean

$$f\hat{\mathbf{u}} \;=\; -g\nabla_h\eta + \frac{\partial}{\partial z}\tau, \tag{3.93}$$

$$\nabla_h \cdot \mathbf{u} + \frac{\partial}{\partial z}w \;=\; 0. \tag{3.94}$$

τ is the vertical momentum flux, i.e., that part of turbulent friction also responsible for the momentum flux between ocean and atmosphere and for a momentum transfer into the sea floor as well. The surface boundary condition is

$$\tau \;=\; \tau_0 \qquad \text{for} \quad z = 0. \tag{3.95}$$

Previously, we have used the approximation of a volume force for this momentum flux. Assuming a constant downward vertical loss of entrained momentum from the small scale surface currents (breaking gravity waves) to the large scale horizontal current, we find

$$\tau(z) \;=\; \tau_0 \left(z + H_{mix}\right) \theta \left(z + H_{mix}\right). \tag{3.96}$$

Hence, within the surface mixing layer the wind acts on the ocean like a volume force,

$$\frac{\partial}{\partial z}\tau(\mathbf{z}) \;=\; \mathbf{X} = \tau_0 \theta \left(z + H_{mix}\right). \tag{3.97}$$

Alternatively, the downward flow of momentum may be considered as a downgradient process similar to Newtonian friction,

$$\tau(\mathbf{z}) \;=\; A_v \frac{\partial}{\partial z}\mathbf{u}. \tag{3.98}$$

The turbulent viscosity A_v is known to be about $A_v \approx 0.01..0.1\mathrm{m}^2\,\mathrm{s}^{-1}$ in the surface and bottom layer, but is significantly smaller in the ocean interiour, i.e, $A_v \approx 10^{-5}..10^{-4}\mathrm{m}^2\,\mathrm{s}^{-1}$. Usually the turbulent bottom and surface boundary layers are very thin compared with the total ocean depth. This assumption is justified below from the result for the Ekman surface flow. Hence, friction is of importance only withing the thin boundary layers but is small within the ocean interior. This motivates a splitting of the solution of the Eq. 3.94 into geostrophic part u_g dominating in the ocean interiour and an Ekman flow for the friction dominated surface and bottom boundary layer,

$$f\hat{\mathbf{u}}_g \;=\; -g\nabla_h\eta, \tag{3.99}$$

$$f\hat{\mathbf{u}}_E \;=\; \frac{\partial}{\partial z}\tau. \tag{3.100}$$

We define the vertical velocity components in such a way that also the equations of continuity can be separated,

$$\nabla_h \cdot \mathbf{u}_g + \frac{\partial}{\partial z}w_g \;=\; 0, \tag{3.101}$$

$$\nabla_h \cdot \mathbf{u}_E + \frac{\partial}{\partial z}w_E \;=\; 0. \tag{3.102}$$

It seems, that the Ekman flow and the geostrophic flow are fully decoupled. However, the surface and the bottom boundary condition need more attention. If the dynamic equations decouple, both vertical velocity components should vanish at the sea surface separately,

$$w_E \;=\; 0, \qquad w_g = 0, \qquad \text{for} \quad z = 0. \tag{3.103}$$

(Note, we ask for the steady solution, the sea level does not depend on time.) This simplified form of a boundary condition is called *rigid lid condition*. It plays a central role in the theory of large scale ocean flows.

As the next step we assume a flat bottom and total vertical velocity must vanish there,

$$w_E + w_g \;=\; 0, \qquad \text{for} \quad z = -H. \tag{3.104}$$

This relation couples the geostrophic flow and the Ekman flow. The vertical integral of the full equation of continuity reads,

$$\nabla_h \cdot \int_{-H}^{0} dz \, (\mathbf{u}_g + \mathbf{u}_E) \;\; = \;\; w(-H) - w(0) = 0. \tag{3.105}$$

Hence, the total horizontal flow is non-divergent,

$$\nabla_h \cdot \mathbf{U} \;\; = \;\; 0. \tag{3.106}$$

If we consider a bottom boundary layer with friction we need a dynamic bottom boundary condition. The lowest water layer should stick at the sea floor, i.e., we assume a "no slip" boundary condition,

$$\mathbf{u} \;\; = \;\; \mathbf{u}_g + \mathbf{u}_E = 0, \qquad \text{for} \quad z = -H. \tag{3.107}$$

3.5.1. The Ekman solution

A basic assumption of the Ekman theory is the decoupling of the bottom and the surface boundary layer. This is well justified, since the Ekman flow is declining exponentially distant from its boundary. A typical vertical scale is the *Ekman depth*

$$d \;\; = \;\; \sqrt{2A_v/|f|}. \tag{3.108}$$

This parameter amounts usually about 50 m, which is significantly less than a total ocean depth of 5000 m.

Classical Ekman solution

The Ekman flow is governed by the equation

$$f\hat{\mathbf{u}}_E \;\; = \;\; \frac{\partial}{\partial z} A_v \frac{\partial}{\partial z} \mathbf{u}_E. \tag{3.109}$$

The classical Ekman solution for the surface layer reads

$$\mathbf{u}_E(z) \;\; = \;\; \mathrm{sgn}(f)\frac{d}{2A_v} e^{z/d} \left((\tau_0 - \hat{\tau}_0) \cos(z/d) + (\tau_0 + \hat{\tau}_0) \sin(z/d) \right). \tag{3.110}$$

For the bottom layer one finds

$$\mathbf{u}_E(z) \;\; = \;\; e^{-(z+H)/d} \left(-\mathbf{u}_g \cos((z + H)/d) + \hat{\mathbf{u}}_g \sin((z + H)/d) \right). \tag{3.111}$$

At the bottom it flows against the geostrophic flow, which renders the bottom boundary condition. The bottom stress (the momentum flux into the bottom) is calculated from the vertical shear,

$$\tau_b \;\; = \;\; A_v \left. \frac{\partial}{\partial z}\mathbf{u}_E \right|_{z=-H} = \frac{d|f|}{2}\left(\mathbf{u}_g + \hat{\mathbf{u}}_g \right). \tag{3.112}$$

It is turned clockwise by an angle of $\pi/4$ to the direction of the geostrophic flow.

The **Ekman transport**, i.e., the total mass flux related to the Ekman flow is the vertical integral of the Ekman velocity, It consists of a surface and a bottom contribution,

$$\mathbf{U}_E = \int_{-H}^{0} dz \mathbf{u}_E = -f^{-1}\left(\hat{\tau}_0 - \hat{\tau}_b\right),$$
(3.113)

$$= -f^{-1}\hat{\tau}_0 + \frac{d\,\mathrm{sgn}(f)}{2}\left(\hat{\mathbf{u}}_g - \mathbf{u}_g\right).$$
(3.114)

The first term is the wind driven Ekman transport in the surface layer. It is independent off the choice of the friction parameter A_v. Its modulus is proportianally to the stress, the direction is perpendicularly to the wind stress, to the right at the northern hemisphere and to the left on the southern hemisphere. The transport within the bottom friction layer is also proportionally to the stress, but it depends on the parameter d, which is not well known. Note, that its direction depends on the sign of the Coriolis force. On the northern hemisphere the bottom Ekman transport flows turned by an angle of $3\pi/4$ anticlockwise to the direction of the geostrophic flow.

The total transport is the sum of the geostrophic transport and the Ekman transport,

$$\mathbf{U} = H\mathbf{u}_g - f^{-1}\hat{\tau}_0 + \frac{d\,\mathrm{sgn}(f)}{2}\left(\hat{\mathbf{u}}_g - \mathbf{u}_g\right).$$
(3.115)

Usually the thickness of the bottom layer is much smaller than the total depth, $d \ll H$, and the contribution of the bottom layer may be neglected,

$$\mathbf{U} \approx H\mathbf{u}_g - f^{-1}\hat{\tau}_0.$$
(3.116)

3.5.2. Vertical velocity

Since the Coriolis parameter varies meridionally, the geostrophically balance flow component becomes divergent. Integrating downward from the sea surface we get

$$\begin{aligned}
w_g(z) &= \nabla_h \cdot \int_z^0 dz'\, \mathbf{u}_g \\
&= zg\frac{\beta}{f^2}\frac{\partial}{\partial x}\eta \\
&= zg\frac{\beta}{f}v_g
\end{aligned}$$
(3.117)

The vertical velocity is related to the variability of the Coriolis force. It does not vanish at the bottom and must be compensated, i.e. by the vertical velocity from the Ekman flow.

The divergence of the wind driven Ekman flow also defines a vertical velocity

$$\begin{aligned}
w_E^s(z) &= \frac{\mathrm{sgn}(f)\,d}{2A_v}\nabla_h \cdot \tau_0 \int_z^0 dz'\, e^{z/d}\left(\sin(z/d) + \cos(z/d)\right) \\
&+ \frac{\mathrm{sgn}(f)\,d}{2A_v}\nabla_h \cdot \hat{\tau}_0 \int_z^0 dz'\, e^{z/d}\left(\sin(z/d) - \cos(z/d)\right).
\end{aligned}$$
(3.118)

With the integrals

$$\int dx\, e^{ax}\left\{\begin{array}{c}\sin x \\ \cos x\end{array}\right\} = \frac{e^{ax}}{1+a^2}\left[a\left\{\begin{array}{c}\sin x \\ \cos x\end{array}\right\} \mp \left\{\begin{array}{c}\cos x \\ \sin x\end{array}\right\}\right]$$
(3.119)

we find

$$w_E^s(z) \;=\; -\nabla_h \cdot \left(\frac{\tau_0}{f}\right) e^{z/d} \sin(z/d) - \nabla_h \cdot \left(\frac{\hat{\tau}_0}{f}\right) \left((1 - e^{z/d} \cos(z/d)\right). \tag{3.120}$$

Note the variable Coriolis parameter in d is used! Significantly below the Ekman depth $z = -d$ the vertical velocity becomes constant. Usually this value of w_E^s is attributed to the Ekman depth $-d$,

$$w_E^s(-d) \;\approx\; \hat{\nabla}_h \cdot \left(\frac{\tau_0}{f}\right) \tag{3.121}$$

A rotational wind pumps water into the surface Ekman layer. This component of the vertical velocity is constant below $z = -d$. How the bottom boundary conditions may be rendered will be discussed below.

Exercise 3.21 Discuss the case of a negative wind stress curl! What happens at the southern hemisphere?

The Ekman flow excited by bottom friction vanishs distant from the sea floor. This is required by the surface boundary condition, i.e., the vertical velocity related to this flow should vanish near the sea surface. Hence, it reads

$$
\begin{aligned}
w_E^b(z) \;=&\; \nabla_h \cdot \int_z^0 dz' \, e^{-(z+H)/d} \left(-\mathbf{u}_g \cos((z+H)/d) + \hat{\mathbf{u}}_g \sin((z+H)/d)\right), \\
\approx&\; \nabla_h \cdot \frac{d}{2} e^{-(z+H)/d} \left((\hat{\mathbf{u}}_g - \mathbf{u}_g) \cos((z+H)/d) + (\hat{\mathbf{u}}_g + \mathbf{u}_g) \sin((z+H)/d)\right) \tag{3.122}
\end{aligned}
$$

At the sea floor this expession condenses to

$$w_E^b(-H) \;=\; \nabla_h \cdot \frac{d}{2}\left(\hat{\mathbf{u}}_g - \mathbf{u}_g\right) = \nabla_h \cdot \mathbf{U}_E^b = -\hat{\nabla}_h \cdot \left(\frac{\tau_b}{f}\right) \tag{3.123}$$

3.5.3. Combination of Ekman- and geostrophic flow

The three vertical velocity components w_E^s, w_E^b and w_g must be combined to fulfill the bottom boundary condition $w(-H) = 0$. We consider different approximation.

f-plane approximation

Considering small scales the f-approximation should be justified. In this case the geostrophic vertical velocity vanishs. Without a divergent Ekman bottom flow a divergent surface Ekman layer would pump water into the ocean interiour and even through the bottom. From

$$w(-H) \;=\; \hat{\nabla}_h \cdot \frac{\tau_0 - \tau_b}{f} = 0 \tag{3.124}$$

we find for the geostrophic flow

$$\hat{\nabla}_h \cdot \frac{\tau_0}{f} \;=\; \frac{d}{2} \hat{\nabla}_h \cdot \mathbf{u}_g. \tag{3.125}$$

Using the geostropic equations to introduce the surface elevation as approximation for the stream function we get

$$g \frac{d}{2} \nabla_h^2 \eta = \hat{\nabla}_h \cdot \tau_0. \tag{3.126}$$

Such a flow may exist and is consistent with the bottom boundary conditions. However, it does not show the observed asymmetry between the eastern and western coast of the ocean basins. Hence, this balance between Ekman and geostrophic flow is highly unrealistic.

β-plane approximation, the Sverdrup regime

Now we take into account the meridional variability of the Coriolis parameter. In this case the geostrophic flow may have non-vanishing divergence and is related to a vertical velocity. This additional vertical velocity can balance the Ekman pumping,

$$w_g(-H) = -w_E(-H) \approx w_E(-d). \tag{3.127}$$

We neglect for the moment the bottom friction term, which should be much smaller than the geostrophic contribution and find

$$-w_g(-H) = Hg \frac{\beta}{f^2} \frac{\partial}{\partial x} \eta = Hg \frac{\beta}{f} v_g = g \frac{\beta}{f} V_g = \hat{\nabla}_h \cdot \left(\frac{\tau_0}{f} \right). \tag{3.128}$$

The last step uses Eq.s 3.127 and 3.121. Hence, Ekman pumping through the bottom can be compensated by the divergence of the geostrophic flow. The meridional geostrophic flow can be complemented with the meridional surface Ekman transport,

$$\beta(V_g + V_e^s) = \beta V = \hat{\nabla}_h \tau_0. \tag{3.129}$$

Note, the y-dependence of f in the right hand side of Eq. 3.128 is made explicit. This is theso called *Sverdrup balance*. It can be read in several ways. We have found a similar equation as final steady state of the basinwide Rossby wave dynamics, Eq. 3.41. We have seen Rossby waves as vorticity waves, i.e., wave like spreading perturbations of the local vorticity. Here, simply the Ekman pumping driven by a wind stress curl is compensated by the divergence of the geostrophic flow. This divergence is related to a meridional transport. This discussion is mainly based on mass conservation arguments. What is the relation between mass conservation and the vorticity budget? This can be discussed in terms of the conservation of potential vorticity.

Finally we present the stream function defining the total flow. Since the total flow is non-divergent it can be written as,

$$\mathbf{U} = \hat{\nabla}_h \Psi \tag{3.130}$$

With this definition the Sverdrup balance reads

$$\beta V = \beta \frac{\partial}{\partial x} \Psi = \hat{\nabla}_h \tau_0. \tag{3.131}$$

The stream function can be easily calculated as a simple line integral starting at the eastern coast, x_E, where the stream function must vanish

$$\Psi(x, y) = -\beta^{-1} \int_x^{x_E} dx \, \hat{\nabla}_h \tau_0. \tag{3.132}$$

The adjustment process which results in this special flow pattern is discussed in Section 3.4. It shows the special role of the asymmetric propagation of Rossby waves and the existence of an eastern coast as fundamental for the Sverdrup balance.

Now we reconsider the example of a cosine-shaped zonal wind blowing over an ocean with an eastern coast. The wind stress reads

$$\tau_0^{(x)} = -\tau_0 \cos ly, \quad \text{with} \quad l = \frac{\pi}{L}. \tag{3.133}$$

If the eastern boundary is at $x = B$, the stream function reads

$$\Psi(x, y) = (B - x)\frac{\tau_0 l}{\beta} \sin ly, \tag{3.134}$$

and the velocities are

$$U = -(B - x)\frac{\tau_0 l^2}{\beta} \cos ly, \tag{3.135}$$

$$V = -\frac{\tau_0 l}{\beta} \sin ly. \tag{3.136}$$

Hence, the zonal velocity follows the wind field, but the Ekman transport,

$$U_E = 0$$
$$V_E = -f^{-1}\tau_0^{(x)}. \tag{3.137}$$

is perpendicularly to the wind. Figure 3.3 shows these quantities for $B = 5000$ km, $L = 4000$ km, $f_0 = 7 \cdot 10^{-5}$ s^{-1}, $\beta = 2 \cdot 10^{-11}$ m^{-1} s^{-1}, $\tau_0 = 10^{-4}$ m^2 s^{-1}. The resulting stream function has the typical east-west asymmetry, but the solution is not valid at a west coast. Moreover, the total transport is directed southward everywhere, a recirculation is missing. Hence, the theory is not complete.

The Stommel regime

When considering the Sverdrup regime we have neglected the bottom Ekman layer. This is well justified in the open ocean, since the thickness of this layer is much smaller than the total ocean depth. Now we take the Ekman layer due to bottom friction into account,

$$\nabla_h \cdot \mathbf{U} = \nabla_h \cdot (\mathbf{U}_E + \mathbf{U}_g) = \hat{\nabla}_h \frac{\tau_0 - \tau_b}{f} - \frac{\beta}{f} V_g = 0. \tag{3.138}$$

Using the y-dependency of f in the derivative we get terms $\tau_0^{(x)}/f = -V_E^s$ and $\tau_b^{(x)})/f = V_E^b$, which allows to rearrange the total mass (volume) budget like

$$\beta V = \beta \left(V_g + V_E^s + V_E^b \right) = \hat{\nabla}_h \left(\tau_0 - \tau_b \right). \tag{3.139}$$

This looks like a generalised Sverdrup balance but modified by a bottom boundary layer contribution.

Like for the Sverdrup equation in the prevoius section we ask for a way to determine the related currents and stream function. It is possible to find a clodes equation for the sea level elevation, but the related coastal boundary condition reveals as very complex.
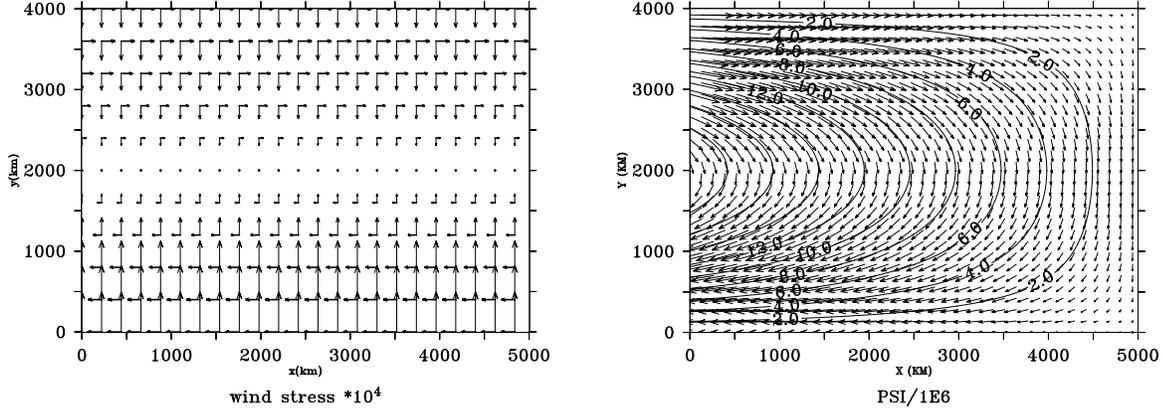
Figure 3.3. Left: The wind stress (thick arrows) and the resulting Ekman transport (northern hemisphere, thin arrows). Right: The Sverdrup stream function and the resulting Sverdrup transport.

Introducing the stream function for V and the relation of τ_b to the geostrophic current we find

$$\beta \frac{\partial}{\partial x} \Psi = \hat{\nabla}_h \tau_0 - \hat{\nabla}_h \cdot |f| \frac{d}{2} \left(\mathbf{u}_g + \hat{\mathbf{u}}_g \right). \tag{3.140}$$

To relate the geostrophic velocity to the stream function we make a simplifying approximation,

$$\mathbf{u}_g \approx \mathbf{U}/H. \tag{3.141}$$

This results in closed equation for the stream function,

$$r \nabla_h^2 \Psi + \beta \frac{\partial}{\partial x} \Psi = \hat{\nabla}_h \tau_0. \tag{3.142}$$

The parameter

$$r = |f| \frac{d}{2H} \tag{3.143}$$

is an inverse time scale. Comparing with the quasigeostrophic wave equation for the west coast in the previous secions, this is the scale for frictional damping of Rossby waves.
Equation 3.142 is called **Stommel**'s equation. It is an approximation but the advantage is a very simple boundary condition $\Psi = const$ at the coasts. It is still complex especially if complex continents like Australia or even islands are considered. Like for the Sverdrup equation the restriction "away from the equator, i.e., $f \neq 0$ does not apply.

We return again to the example of a cosine-shaped zonal wind but now blowing over an ocean with an eastern coast at $x = B$ and a western coast at $x = 0$. The wind stress reads again

$$\tau_0^{(x)} = -\tau_0 \cos ly, \quad \text{with} \quad l = \frac{\pi}{L}. \tag{3.144}$$

The stream function reads

$$\Psi(x, y) \ = \ \phi(x)\tau_0 \sin ly, \tag{3.145}$$

where $\phi(x)$ has to fulfill the zonal boundary conditions. The resulting equation for ϕ reads

$$r\left(\phi_{xx} - l^2\phi\right) + \beta\phi_x \ = \ -l. \tag{3.146}$$

For the special case $r = 0$ we retain the Sverdrup solution

$$\phi_{Sver} \ = \ \frac{l}{\beta}B\left(1 - \frac{x}{B}\right). \tag{3.147}$$

Now we consider the length scale $\delta = r/\beta$ as a parameter of the theory. The general solution reads

$$\phi \ = \ \frac{L}{\pi\beta\delta}\left[1 - \frac{\left(1 - e^{a_2}\right)e^{a_1 x/B} - \left(1 - e^{a_1}\right)e^{a_2 x/B}}{e^{a_1} - e^{a_2}}\right]. \tag{3.148}$$

ψ vanishs for both, $x = 0$ and $x = B$. The constants $a_{1,2}$ are

$$a_{1,2} \ = \ -\frac{B}{2\delta}\left[1 \pm \sqrt{1 + \left(\frac{2\pi\delta}{L}\right)^2}\right] \tag{3.149}$$

The case of small values of δ is of interest, just to see, how the solution deviates from the Sverdrup solution. Usually δ is significantly smaller than the meridional scale L,

$$a_1 \ = \ -\frac{B}{\delta}, \qquad a_2 = \frac{B\delta\pi^2}{L^2} = B\delta l^2. \tag{3.150}$$

Analysing ϕ in the limit $x \ll \delta$ we find

$$\phi \ \approx \ x\frac{l}{\beta}\frac{B}{\delta}. \tag{3.151}$$

For $x \gg \delta$ we find

$$\phi \ \approx \ (B - x)\frac{l}{\beta}. \tag{3.152}$$

Hence, at both the coasts the slope of ψ has opposite sign. Notably, the meridional flow at the western coast is directed against the Sverdrup transport. The modulus of the slope is enhanced by a factor B/δ near the western boundary. This means that the maximum of the stream function is near the western boundary and the flow is significantly enhanced there.

Exercise 3.22 Show that the Sverdrup southward flow is balanced exactly by the western boundary current! Show this independently off the specific form of the wind stress.
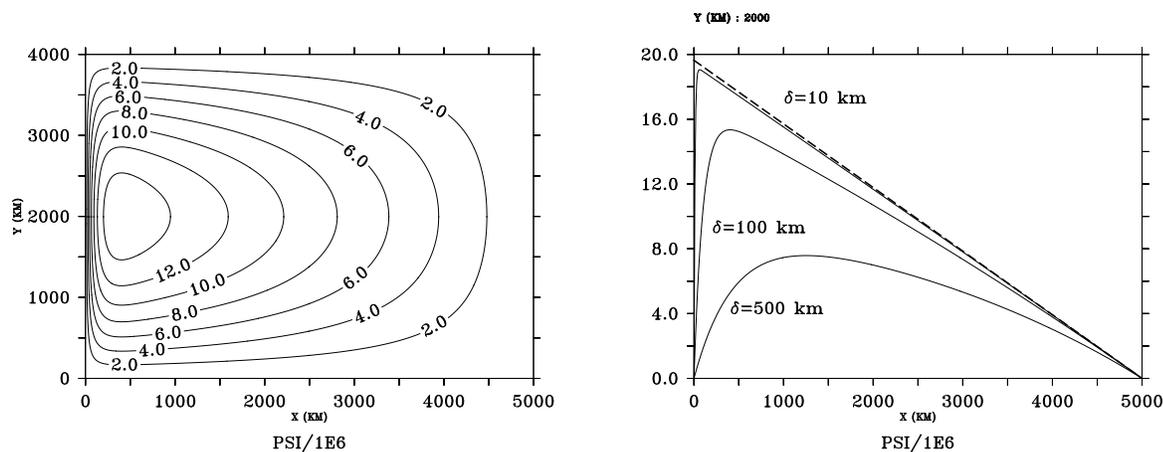
Figure 3.4. Left: The stream function in the Stommel regime. Right: Shape of the Stommel stream function for varying width of the western boundary layer. The dashed line markes the Sverdrup stream function.

The Stommel regime is the most simple solution of the quasigeostrophic equations for the wind driven basin wide ocean flow that shows the observed differences between the eastern and western ocean boundaries. The result is a closed steady state circulation, the Rossby wave dynamics behind the adjustment process was sketched in Section 3.4. It is stable for long times and deserves to be considered as a part of earth's *climate dynamics.*

The result discussed here is over-simplified, but it is straightforward to solve the Stommel equation for a realistic wind field. Doing so requires a mostly numerical treatment of the problem. Realistic topography and stratification can be also included.

A significant improvement of the Stommel theory is the inclusion of lateral friction by Walter Munk (1950). The extended momentum equation reads

$$f\hat{\mathbf{u}} = -g\nabla_h\eta + \frac{\partial}{\partial z}\tau + A_h\nabla_h^2\mathbf{u}. \tag{3.153}$$

Similarly to the discussion of the Stommel equation the *Stommel-Munk* equation can be derived,

$$r\nabla_h^2\Psi + A_h\nabla_h^4\Psi + \beta\frac{\partial}{\partial x}\Psi = \hat{\nabla}_h\tau_0. \tag{3.154}$$

The general structure of the solution is the same like that of the Stommel equation, but if the lateral friction dominates, the width of the western boundary layer is different and becomes $\delta = (A_h/\beta)^{1/3}$.

The Stommel-Munk equation has a specific importance for the development of numerical circulation models. Usually, in the ocean interiour the lateral turbulent momentum flux is small, but some amount of friction is required to get a realistic width of the western boundary currents. This reveals as unresolvable with a constant horizontal viscosity A_h. The solution is a turbulent viscosity depending on stress and strain of the flow field.

The result is the so called *Smagorinski eddy viscosity* that is today a standard for the representation of turbulent viscosity in large scale ocean models.
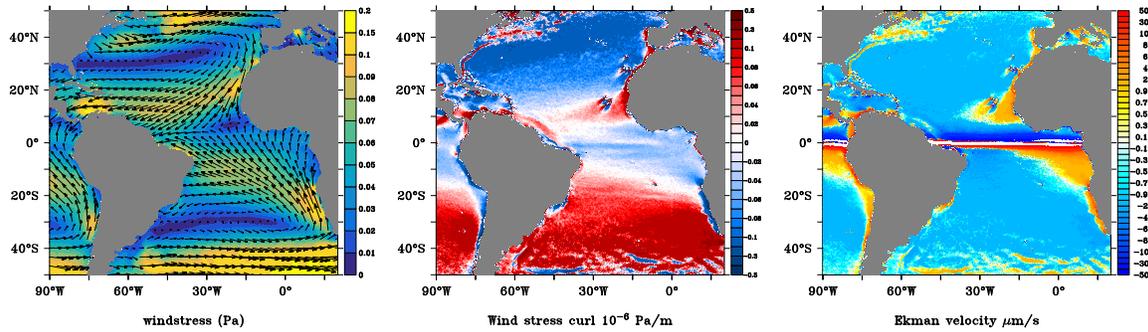

Figure 3.5. 10 year average of QuikSCAT derived wind stress. Left: The wind stress. Middle: Wind stress curl. Right: Vertical Ekman velocity.

3.5.4. The Sverdrup and Stommel regime as vorticity balance

Chapter 4

Wind driven equatorial currents

4.1. The basic equations

Near the equator the Coriolis force becomes negligibly small. So one may expect that the cross wise coupling of meridional and zonal motion by the Coriolis acceleration does not play any role here. Indeed, one may assume a simple balance: In the surface layer zonal wind stress accelerates a zonal current. Since there are continents intersecting this current, pressure gradients build up. In the surface layer the wind stress becomes balanced by a gradient of the sea surface heigt η,

$$\rho_1 g \frac{\partial}{\partial x} \eta = \rho_s X, \tag{4.1}$$

an east wind (blowing westward, negative X) is balanced by a negative (high sea level in the west) sea surface elevation gradient. Below the wind driven surface layer the surface pressure gradient is compensated by an opposite gradient of the thermocline,

$$\rho_1 g \frac{\partial}{\partial x} \eta = (\rho_2 - \rho_1) g \frac{\partial}{\partial x} h. \tag{4.2}$$

As a result the acceleration becomes small throughout the water column. Indeed, measurements of temperature and salinity in the equatorial area show westward enhanced mixed layer depth and westward enhanced sea level elevation. However, this simplistic view does not show, how this balance is established. Morevoer, it does not reveal any information on the currents except that the acceleration is zero.

In the last chapter we have seen that the zonal variation of the Coriolis parameter permits wave like current patterns from the conservation of potential vorticity. This conservation is also valid at the equator with zero Coriolis force, any zonal movement corresponds to changing relative (local) vorticity. To understand these waves we start here a detailed analysis of the dispersion relation of equatorial wavs and the corresponding wind driven flow pattern.

We start with the linearised frictionless Boussinesq equations

$$\frac{\partial}{\partial t} u - \beta y v + \frac{\partial p}{\partial x} = X \tag{4.3}$$

$$\frac{\partial}{\partial t} v + \beta y u + \frac{\partial p}{\partial y} = Y \tag{4.4}$$
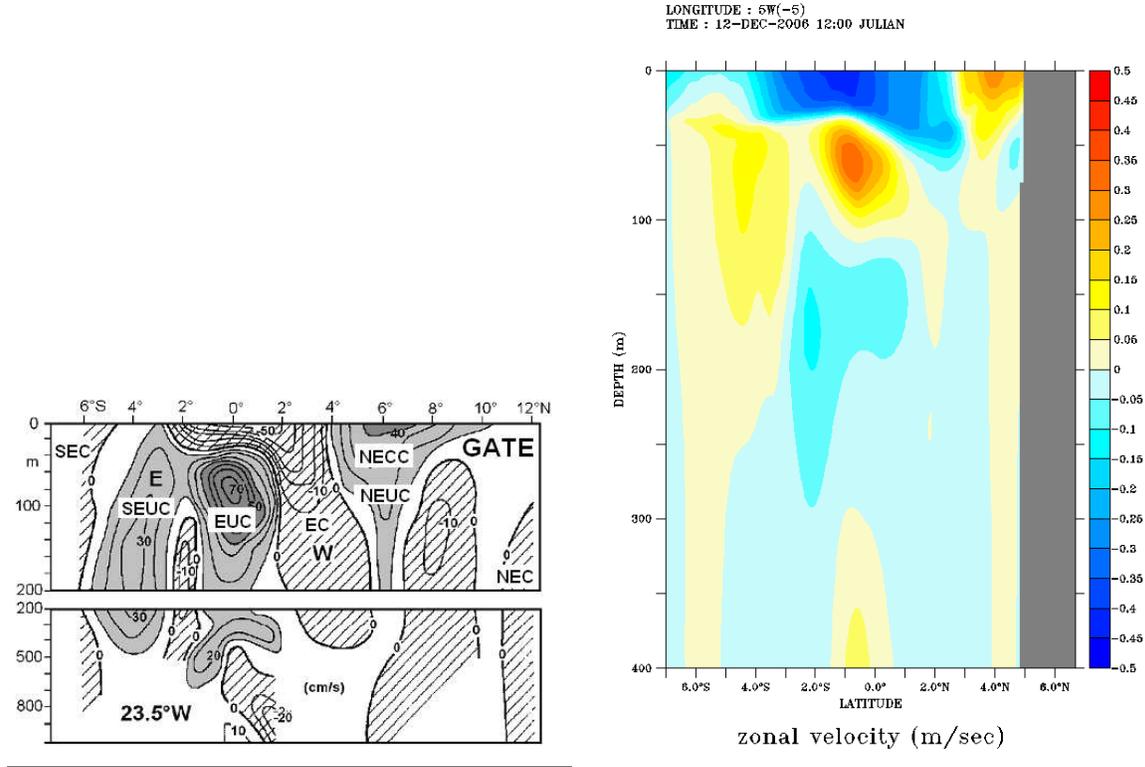
Figure 4.1. The equatorial currents found during the GATE experiment in the 60th (left) and seen in a numerical simulation (right).

$$\frac{\partial u}{\partial x} + \frac{\partial v}{\partial y} \;=\; \mathcal{Z}\frac{\partial}{\partial t}p. \tag{4.5}$$

The operator $\mathcal{Z}$ stands for

$$\mathcal{Z} = \frac{\partial}{\partial z}\frac{1}{N^2}\frac{\partial}{\partial z}. \tag{4.6}$$

and implies as usual the decomposition into vertical eigenfunctions F_n. The index n will be dropped below. After Fourier transformation over x and t we find

$$-i\bar{\omega}u - \beta yv + ikp \;=\; X, \tag{4.7}$$

$$-i\bar{\omega}v + \beta yu + \frac{\partial p}{\partial y} \;=\; Y, \tag{4.8}$$

$$iku + \frac{\partial v}{\partial y} - i\bar{\omega}\lambda^2 p \;=\; 0, \tag{4.9}$$

with $\bar{\omega} = \omega + i\varepsilon$. After a little algebra this can be resolved to single equation for v,

$$\frac{\partial^2 v}{\partial s^2} + \left(q + \frac{1}{2} - \frac{s^2}{4}\right)v \;=\; i\frac{(\bar{\omega}^2\lambda^2 - k^2)\,Y}{2\lambda\beta\bar{\omega}} + \sqrt{\frac{\lambda}{2\beta}}\frac{s}{2}X + \frac{k}{\bar{\omega}\sqrt{2\lambda\beta}}X_s, \tag{4.10}$$
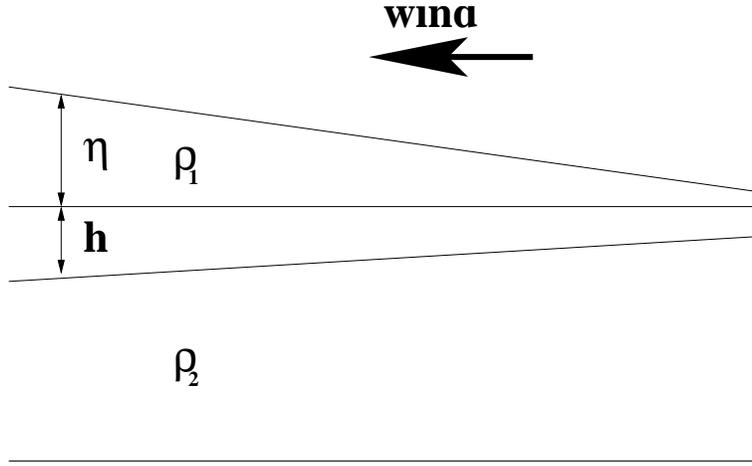
Figure 4.2. The wind induced surface elevation and the thermocline elevation.

with the scaled coordinate $s = \sqrt{2\lambda\beta}y$ and

$$2q + 1 \;=\; \frac{\bar{\omega}^2\lambda^2 - k^2}{\lambda\beta} - \frac{k}{\lambda\bar{\omega}}. \tag{4.11}$$

We assume the boundary conditions

$$v \;\to\; 0 \quad \text{for} \quad y \to \pm\infty. \tag{4.12}$$

4.2. Green's function

The Green's function is defind by the equation

$$\frac{\partial^2}{\partial s^2}G(s, s') + \left(q + \frac{1}{2} - \frac{s^2}{4}\right)G(s, s') \;=\; \delta(s - s'). \tag{4.13}$$

The homogeneous equation has the so called parabolic cylinder functions $Dq(s$ and $D_q(-s)$ as solution. Without a proof we note, that the Wronskian of the D is

$$W \;=\; D_q(s)\frac{\partial}{\partial s}D_q(-s) - D_q(-s)\frac{\partial}{\partial s}D_q(s) = -\frac{\sqrt{2\pi}}{\Gamma(-q)}. \tag{4.14}$$

Hence, as described in Section 2.5.2 the resulting Green's function reads

$$G_q(s, s') \;=\; \theta(s - s')G^>(q, s, s') + \theta(s' - s)G^<(q, s, s'), \tag{4.15}$$

with

$$G^>(q, s, s') \;=\; -\frac{\Gamma(-q)}{\sqrt{2\pi}}D_q(s)D_q(-s') = G^<(q, s', s) \tag{4.16}$$

The function Γ has poles for integer values of q and reads approximately,

$$\Gamma(-q) \;\approx\; \frac{(-1)^m}{m!(m - q)}, \tag{4.17}$$

Hence, we consider the Green's function near these poles for integer values of $q = n$. In this case the parabolic cylinder functions simplify to Hermite polynominals

$$D_n(s) = \frac{1}{\sqrt{2^m}} e^{-\frac{s^2}{4}} H_m\left(\frac{s}{\sqrt{2}}\right), \tag{4.18}$$

and the Green's function becomes a sum over all residuals of the poles of the Γ-function

$$G_q(s, s') = \sum_{n=0}^{\infty} \frac{e^{-\frac{s^2+s'^2}{4}}}{2^m m! \sqrt{2\pi}(q-m)} H_m\left(\frac{s}{\sqrt{2}}\right) H_m\left(\frac{s'}{\sqrt{2}}\right) \tag{4.19}$$

The Hermite polynominals are either symmetric or antisymmetric,

$$\begin{aligned}
H_0(x) &= 1, \\
H_1(x) &= 2x, \\
H_2(x) &= 4x^2 - 2, \\
H_3(x) &= 8x^3 - 12x. \tag{4.20}
\end{aligned}$$

Here we can derive our first result. The solution is localised at the equator and decays exponentially with y. The typical scale is

$$R_n = \sqrt{\beta\lambda}^{-1}, \tag{4.21}$$

the so called equatorial Rossby radius. The special waves described by the Green's function are confined to the so called equatorial wave guide.

4.3. Formal solution

The formal solution for this Green's function is found like in the previous examples.

$$v(\bar{\omega}, k, s) = i \frac{(\bar{\omega}^2\lambda^2 - k^2) G_q \star Y}{2\lambda\beta\bar{\omega}} + \sqrt{\frac{\lambda}{2\beta}} G_q \star \frac{s'}{2} X + \frac{k}{\bar{\omega}\sqrt{2\lambda\beta}} G_q \star X'_s, \tag{4.22}$$

the zonal velocity and the pressure read

$$\begin{aligned}
u(\bar{\omega}, k, s) = {}& \sqrt{\frac{\lambda}{2\beta}} \left(\frac{k}{\bar{\omega}\lambda}\frac{\partial}{\partial s} - \frac{s}{2}\right) G \star Y \\
& + \frac{i\bar{\omega}\lambda^2}{\bar{\omega}^2\lambda^2 - k^2} \left(X + \left(\frac{s}{2} - \frac{k}{\bar{\omega}\lambda}\frac{\partial}{\partial s}\right)\left(G \star \frac{s'}{2} X + \frac{k}{\bar{\omega}\lambda} G \star X'_s\right)\right), \tag{4.23}
\end{aligned}$$

$$\begin{aligned}
p(\bar{\omega}, k, s) = {}& \sqrt{\frac{1}{2\beta\lambda}} \left(\frac{\partial}{\partial s} - \frac{k}{\bar{\omega}\lambda}\frac{s}{2}\right) G \star Y \\
& + \frac{ik}{\bar{\omega}^2\lambda^2 - k^2} \left(X + \left(\frac{s}{2} - \frac{\bar{\omega}\lambda}{k}\frac{\partial}{\partial s}\right)\left(G \star \frac{s'}{2} X + \frac{k}{\bar{\omega}\lambda} G \star X'_s\right)\right) \tag{4.24}
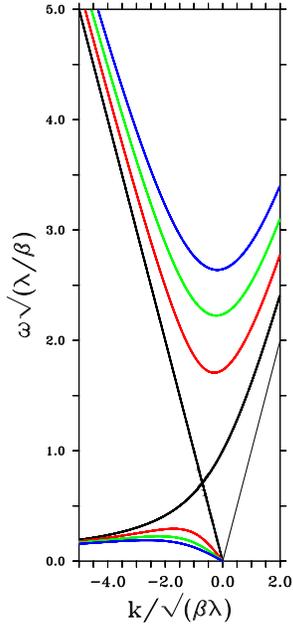\end{aligned}$$

Figure 4.3. The positive frequency part of the dispersion relation for equatorial waves. Black is the result for $m = 0$, the so called Yanai-wave. Red the Rossby and gravity waves for $m = 1$ and so on. The thin black curve is a Kelvin wave that does not result from the dispersion relation (4.26).

4.4. The dispersion relation

The dispersion relation is given by the integer values of q, or,

$$2n + 1 \;\; = \;\; \frac{\bar{\omega}^2 \lambda^2 - k^2}{\lambda \beta} - \frac{k}{\lambda \bar{\omega}}. \tag{4.25}$$

This defines a third order polynominal

$$\bar{\omega}^3 - \left(\frac{k^2}{\lambda^2} + \frac{\beta}{\lambda}(2m + 1) \right) \bar{\omega} - \frac{\beta k}{\lambda^2} \;\; = \;\; 0, \tag{4.26}$$

that is the dispersion relation for equatorial waves. An explicit solution does not exist and we will discuss approximations. To this end we introduce the scaling

$$\tilde{\omega} \;\; = \;\; \bar{\omega}\sqrt{\frac{\lambda}{\beta}}, \quad \tilde{k} = \frac{k}{\sqrt{\lambda \beta}} \tag{4.27}$$

$$\tilde{\omega}^3 - \left(\tilde{k}^2 + 2m + 1 \right) \tilde{\omega} - \tilde{k} \;\; = \;\; 0. \tag{4.28}$$

This is a reduced cubic equation of the general form

$$y^3 + 3py + 2q \;\; = \;\; 0, \tag{4.29}$$

The discriminant $D = p^3 + q^2$ is

$$D = \frac{k^2}{4} - \left(\frac{1}{3}\left(k^2 + 2m + 1\right)\right) < 0 \tag{4.30}$$

is negative and 3 reals roots of the dispersion relation must exist. Figure 4.3 shows the positive frequency branches for the equatorial ocean. The thick black lines are the curves for $m = 0$, the so called Yanai-wave. Equation 4.26 can be solved for the wave number and has two roots

$$\tilde{k}_{0;1/2} = -\frac{1}{2\tilde{\omega}} \pm \sqrt{\frac{1}{4\tilde{\omega}^2} + \tilde{\omega}^2 - 1} = -\frac{1}{2\tilde{\omega}} \pm \left(\frac{1}{2\tilde{\omega}} - \tilde{\omega}\right)$$

$$\tilde{k}_{01} = \tilde{\omega} - \frac{1}{\tilde{\omega}}, \quad k_{02} = -\tilde{\omega}. \tag{4.31}$$

The second root k_{02} corresponds to a Kelvin wave. We will show below, that this wave cannot propagate within an unbounded ocean. For large negative wave numbers the Yanai wave is similar to short wave Rossby waves with east-ward propagating phases. For large positive wave numbers is behaves similarly to gravity waves.

For $m \geq 1$ there is a large frequency gap between Rossby waves with low frequency and gravity waves with high frequency. For low frequency the dispersion relation reads approximately

$$\bar{\omega} \approx -\frac{\beta k}{k^2 + (2m + 1)\beta\lambda}, \tag{4.32}$$

which is similar to that of mid-latitude Rossby waves, but now with the equatorial Rossby radius $R^2 = 1/(\beta\lambda)$. The phase velocity is also west-ward, the groop velocity changes sign and is negative for small wave number (long waves) and positive for large (negative) wave numbers. For large frequency we find

$$\bar{\omega}^2 \approx \frac{\beta}{\lambda}(2m + 1) + \frac{k^2}{\lambda^2}, \tag{4.33}$$

similar to gravity waves. But note, the different limit $k \to 0$ (dependent on λ_n) for the different vertical modes.

The zonal velocity u as well as the pressure p have additional poles at

$$\tilde{\omega} = \pm\frac{k}{\lambda}, \tag{4.34}$$

corresponding to Kelvin waves spreading along the equator. One Kelvin pole coincides with one of the Yanai wave modes, the other one is a simple Kelvin pole to be discussed below.

4.5. The equatorial Kelvin wave

We consider the residuum of the poles at $\bar{o}mega = \pm k$ and $\bar{o}mega = 0$. These poles can be found in the expression for the zonal velocity u and the pressure p. It is of some

help to separate the poles using the relations

$$\frac{k}{\omega^2 - \left(\frac{k}{\lambda}\right)^2} = \frac{\lambda}{2}\left(\frac{1}{\omega - \frac{k}{\lambda}} - \frac{1}{\omega + \frac{k}{\lambda}}\right), \tag{4.35}$$

$$\frac{\omega}{\omega^2 - \left(\frac{k}{\lambda}\right)^2} = \frac{1}{2}\left(\frac{1}{\omega - \frac{k}{\lambda}} + \frac{1}{\omega + \frac{k}{\lambda}}\right), \tag{4.36}$$

$$\frac{1}{\omega\left(\omega^2 - \left(\frac{k}{\lambda}\right)^2\right)} = \frac{\lambda^2}{k^2}\left(\frac{1}{\omega} - \frac{1}{2}\left(\frac{1}{\omega - \frac{k}{\lambda}} + \frac{1}{\omega + \frac{k}{\lambda}}\right)\right). \tag{4.37}$$

We sort contribution of the different poles for the zonal velocity,

$$
\begin{aligned}
u(\bar{\omega}, k, s) &= \sqrt{\frac{\lambda}{2\beta}}\left(\frac{k}{\bar{\omega}\lambda}\frac{\partial}{\partial s} - \frac{s}{2}\right)G \star Y \\
&+ \frac{i}{2}\frac{1}{\omega - \frac{k}{\lambda}}\left(X + X \star \Lambda^-(s)\Lambda^-(s')G\right) \tag{4.38} \\
&+ \frac{i}{2}\frac{1}{\omega + \frac{k}{\lambda}}\left(X + X \star \Lambda^+(s)\Lambda^+(s')G\right) \tag{4.39} \\
&+ \frac{i}{\omega}\frac{\partial}{\partial s}G \star X_{s'}. \tag{4.40}
\end{aligned}
$$

To achieve this result the term with $G \star X_{s'}$ has been integrated by parts. The operator $\Lambda^\pm$ is short for

$$\Lambda^\pm(s) = \left(\frac{\partial}{\partial s} \pm \frac{s}{2}\right). \tag{4.41}$$

The choice of this operator is motivated by the property of the parabolic cylinder functions

$$\Lambda^+(s)D_q(\pm s) = \pm q D_{q-1}(\pm s), \tag{4.42}$$
$$\Lambda^-(s)D_q(\pm s) = \mp D_{q+1}(\pm s). \tag{4.43}$$

Applying Λ to the Green's function yields

$$\Lambda^+(s)G(q, s, s') = -\frac{\Gamma(-q)}{\sqrt{2\pi}}q\left(\theta(s - s')D_{q-1}(s)D_q(-s') - \theta(s' - s)D_{q-1}(-s)D_q(s')\right) \tag{4.44}$$

and

$$
\begin{aligned}
\Lambda^+(s)\Lambda^+(s') \quad & G_q(s, s') \\
&= -\frac{\Gamma(-q)}{\sqrt{2\pi}}q^2\left(-\theta(s - s')D_{q-1}(s)D_{q-1}(-s') - \theta(s' - s)D_{q-1}(-s)D_{q-1}(s')\right) \\
&+ \frac{\Gamma(-q)}{\sqrt{2\pi}}q\delta(s - s')\left(D_{q-1}(s)D_q(-s) + D_{q-1}(-s)D_q(s)\right), \tag{4.45}
\end{aligned}
$$

With the help of the Wronskian and the property of the Γ-function

$$z\Gamma(z) = \Gamma(z + 1), \quad \text{or} \quad (-q)\Gamma(-q) = \Gamma(-q + 1), \tag{4.46}$$

we find

$$\Lambda^+(s)\Lambda^+(s')G_q(s,s') = -\delta(s-s') + qG_{q-1}(s,s') \tag{4.47}$$
$$\Lambda^-(s)\Lambda^-(s')G_q(s,s') = -\delta(s-s') + (q+1)G_{q+1}(s,s') \tag{4.48}$$
$$\tag{4.49}$$

and finally

$$
\begin{aligned}
u(\bar{\omega},k,s) &= \sqrt{\frac{\lambda}{2\beta}}\left(\frac{k}{\bar{\omega}\lambda}\frac{\partial}{\partial s} - \frac{s}{2}\right)G_q \star Y \\
&+ \frac{i}{2}\frac{1}{\omega - \frac{k}{\lambda}}\left((q+1)G_{q+1} \star X\right) \tag{4.50} \\
&+ \frac{i}{2}\frac{1}{\omega + \frac{k}{\lambda}}\left(qG_{q+1} \star X\right) \tag{4.51} \\
&+ \frac{i}{\omega}\frac{\partial}{\partial s}G_q \star X_{s'}. \tag{4.52}
\end{aligned}
$$

Remains the determination of q from

$$2q+1 = \frac{\bar{\omega}^2\lambda^2 - k^2}{\lambda\beta} - \frac{k}{\lambda\bar{\omega}}. \tag{4.53}$$

For $\omega = 0$ this results in a singularity and the k-integrals have to be calculated first. For $\omega = k/\lambda$ we find $q = -1$ and $q = 0$ for $\omega = -k/\lambda$. Hence, with

$$-(q+1)\Gamma(-(q+1)) = \Gamma(-(q+1)+1) \to \Gamma(1) \tag{4.54}$$

we find for the $\omega = k/\lambda$-contribution

$$\frac{i}{2}\frac{1}{\omega - \frac{k}{\lambda}}\left((q+1)G_{q+1} \star X\right) \to \frac{i}{2}\frac{1}{\omega - \frac{k}{\lambda}}\left(\frac{1}{\sqrt{2\pi}}e^{-\frac{s^2+s'^2}{4}} \star X\right). \tag{4.55}$$

The $\omega = -k/\lambda$ does not contribute, since $\Gamma(-(q-1))$ remains finite for $q = 0$ and the explicit factor $q \to 0$ cancels this contribution out,

$$
\begin{aligned}
u(\bar{\omega},k,s) &= \sqrt{\frac{\lambda}{2\beta}}\left(\frac{k}{\bar{\omega}\lambda}\frac{\partial}{\partial s} - \frac{s}{2}\right)G_q \star Y + \frac{i}{\omega}\frac{\partial}{\partial s}G_q \star X_{s'} \\
&+ \frac{i}{2}\frac{1}{\omega - \frac{k}{\lambda}}\left(\frac{1}{\sqrt{2\pi}}e^{-\frac{s^2+s'^2}{4}} \star X\right). \tag{4.56}
\end{aligned}
$$

Similarly we get for the pressure

$$
\begin{aligned}
p(\bar{\omega},k,s) &= \sqrt{\frac{1}{2\lambda\beta}}\left(\frac{\partial}{\partial s} - \frac{k}{\bar{\omega}\lambda}\frac{s}{2}\right)G_q \star Y - \frac{i}{\lambda\omega}\frac{s}{2}G_q \star X_{s'} \\
&- \frac{i}{2\lambda}\frac{1}{\omega - \frac{k}{\lambda}}\left(\frac{1}{\sqrt{2\pi}}e^{-\frac{s^2+s'^2}{4}} \star X\right) \tag{4.57}
\end{aligned}
$$

In summary:

- the equator serves as a wave guide. The characteristic meridional extension is the equatorial Rossby radius $R_n = \sqrt{\beta\lambda}^{-1}$.

- Several wave types may be excited in this wave guide. Rossby waves may spread (group velocity) east- and west-ward. Kelvin waves are non-dispersive, localized in the equatorial wave guide and can spread only east-ward.

- From a uniform zonal wind even in absence of the Coriolis acceleration a meridional flow can be driven. It can be shown, that this flow is antisymmetric across the equator and drives upwelling confined to the equatorial wave guide.

4.6. Kelvin waves and equatorial currents

Considering a zonal wind patch over the equator with large meridional extension,

$$X = -\frac{u_*^2}{H_{mix}}\theta(t)\theta(z + H_{mix})\theta(a - |x|). \tag{4.58}$$

We will discuss only the contribution of the Kelvin waves. In this case the velocity and the pressure simplifies to

$$v(\bar{\omega}, k, s) = \sqrt{\frac{\lambda}{2\beta}}G_q \star \frac{s'}{2}X = 0,$$

$$u(\bar{\omega}, k, s) = \frac{i}{2}\frac{1}{\omega - \frac{k}{\lambda}}\left(\frac{1}{\sqrt{2\pi}}e^{-\frac{s^2 + s'^2}{4}} \star X\right),$$

$$p(\bar{\omega}, k, s) = -\frac{i}{2\lambda}\frac{1}{\omega - \frac{k}{\lambda}}\left(\frac{1}{\sqrt{2\pi}}e^{-\frac{s^2 + s'^2}{4}} \star X\right). \tag{4.59}$$

Calculating the inverse Fourier transforms and the residuum around the $\omega - \frac{k}{\lambda}$-pole the result for u is

$$u(x, y, t) = -\frac{u_*^2}{h}\Psi_0(y)$$
$$[\theta(t)\theta(a - |x|)t$$
$$- \theta(x + a)\theta(t - \lambda(x + a))(t - \lambda(x + a))$$
$$+ \theta(x - a)\theta(t - \lambda(x - a))(t - \lambda(x - a))]$$

$$p(x, y, t) = \frac{1}{\lambda}u(x, y, t)$$

$$w(x, y, t) = -p_t = \frac{1}{\lambda}u_t = \frac{u_*^2}{h\lambda}\Psi_0(y)$$
$$[\theta(t)\theta(a - |x|) - \theta(x + a)\theta(t - \lambda(x + a)) + \theta(x - a)\theta(t - \lambda(x - a))] \tag{4.60}$$

The response is confined to a stripe near the equator described by the function $\Psi_0(y)$ from the convolution of the wind field with $e^{-\frac{s^2 + s'^2}{4}}$. For u the result is a superposition of three components - a linearly growing jet within the wind patch and two eastward spreading Kelvin waves starting from $x = a$ and $x = -a$. The waves adjust the growing equatorial jet to a fixed value.

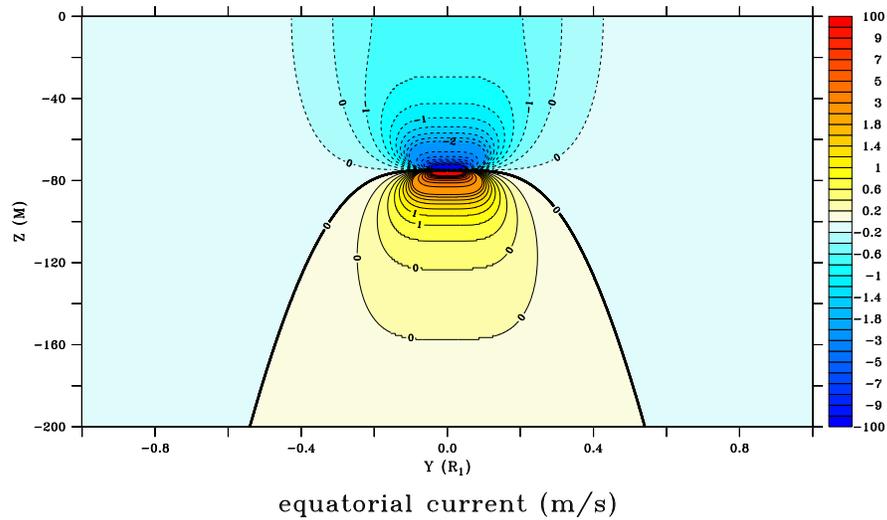Performing the mode sum yields the following picture:

Figure 4.4. The analytical solution for the system of equatorial currents.

- There exists a strong west-ward surface current with an underlying strong east-ward under-current.

- The under-current is established by the Kelvin waves starting from the edges of the wind patch.

- Kelvin waves export the wind response from the area of the wind patch.

Chapter 5

The Antarctic Circumpolar current

5.1. ACC as a zonally periodic system

The Antarctiv Circumpolar Current (ACC) is one of the largest circulation systems of the world. It encircles Antarctica and connects this way all major oceans except the Arctic Ocean. Although the flow is basically a closed stream band, it exhibits strong lateral elevations and embedded eddies. It is strongest in narrow straits between continents, easpecially between the souther tip of South Americal and the Antarctic Peninsula. Here ADCP measurments reveal a permanent east-ward current, see Fig. 5.1. The ACC is approximately in geostrophic balance and can be seen as band with permanent gradient in the sea surface elevation around Antarctica, see Fig. 5.2. Its transport is about 120 Sv. However, snapshots reveal a strong eddy component of the flow, see Fig. 5.3. These eddies are drifting mainly westward and seem to obey Rossby wave dynamics. Differently from the subtropical gyres where the flow is confined to the surface layer, (see Sverdrup's catastrophy), the flow in the ACC extends to deep areas, partly over 2000 m depth. As the result the stratification is more "horizontal" than vertical and Antarctica is surrounded by a complex system of fronts. The northern boundary of the ACC is the so called "Polar front", the southern boundary the "Antarctic front", Fig. 5.4.

The dynamics of the ACC has been subject of intense reasearch and partly controversal discussions during the last decades. Especially its momentum balance is not finally understand yet. Nevertheless, the key processes seem to be clear now and some basic ideas will be outlined here. The ACC is situated within a belt of strong westerly (east-ward) wind around Antarctica. Actually this wind pattern is a sequence of localised low pressure areas born frequentyl in the permanent polar gyres. Those appear in the climatology as a contineous low pressure band with corresponding westerly winds. The first effect of the east-ward wind is an equatorward Ekman transport in the surface layer,

$$-fv_E = X. \tag{5.1}$$

Integrating this Ekman flow over a circle round Antarctica, say following the Polar front, it implies a permanent loss of water from the ACC system. This is not the case and the equator-ward Ekman transport must be compensated by a pole-ward flow in the ocean interiour, v_g or v_b. Here v_g is the approximately qeostrophically balanced flow in the ocean interiour and v_b the flow within a turbulent bottom boundary layer similarly to the Ekman transport in the surface layer. Averaging over a sufficient time period the total
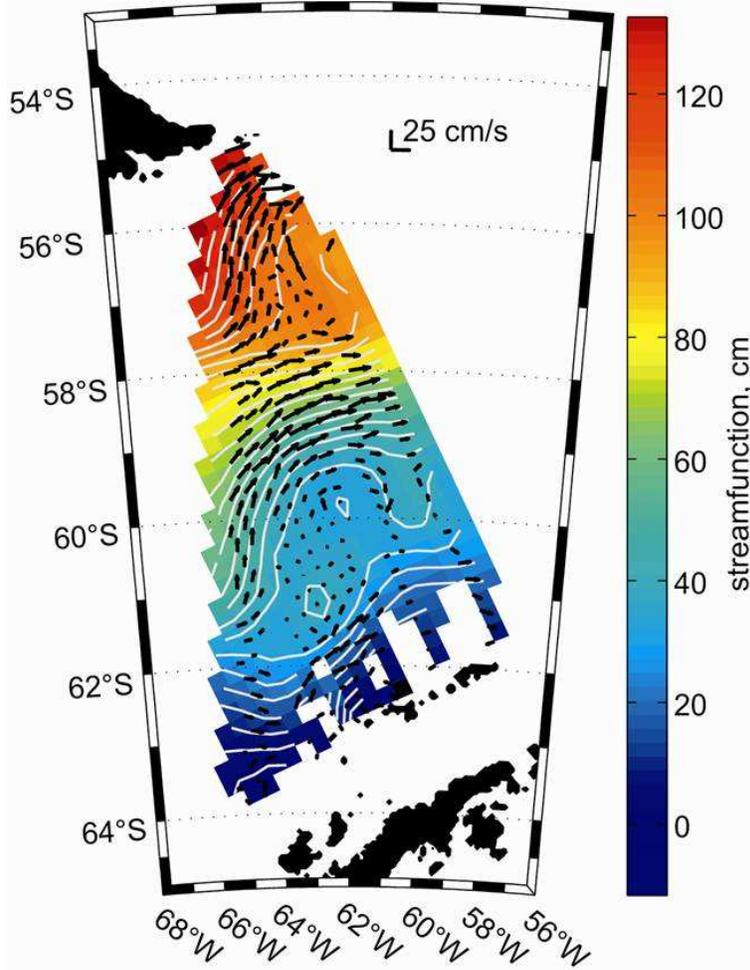
Figure 5.1. The surface component of the ACC in ADCP measurements in the Drake passage.

volume of the water within the ACC area must be constant,

$$\int_{-H}^{0} dz \left(<v>_E + <v>_g + <v>_b \right) \;\; = \;\; 0. \tag{5.2}$$

Here the brackets denote a zonally averaged quantity. This special and unique form of a budget - zonally periodic and meridionally semi-closed seems to be a key to understand the ACC. We will follow this idea with step-wise increased complexity of the analysis. We start from following system of Boussinesq equations

$$\frac{\partial}{\partial t}u + \nabla \cdot (\mathbf{u}u) - fv + \frac{\partial}{\partial x}p \;\; = \;\; \frac{\partial}{\partial z}\tau^x, \tag{5.3}$$

$$\frac{\partial}{\partial t}v + \nabla \cdot (\mathbf{u}v) + fu + \frac{\partial}{\partial y}p \;\; = \;\; \frac{\partial}{\partial z}\tau^y, \tag{5.4}$$

$$\frac{\partial}{\partial x}u + \frac{\partial}{\partial y}v + \frac{\partial}{\partial z}w \;\; = \;\; 0, \tag{5.5}$$
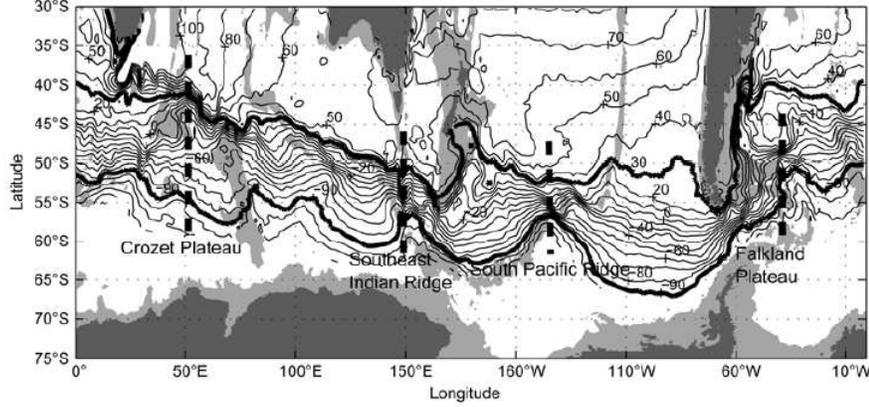
Figure 1 Mean SSH (cm) during 1993–2011 from AVISO (contours). Bold contours represent the northernmost and southernmost streamlines that pass through Drake Passage. Depths less than 3000 m are gray shaded. Dashed lines indicate four regions where the ACC strength has large interannual variations, as described in section 3.

Figure 5.2. The ACC seen in altimeter data. (Zhang et. al, 2012)

$$\frac{\partial}{\partial z}p = -g \tag{5.6}$$

τ is the turbulent vertical momentum flux. We assume, that the sea level elevation $\eta \ll H$ and neglect the upper part between $0 - \eta$ in vertical integrals. For consistency we use the rigid lid approximation $w(z = 0) = 0$. A more general derivation with variable sea surface height is possible. $< .. >$ denotes the zonal average, for vertically integrated quatities we use capital letters.

5.2. Flat bottom, low lateral friction

For an ocean with flat bottom the Boussinesq equations can be averaged zonally and integrated vertically. Since the flow is zonally periodic, some terms are eliminated this way,

$$\frac{\partial}{\partial t} <U> + \int_{-H}^{0} dz \frac{\partial}{\partial y} <vu> - f <V> = \tau_s^x - \tau_b^x, \tag{5.7}$$

$$\frac{\partial}{\partial t} <V> + \int_{-H}^{0} dz \left(\frac{\partial}{\partial y} <vv> + \frac{\partial}{\partial y} <p> \right) + f <U> = \tau_s^y - \tau_b^y, \tag{5.8}$$

$$\frac{\partial}{\partial y} <V> = 0, \tag{5.9}$$

$$p(z) = g\eta + \int_{z}^{0} dz' \frac{\rho(z')}{\rho_0}. \tag{5.10}$$

The remaining term of the continuity equation means, that the total meridional flow is independent off y and, hence, a constant. The existence if the rigid southern boundary Antarctica implies, that
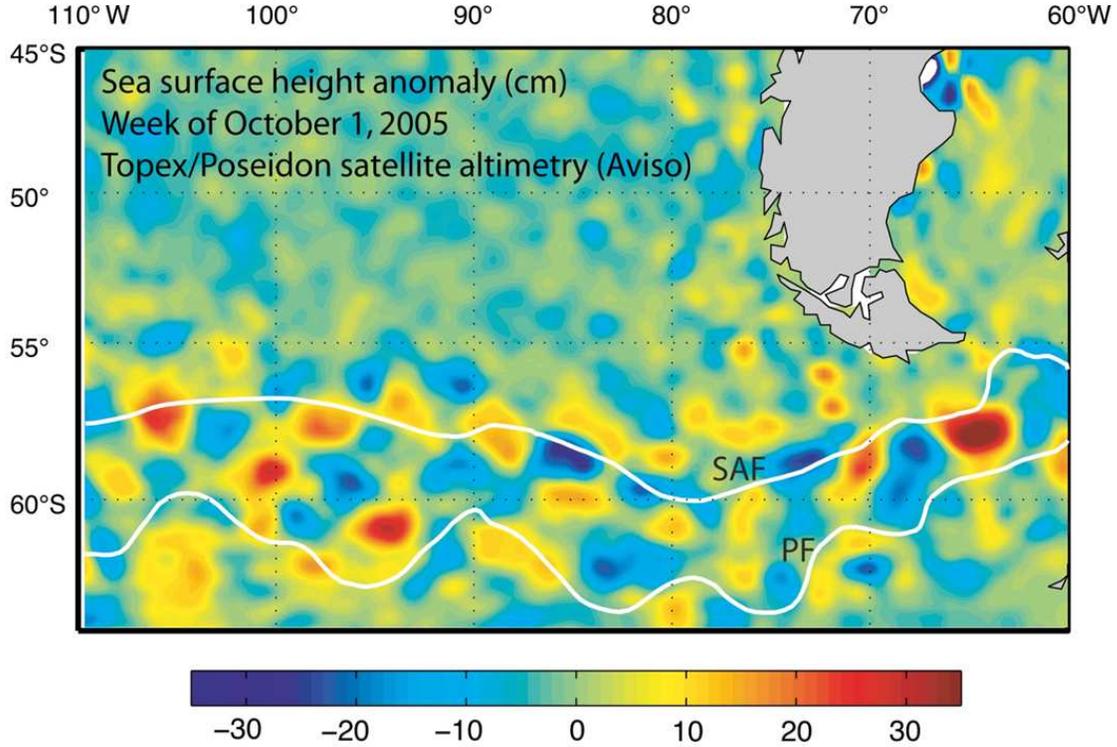
$$<V> = 0. \tag{5.11}$$

Figure 5.3. The ACC variability seen in altimeter data.

Considering a steady limit and neglecting the nonlinear terms for the moment, we find simple momentum budgets promising to reveal the basic physics behind governing the ACC,

$$-f <V> \; = \; 0 = \tau_s^x - \tau_b^x, \tag{5.12}$$

$$f <U> + gH \frac{\partial}{\partial y} <\eta> \; = \; \tau_s^y - \tau_b^y. \tag{5.13}$$

The first equation is simply the statement, that the momentum flux into the ocean from wind stress is balanced by a momentum flux out of the ocean from bottom friction. Although this equation is the zonal moentum equation, is does not simply define the velocity of the ACC. The second equation is the general geostrophic balance of the ACC valid in the ocean interiour except for the surface and the bottom boundary layers. Assuming a pure zonal wind, this equation defines the total transport of the ACC,

$$<U> \; = \; -\frac{gH}{f} \frac{\partial}{\partial y} \eta - \frac{\tau_b^y}{f}. \tag{5.14}$$

τ_s results from the wind field. The flow in the ACC will grow to such an extend, that bottom friction compensates exactly the momentum input from the wind.

To find the bottom friction, we employ the classical Ekman theory of frictional boundayr layers in a rotating system. We consider the steady state solution only, since we are not
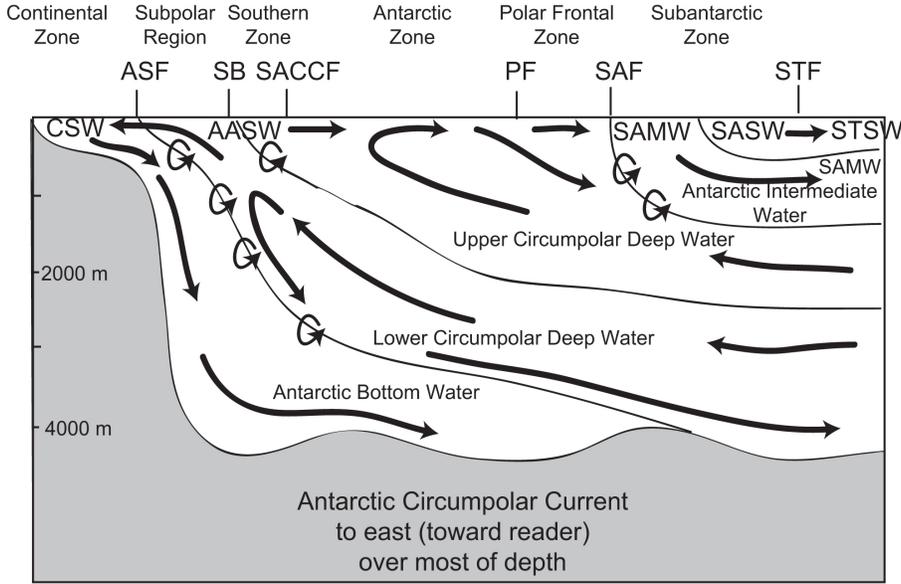
Figure 5.4. The system of fronts between water masses around Antarctica.

interested in the high frequency inertial oscillations. A missing ingredient is the relation between the vertical momentum flux τ and the horizontal flow. We use the standard approximation

$$\tau = \nu \frac{\partial}{\partial z} \mathbf{u} \tag{5.15}$$

where ν is the turbulent viscosity. Omitting the nonlinear terms we get

$$-f < v > = \frac{\partial}{\partial z} \nu \frac{\partial}{\partial z} < u >, \tag{5.16}$$

$$f < u > + g \frac{\partial}{\partial y} < \eta > = \frac{\partial}{\partial z} \nu \frac{\partial}{\partial z} < v >, \tag{5.17}$$

$$\frac{\partial}{\partial y} < v > + \frac{\partial}{\partial z} < w > = 0. \tag{5.18}$$

From the Ekman boundary layer theory we know, that the friction terms are important only within thin boundary layers near the sea surface and the sea floor. Here the wind entrains turbulence or turbulence is formed from the shear between the flow in the ocean interiour and the bottom, where the horizontal flow vanishs,

$$< v > = 0, \quad < u > = 0 \quad \text{for} \quad z = -H. \tag{5.19}$$

This allows to split the total flow into a geostropic part and an ageostrophic part in the boundary layers,

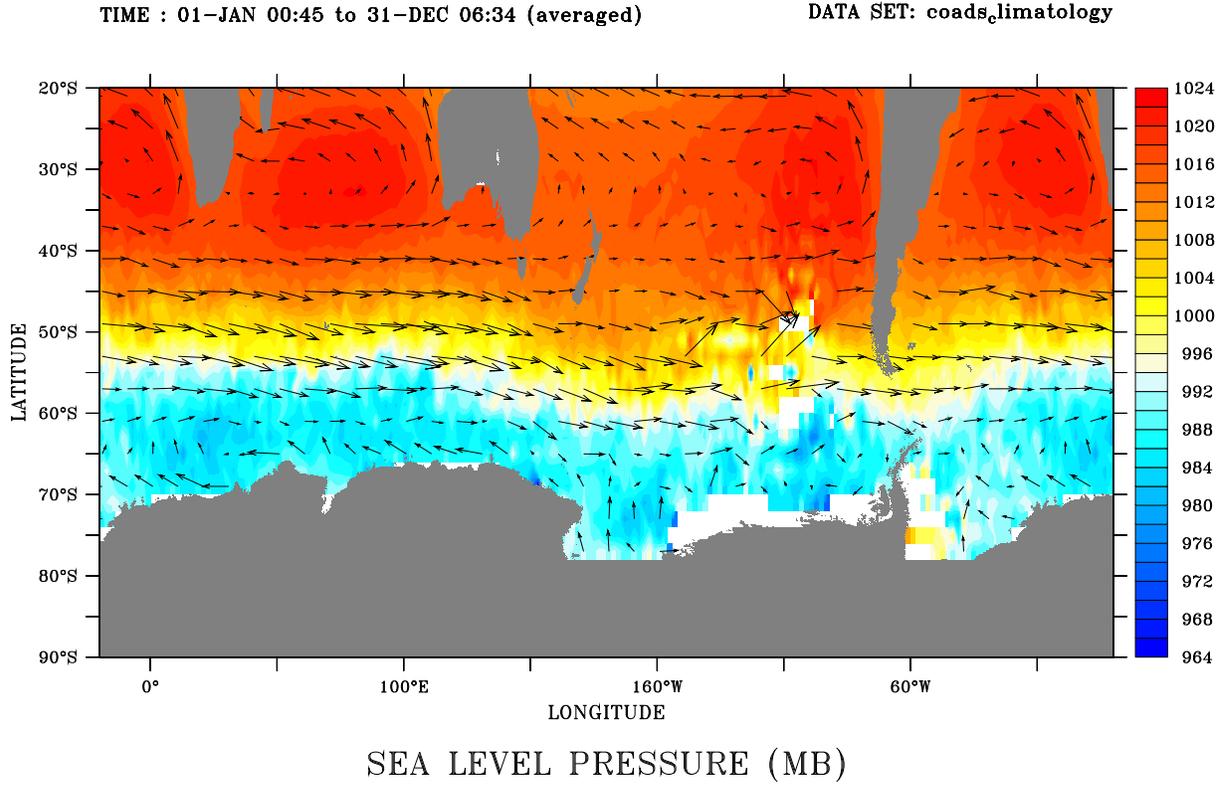$$< u > = u_g + u_b \tag{5.20}$$

$$< v > = v_g + v_b. \tag{5.21}$$

Figure 5.5. The west wind belt encircling Antarctica seen in the time averaged climatology. Actually this wind pattern is a sequence of localised low pressure areas encircling Antartica.

u_b and v_b are confined to a thin bottom layer, hence we require

$$< u > \ = \ u_g, \quad < v >= v_g \quad \text{for} \quad z \gg -H. \tag{5.22}$$

The geostrophic meridional flow vanishs, and we have $v_b =< v >$. The geostrophic zonal flow is balanced (per definition) with the meridional pressure gradient,

$$-f < v > \ = \ \frac{\partial}{\partial z}\nu\frac{\partial}{\partial z} < u >, \tag{5.23}$$

$$f < u > \ = \ fu_g + \frac{\partial}{\partial z}\nu\frac{\partial}{\partial z} < v > . \tag{5.24}$$

This system of equations is solved with the ansatz

$$< u(z) > \ = \ u_g + ae^{\lambda(z+H)}, \tag{5.25}$$
$$< v(z) > \ = \ be^{\lambda(z+H)}. \tag{5.26}$$

Inserting gives an equation for λ,

$$\lambda^4 \ = \ -\frac{f^2}{\nu^2}, \tag{5.27}$$

i.e.

$$\lambda \;=\; \pm(1\pm i)\frac{1}{d}, \tag{5.28}$$

$$d \;=\; \sqrt{\frac{2\nu}{|f|}} \tag{5.29}$$

From the boundary condition all solutions growing exponentially with z must have vanishing coefficients. The remaining part can be written as

$$<u(z)> \;=\; u_g\left(1 - e^{-\frac{z+H}{d}}\cos\frac{z+H}{d}\right), \tag{5.30}$$

$$<v(z)> \;=\; sig(f)\,u_g\,e^{-\frac{z+H}{d}}\sin\frac{z+H}{d}. \tag{5.31}$$

To find the vertical momentum flux we calculate the first derivative,

$$\tau^x \;=\; \nu\frac{\partial}{\partial z}<u(z)> = \frac{\nu u_g}{d}e^{-\frac{z+H}{d}}\left(\cos\frac{z+H}{d} + \sin\frac{z+H}{d}\right), \tag{5.32}$$

$$\tau^y \;=\; \nu\frac{\partial}{\partial z}<v(z)> = -sig(f)\frac{\nu u_g}{d}e^{-\frac{z+H}{d}}\left(\sin\frac{z+H}{d} - \cos\frac{z+H}{d}\right). \tag{5.33}$$

With this finding we can express the bottom stress in terms of the geostrophic flow in the ocean interiour,

$$\tau_b^x \;=\; \frac{\nu u_g}{d} = u_g\frac{d|f|}{2}, \tag{5.34}$$

$$\tau_b^y \;=\; sig(f)\frac{\nu u_g}{d} = u_g\frac{d\,f}{2}. \tag{5.35}$$

In the next step we use the exact balance of the wind stress and the bottom friction in zonal direction. Note, it is a consequence of the volume conservation in the ACC-area! Solving for the geostrophic quantities "zonal flow" and " sea level elevation" we find,

$$u_g \;=\; \frac{2\tau_s^x}{d|f|}, \quad \frac{\partial}{\partial y}\eta = -sig(f)\frac{2\tau_s^x}{dg}. \tag{5.36}$$

The geostrophic flow is proportional to the wind stress and the inverse thickness of the bottom boundary layer as a measure for bottom friction. The sea level is rising north-ward at the southern hemisphere.

This result is interesting and suggests the possibility of geostrophic adjustment by bottom friction instead of inertial waves, Kelvin- or Rossby waves. It would explain the extension of the ACC into deep layers. From typical parameters like the observed width and depth of the ACC and friction parameters results a zonal transport and meridional overturning with a reasonable magnitude, but the surface tilt is much to small compared with altimeter observations. Choosing a smaller value for d enhances the tilt, but also the transport. Hence the theory is not complete and some important ingredient seems to be missing.

5.3. Lateral friction, Hidarkas dilemma

Some areas of the ACC exhibit a large eddy acitivity, hence, many mesoscale eddies are embedded in the mean current. These eddies may drift into the area north of the ACC and carry some momentum of the ACC. In turn water with low zonal momentum may enter the ACC with the tendency of slowing down the mean current. This way the exchange of eddies between the ACC and the adjacent seas acts like a meridional diffusion of momentum, or like friction between the ACC and the adjacent sea. This meridional momentum flux becomes part of the total momentum budget an is an alternative for the bottom friction to balance the wind driven acceleration.

Adding the therm

$$A_h \frac{\partial^2 u}{\partial y^2} \tag{5.37}$$

to the right hand side of the zonal momentum equation gives the balance equations

$$-f <V> \;=\; 0 = \tau_s^x - \tau_b^x + A_h \frac{\partial^2 <U>}{\partial y^2}, \tag{5.38}$$

$$f <U> +gH \frac{\partial}{\partial y} <\eta> \;=\; \tau_s^y - \tau_b^y. \tag{5.39}$$

For zero bottom stress, the system can be solved for simple assumptions on the form of the wind field. Choosing realistic value for $A_h = 10^4 \mathrm{m}^2 \mathrm{s}^{-1}$ derived from the observed eddy size and probability the calculated transport of the ACC amounts ≈ 2500 Sv which is completely unrealistic. Increasing A_h may give realistic transport values, but the resulting tilt of the sea surface becomes much to high. This finding is called in the literature "Hidarkas dilemma" - it is impossible to find a momentum budget of the ACC based on friction, that is compatible with the measurements for the transport of the ACC, the meridional surface tilt and the observed eddy size and activity within the ACC.

5.4. Topographic form stress

Figure 5.6 shows the position of the polar front as the northern rim of the ACC derived from microwave sea surface temperature data. Obviously it follows the bottom topography which suggests the hypothesis, that the ACC interacts strongly with the bottom topography. Indeed the ACC is not confined to the surface but extends into the depth.

Introducing a zonally variable bottom topography

$$z \;=\; -H(x,y), \tag{5.40}$$

the vertical and zonal average of the pressure gradient reads,

$$<P> \;=\; \int dx \int_{-H}^{0} dz\, p_x = \int dx \left(\frac{\partial}{\partial x} \int_{-H}^{0} dz\, p - p(x,y,-H) \frac{\partial}{\partial x} H(x,y) \right). \tag{5.41}$$

The first term vanishs for a periodic integral, the second term

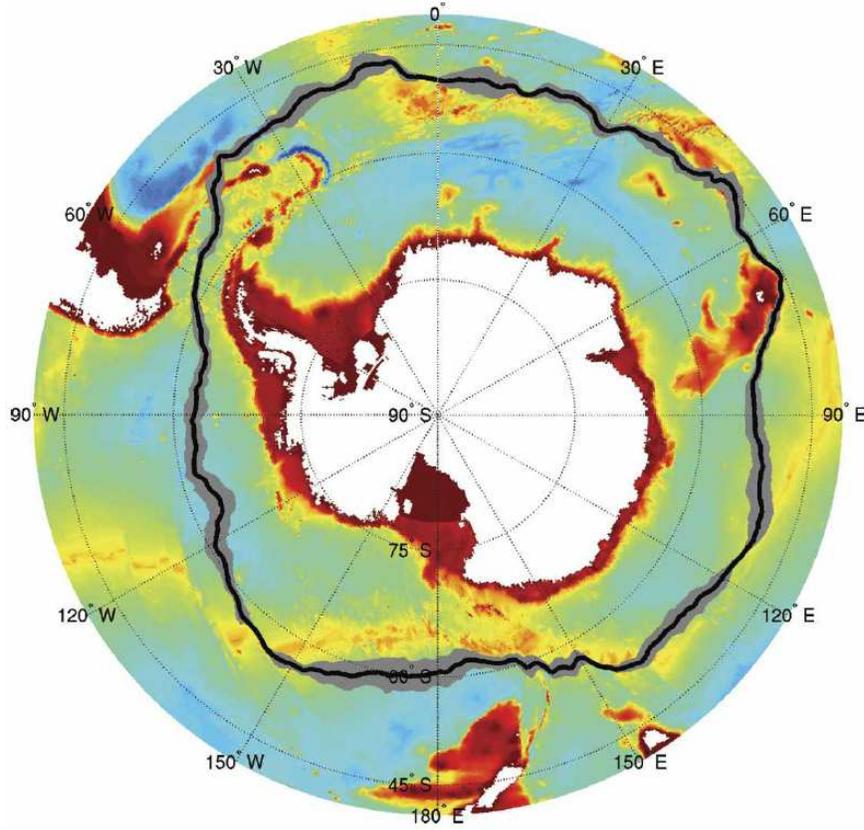$$\tau_f \;=\; - <p \frac{\partial}{\partial x} H> = <H \frac{\partial}{\partial x} p> \tag{5.42}$$

FIG. 5. Mean PF (black line) from the 3 yr of AMSR-E SST measurements and bottom topography (colors). The shaded area shows one std dev of the PF location.

Figure 5.6. The polar front seen in microwave data and its relation to bottom topography. (Dong et. al, 2005)

is called the bottom form stress. Hence, the momentum balance for the ACC with variable bottom topography reads

$$\tau_f - A_h \frac{\partial^2 <U>}{\partial y^2} = \tau_s^x - \tau_b^x, \tag{5.43}$$

$$f <U> + gH \frac{\partial}{\partial y} <\eta> = \tau_s^y - \tau_b^y. \tag{5.44}$$

So far we have introduced a new term into the balance equations, but the calculation of this term is not simple. Neither the bottom presssure nor its derivative can be expressed in one of the zonally averaged quantities. Our system of equations is not complete and the determination of the bottom form stress requires the detailed knowledge of the current (pressure) field.

The calculation of the bottom pressure field for realistic topography is a complex task and is solved mostly numerically. Even for very simple topography like a ridge or symmetric obstacle the solution reveals as complex. A first guess for the solution can be derived from the fact, that a steady geostrophic vertically averaged flow follows approximately contours of f/H. Hence, the stream function must be some function of f/H. Neglecting for a moment the meridional variability of f, we find

$$\tau_f \quad \approx \quad < g(H)\frac{\partial}{\partial x}H >=< \frac{\partial}{\partial x}G(H) >= 0. \tag{5.45}$$

Hence, a purely topographically steered flow does not produce any form stress. Some mechanism must be taken into account that generates a zonal shift of the pressure field against the topography causing a "phase shift" between the pressure and the topography. Candidates for processes generating this shift is bottom friction and lateral friction, but also Rossby waves propagating west-ward within the eastward ACC. The design of such so called "low order models" to find solutions of this problem exceeds the frame of these lecture.

Chapter 6

The oceanic wave guide

equatorial Kelvin waves

no reflection possible
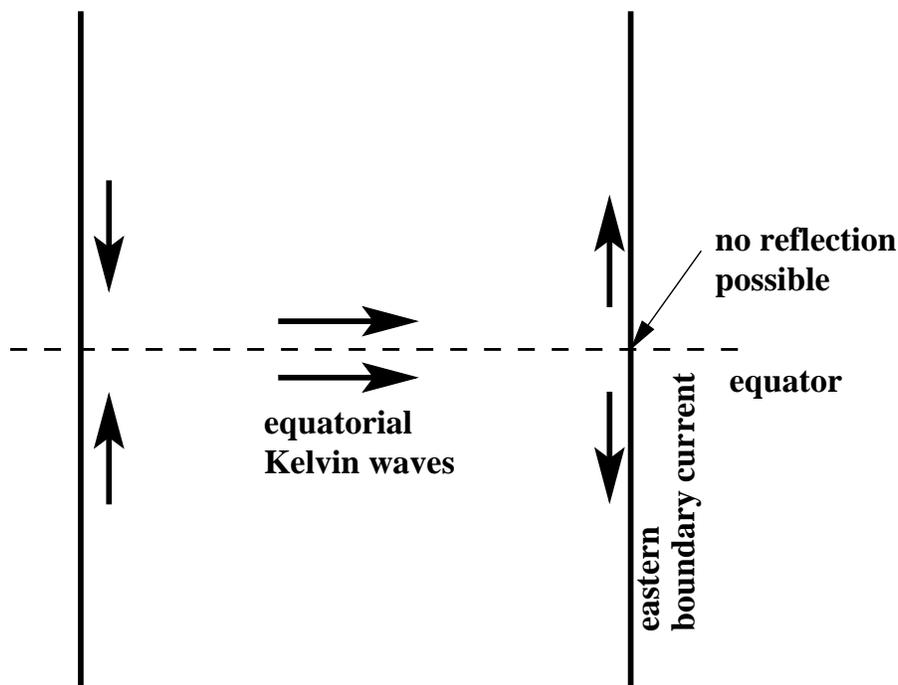
equator

eastern boundary current

Figure 6.1. The equatorial wave guide and the eastern boundary currents.

In the previous chapters the ocean response to wind forcing was governed by waves. These waves may carry signals on wind events into areas far away from the wind forcing. Examples are coastal or equatorial Kelvin waves exporting up- or downwelling signals, adjusting jet-like surface currents or generating undercurrents. Rossby waves may cross the oceans generating strong western boundary currents. Putting all these pieces together there emerges a new view on the ocean. There are several wave guides connecting distant areas of the ocean. The group speed of the waves defines times scales for the connectivity.
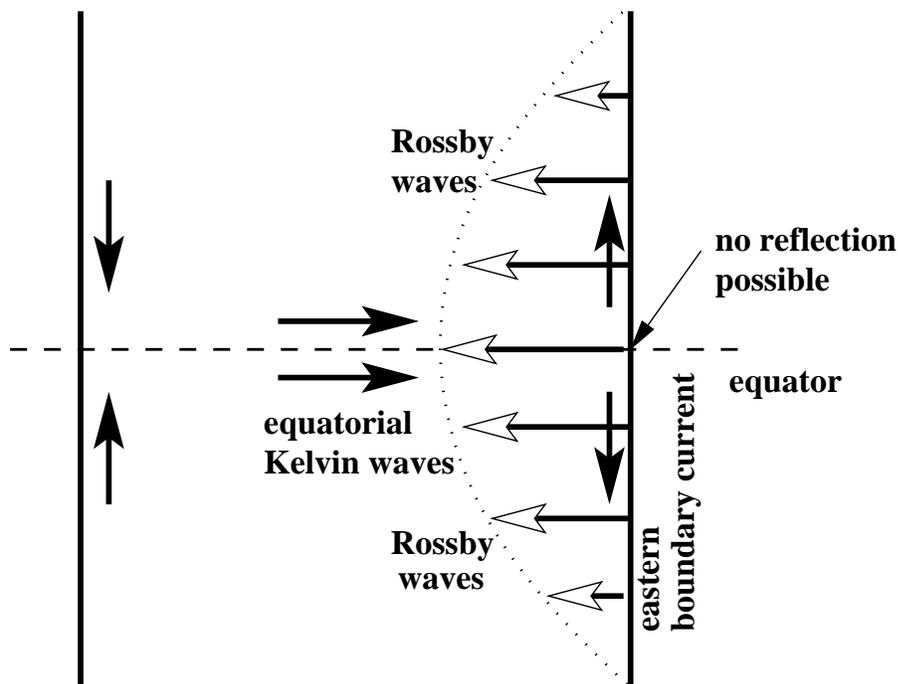
Figure 6.2. The equatorial wave guide, eastern boundary currents and Rossby waves closing the cycle.

This transport of signals and energy over long distances may have consequences for the state of the ocean on long time scales, hence, may be relevant for the ocean component of the earth climate. Fig. 6.1 shows the equatorial wave guide. Kelvin waves propagating equator-wards at the west coast cannot cross the equator but may bend east-ward and cross the ocean toward the east coast. Similarly, signals generated in the equatorial ocean propagate toward the east coast. At the east coast, Kelvin waves cannot be reflected because they have only east-ward phase and group velocity. Moreover, it can be shown that west-ward moving Rossby wave cannot be excited. Hence, the wave energy accumulates at the east coast and is the source of pole-ward moving Kelvin waves, now trapped at the oceans east coast.

This mechanism is one driver of the El Niño phenomenon observed in the Pacific ocean. Weaken trade winds over the equator disturb the balance of the barotropic (sea level) and baroclinic (tilt of the thermocline) gradients. As a result a wave is generated that goes along with an pulse of warm water in the east-ward undercurrent. Hence, at the coast of South America a warm temperature anomaly can be observed. The undercurrent bends pole-ward and can propagate the warm water north- and south-ward. A result is reduced upwelling and a thick layer of warm nutrient depleted surface water with far reaching consequences for the food chain at the coast of Peru. There is a strong feedback to the atmosphere circulation altering the weather for months or even longer.

This so called El Niño Southern Oscillation (ENSO) is subject of climate research since many years. One key for the understanding are Kelvin waves in the equatorial and coastal

wave guides which convey the directed transfer of energy and matter between the western and the eastern part of the Pacific. A similar, but less energetic phenomenon is known for the Atlantic ocean, the so called Benguela Niños.

As it was shown previously, a disturbance at an eastern coast generates Rossby waves that propagate west-ward. Without a proof or derivation we note that after a much longer time than the Kelvin waves need to cross the Pacific, the Rossby waves arrive at the west-coast and generate Kelvin waves there that move again equator-ward and cross the equator within the equatorial wave guide, but now carrying a signal in the oposite direction. Hence, we have a closed cycle of signal propagation. There is a phase shift from the finite wave group velocity. Positive feedbacks to the atmosphere may counteract to wave damping and the ocean with its system of wave guides may behave like some oscillator. Although the Kelvin- and Rossby waves can be described with linear Boussinesq equations the coupling to the atmosphere with positive feedback introduce non-linearity. This way we stumble into the wide field of the theory of non-linear systems with possibly chaotic or unpredictable behaviour. To deal with such systems requires an approach beyond this lecture.
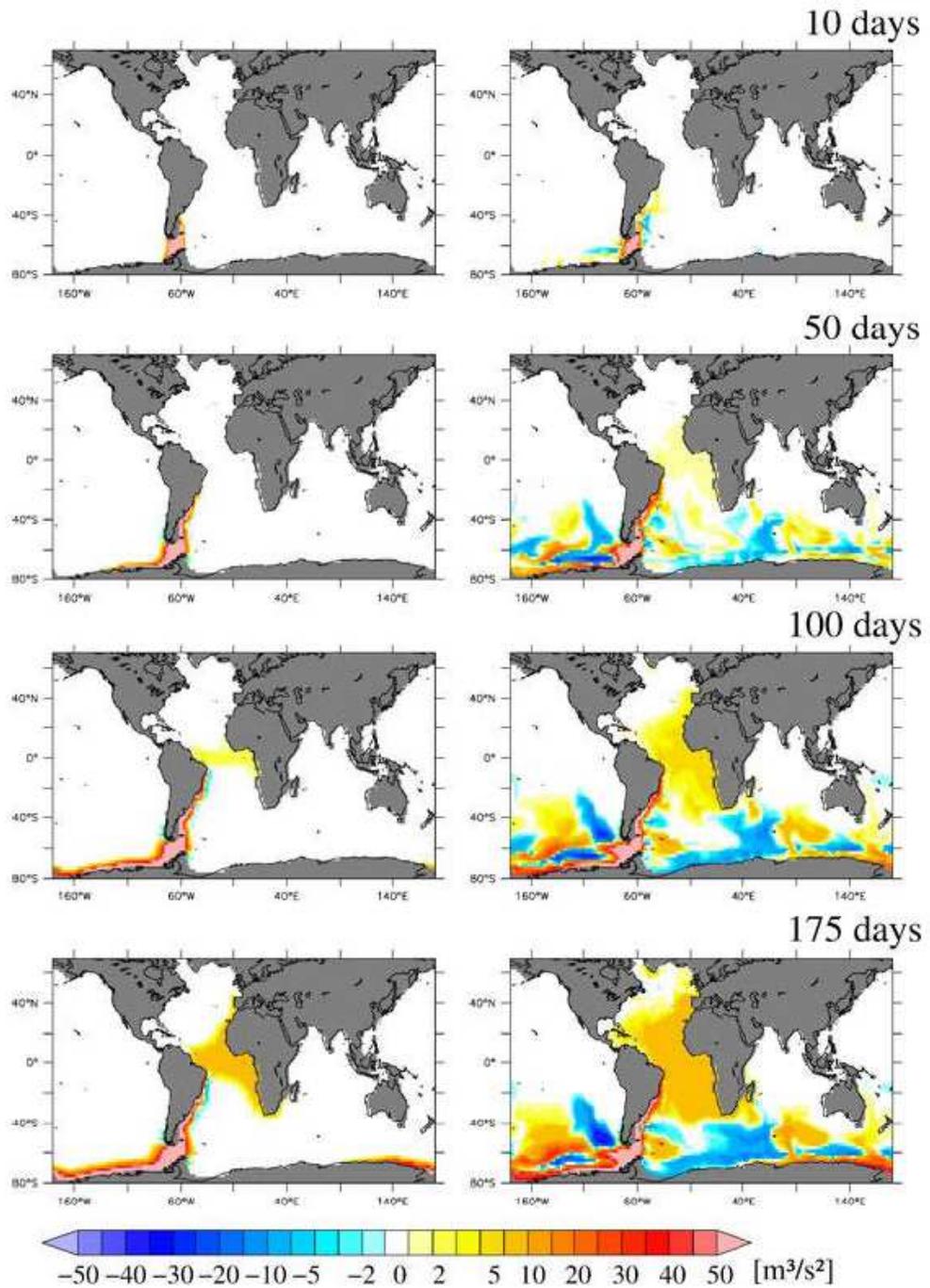
Fig. 8.22   Aspects of oceanic wave propagation, as simulated with the BARBI model (see Ap
pendix B.2). The wave is initiated in Drake Passage by a baroclinic perturbation and propagates i
the ocean wave guide around the globe. Left without topography, right with realistic topography
Both simulations are for a mean state with prescribed Brunt–Väisälä frequency without any mea
flow

Appendix A

Frequently used Fourier integrals

$$F(t) = \int\limits_{-\infty}^{\infty} \frac{d\omega}{2\pi} e^{-i\omega t} \tilde{F}(\omega) \, , \; \tilde{F}(\omega) = \int\limits_{-\infty}^{\infty} dt e^{i\omega t} F(t)$$

$F(t)$	$\tilde{F}(\omega)$
1	$2\pi\delta(\omega)$
e^{ift}	$2\pi\delta(\omega + f)$
$\cos(ft)$	$\pi\left(\delta(\omega + f) + \delta(\omega - f)\right)$
$\sin(ft)$	$\frac{\pi}{i}\left(\delta(\omega + f) - \delta(\omega - f)\right)$
t^n	$\frac{2\pi}{i^n} \frac{d^n}{d\omega^n} \delta(\omega)$
$\theta(t)$	$\frac{i}{\omega + i\epsilon}$
$\theta(t)\sin(ft)$	$\frac{-f}{(\omega + i\epsilon)^2 - f^2}$
$\theta(t)\cos(ft)$	$\frac{i\omega}{(\omega + i\epsilon)^2 - f^2}$
$\theta(t)t$	$\frac{-1}{(\omega + i\epsilon)^2}$

For spatial integrals substitute $x = t$ and $k = -\omega$.

Fennel, W., Lass, H.U., 1989. *Analytical theory of forced oceanic waves.* Akademie-Verlag.

Appendix B

Example for the eigenfunction decomposition

Consider a volume force with exponential shape. All factors not needed here are dropped.

$$f(z) = e^{\frac{z}{H_{mix}}} = e^{bz}. \tag{B.1}$$

Recall the eigenfunctions

$$F_0(z) \approx 1$$
$$F_n(z) \approx \sqrt{2}(-1)^n \cos \frac{n\pi z}{H}. \tag{B.2}$$

The coefficients of $f(z)$ are

$$f_0 = \frac{1}{Hb} \left(1 - e^{-bH}\right),$$
$$f_n = \int_{-H}^{0} \frac{dz}{H} e^{bz} F_n(z),$$
$$= \frac{\sqrt{2}}{H}(-1)^n \frac{e^{bz}}{b^2 + \left(\frac{n\pi}{H}\right)^2} \left(b \cos \frac{n\pi z}{H} + \frac{n\pi z}{H} \sin \frac{n\pi z}{H}\right)\Big|_{-H}^{0}$$
$$= \frac{\sqrt{2}}{H}(-1)^n \frac{b}{b^2 + \left(\frac{n\pi}{H}\right)^2} \left(1 - (-1)^n e^{-bH}\right)$$
$$= \frac{\sqrt{2}}{\pi}(-1)^n \frac{q}{q^2 + n^2} \left(1 - (-1)^n e^{-bH}\right) \tag{B.3}$$

The abbreviation

$$q = \left(\frac{bH}{\pi}\right) \tag{B.4}$$

was used.

It is interesting to demonstrate, how the original exponential function is reconstructed from the sum over the eigenfunctions, i.e., to provef

$$f(z) = \sum_n F_n(z) f_n. \tag{B.5}$$

The calculation of such sums is complex. Basically, a decomposition into eigenfunctions is used. Hence, we just check consistency and use a table of infinite series (see for example Prudnykov, Brytchkov and Marytchev: Integrals and Series)

$$\sum_{n=1}^{\infty} \frac{1}{q^2 + n^2} \cos kx \;=\; +\frac{\pi}{2q} \cosh((\pi - x)q) \sinh^{-1} \pi q - \frac{1}{2q^2} \qquad 0 \le x \le 2\pi \qquad (\text{B.6})$$

and

$$\sum_{n=1}^{\infty} \frac{(-1)^{n-1}}{q^2 + n^2} \cos kx \;=\; -\frac{\pi}{2q} \cosh xq \sinh^{-1} \pi q + \frac{1}{2q^2} \qquad -\pi \le x \le \pi \qquad (\text{B.7})$$

Note the restricted domain of x! Since x is negative, we have to use

$$F_n(z) \;=\; F_n(-z) \qquad (\text{B.8})$$

in the first sum. We find

$$
\begin{aligned}
f(z) \;=\;& \frac{1}{Hb} \left(1 - e^{-bH} \right) \\
&+ \frac{2q}{\pi} \left(\frac{\pi}{2q} \frac{\cosh((\pi + x)q)}{\sinh \pi q} - \frac{1}{2q^2} - \frac{\pi}{2q} \frac{e^{-bH} \cosh xq}{\sinh \pi q} + \frac{e^{-bH}}{2q^2} \cdot \right)
\end{aligned}
\qquad (\text{B.9})
$$

With a little algebra this collapses to

$$f(z) \;=\; e^{\frac{z}{H_{mix}}} = e^{bz}. \qquad (\text{B.10})$$

Appendix C

Properties of the Bessel functions

Many mathematical problems related to the potential equation, diffusion equation or oscillating bodies lead to a ordinary differential equation of the general form

$$z^2\frac{d^2f}{dz^2} + z\frac{df}{dz} + \left(z^2 - \nu^2\right)f = 0. \tag{C.1}$$

The solution defines a special type of functions, so called Bessel-functions. They are defined by a series decomposition. The analytical properties of these functions are well investigated, see for example

Milton Abramowitz, Irene Stegun: *Handbook of Mathematical Functions.* Dover, New York 1972, S. 355.

C.1. Bessel functions of first kind

Solutions of Bessel's differential equation can be written as a power series,

$$J_\nu(z) = \left(\frac{1}{2}z\right)^\nu \sum_{n=0}^\infty \frac{\left(-\frac{z^2}{4}\right)^n}{\Gamma(\nu + n + 1)\,n!}. \tag{C.2}$$

The Γ-function may be defined by Euler's integral

$$\Gamma(z) = \int_0^\infty dt\, t^{z-1} e^{-t}, \qquad (\mathcal{R}z > 0) \tag{C.3}$$

for integer arguments it reads simply

$$\Gamma(n+1) = n!. \tag{C.4}$$

Since $\Gamma(n)$ growth faster then the z^n the sum converges and J_ν is finite for all z.

C.2. Bessel functions of second kind

A second solution of Bessel's differential equation reads

$$Y_\nu(z) = \frac{J_\nu(z)\cos(\nu\pi) - J_{-\nu}(z)}{\sin(\nu\pi)}. \tag{C.5}$$

For $\nu = 0$ this function has a logarithmic singularity at $z = 0$, otherwise a ploe of the order n. Since this function is not needed here, we skip more details.
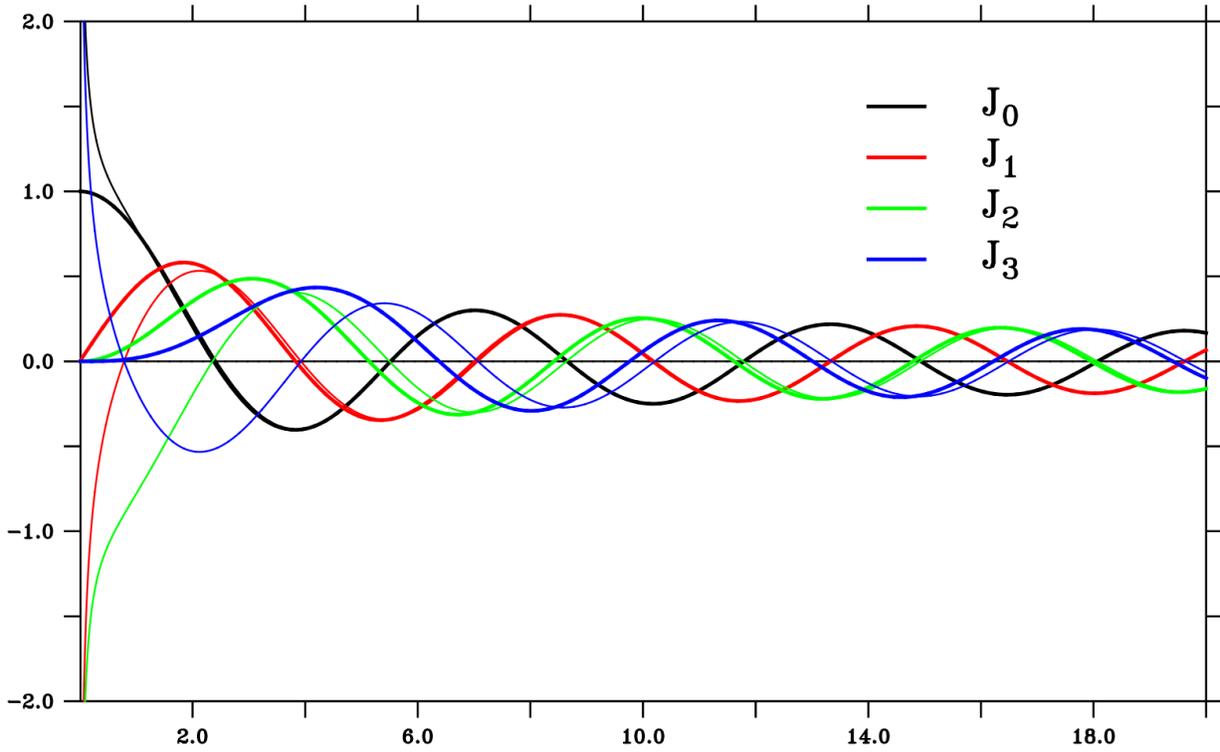
Figure C.1. Bessel functions of the first kind. Thick lines mark the full soltion, thin lines the asymptotic approximation.

C.3. Limiting forms for small arguments

$$J_\nu(z \to 0) \quad \approx \quad \frac{\left(\frac{1}{2}z\right)^\nu}{\Gamma(\nu+1)}, \qquad (\nu \neq -1, -2, ...) \tag{C.6}$$

$$Y_0(z \to 0) \quad \approx \quad \frac{2}{\pi}\left(\left(\ln\left(\frac{z}{2}\right) + \gamma\right)\right) \tag{C.7}$$

$$Y_\nu(z \to 0) \quad \approx \quad \frac{1}{\pi}\Gamma(\nu)\left(\frac{z}{2}\right)^{-\nu} (\mathcal{R}\nu > 0) \tag{C.8}$$

C.4. Asymptotic forms for large arguments

For fixed ν and $|z| \to \infty$ the Bessel functions describe a damped oscillation

$$J_\nu(z) \approx \sqrt{\frac{2}{\pi z}} \cos\left(z - \frac{1}{2}\nu\pi - \frac{1}{4}\pi\right) + \mathcal{O}(|z|^{-1}) \tag{C.9}$$

$$Y_\nu(z) \approx \sqrt{\frac{2}{\pi z}} \sin\left(z - \frac{1}{2}\nu\pi - \frac{1}{4}\pi\right) + \mathcal{O}(|z|^{-1}) \tag{C.10}$$

C.5. Recurrents relations

Let $\mathcal{C}$ be either J or Y. The following recurrence relations can be derived:

$$\mathcal{C}_{\nu-1}(z) + \mathcal{C}_{\nu+1}(z) = \frac{2\nu}{z}\mathcal{C}_\nu(z) \tag{C.11}$$

$$\mathcal{C}_{\nu-1}(z) - \mathcal{C}_{\nu+1}(z) = 2\mathcal{C}'_\nu(z) \tag{C.12}$$

$$\mathcal{C}'_\nu(z) = \mathcal{C}_{\nu-1}(z) - \frac{\nu}{z}\mathcal{C}_\nu(z) \tag{C.13}$$

$$\mathcal{C}'_\nu(z) = -\mathcal{C}_{\nu+1}(z) + \frac{\nu}{z}\mathcal{C}_\nu(z) \tag{C.14}$$

Especially

$$J'_0(z) = -J_1(z) \tag{C.15}$$

$$Y'_0(z) = -Y_1(z). \tag{C.16}$$

Appendix D

Calculation of convolution integrals

The inverse Fourier integrals to be carried out are of the type

$$C^{(1)}(|y|,t) = \int_{-\infty}^{\infty} \frac{d\omega}{2\pi i} \frac{e^{i|y|\lambda\sqrt{\tilde{\omega}^2-f^2}-i\tilde{\omega}t}}{\tilde{\omega}^2\sqrt{\omega^2-f^2}}, \tag{D.1}$$

$$C^{(2)}(|y|,t) = \int_{-\infty}^{\infty} \frac{d\omega}{2\pi} \frac{f^2 e^{i|y|\lambda\sqrt{\tilde{\omega}^2-f^2}-i\tilde{\omega}t}}{\tilde{\omega}^2(\omega^2-f^2)}, \tag{D.2}$$

$$\tag{D.3}$$

Let us first discuss the integration path. We complete it again by a semicircle in the lower or upper complex half plane. This is possible, since the length of the path growth like ω, but the function decreases exponentially when

> closing in the upper half plane for $t < \lambda|y|$,

> closing in the lower half plane for $t > \lambda|y|$.

In the first case the resulting contour integral encloses no singulatities and vanishs. Hence, we have to close the contour in the lower half plane and the result carries a factor $\theta(t - \lambda|y|)$. Away from the cut the integrand is an analytical function and we can contract the integration path around the singularities. Figure D.1 depicts the contour of the integration path. The fact, that a time $t > \lambda|y|$ is needed until the perturbation (pressure or velocity) differs from the Ekman solution is very important. It shows that the signal carrying the information on the existence of the wind edge spreads with waves. The maximum phase velocity is λ^{-1}. The response is zero, until a wave from the wind edge has arrived. Causality is ensured!

Evaluation of $C^{(1)}$

Following the idea of Fennel, as a first step $C_{tt}^{(1)}$ is transformed into a time integral. $C_{tt}^{(1)}$ reads

$$C_{tt}^{(1)} = -\int_{-\infty}^{\infty} \frac{d\omega}{2\pi i} \frac{e^{i\sqrt{\tilde{\omega}^2-f^2}\lambda y-i\omega t}}{\sqrt{\tilde{\omega}^2-f^2}}. \tag{D.4}$$

The integration path can be completed again to a closed contour. Figure D.1 shows details. For $\lambda y - t > 0$ the semi-circle in the upper half-plane does not contribute to
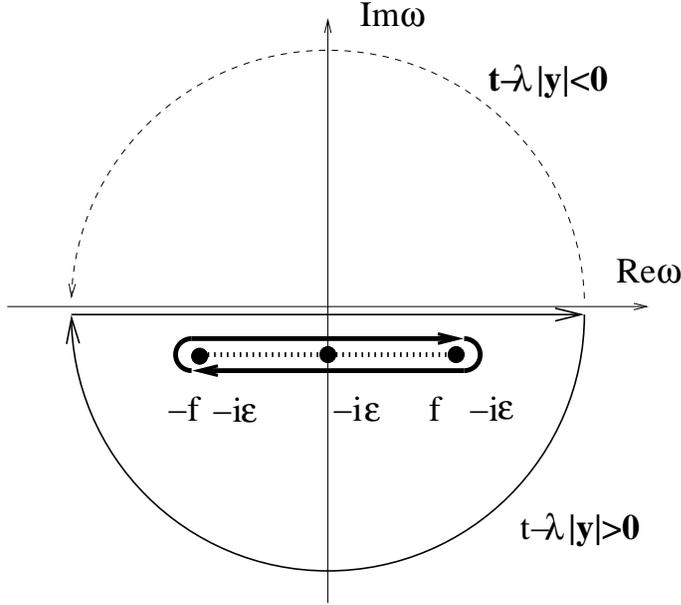
Figure D.1. Choice of the integration path for the general integrals $C^{(1)}$ and $C^{(2)}$. A separate integration around the singularities is not possible, since the real part of the square root changes sign when crossong the cut in the complex plane (dashed line).

the integral. In this case the integration path does not include any singularity and the integral vanishs. For $\lambda y - t < 0$ the integral can be closed in the lower half-plane. Using Cauchy's theorem, the contour can be contracted to the thick closed line. At the upper line the square root $\sqrt{\tilde{\omega}^2 - f^2}$ has the positive sign, at the lower line the negative sign. Hence,

$$
\begin{aligned}
C_{tt}^{(1)} &= -\theta(t - \lambda y) \int_{-f}^{f} \frac{d\omega}{2\pi i} \frac{e^{i\sqrt{\omega^2 - f^2}\lambda y - i\omega t}}{\sqrt{\omega^2 - f^2}} - \theta(t - \lambda y) \int_{f}^{-f} \frac{d\omega}{2\pi i} \frac{e^{-i\sqrt{\omega^2 - f^2}\lambda y - i\omega t}}{(-1)\sqrt{\omega^2 - f^2}} \\
&= \theta(t - \lambda y) \frac{2}{\pi} \int_{0}^{f} d\omega \frac{\cosh\sqrt{f^2 - \omega^2}\lambda y}{\sqrt{f^2 - \omega^2}} \cos\omega t.
\end{aligned}
\tag{D.5}
$$

This integral can be found in standard integral tables and leads to a Bessel function of first kind,

$$
C_{tt}^{(1)} = \theta(t - \lambda y) J_0\left(f\sqrt{t^2 - \lambda^2 y^2}\right).
\tag{D.6}
$$

The two time integrals can be found either by using the convolution theorem or by direct time integration using a partial integral and the properties of the step function,

$$
C_t^{(1)} = \int_{-\infty}^{t} dt' \theta(t' - \lambda y) J_0\left(f\sqrt{t'^2 - \lambda^2 y^2}\right),
\tag{D.7}
$$

$$
C^{(1)} = \int_{-\infty}^{t} dt'(t - t') \theta(t' - \lambda y) J_0\left(f\sqrt{t'^2 - \lambda^2 y^2}\right).
\tag{D.8}
$$

So far we have replaced only the ω-integral by a time integral. This integral can be carried out numerically, using standard techniques, e.g. a Romberg or Runge-Kutta scheme.

For our purpose analytical approximation may help to understand some more details. The first finding ist, that the integrals vanish for $t < \lambda y$. Hence, considering some special place with a distance y to the coast. The pressure perturbation given by $C^{(1)}$ remains zero until a wave with phase speed λ^{-1}, (remember, this is the upper limit for the group speed), arrives at this special position. Again, waves are responsible for propagation of pressure signals away from the coast.

To consider the response for large times, $t \gg \lambda y$, we search for asymptotic expressions. With the transformation

$$
\begin{aligned}
t^2 - \lambda^2 y^2 &= q^2, \qquad t^2 = q^2 + \lambda^2 y^2, \\
dt &= \frac{q}{t} dq = \frac{q}{\sqrt{q^2 + \lambda^2 y^2}} dq
\end{aligned}
\tag{D.9}
$$

we find

$$
\begin{aligned}
C^{(1)} &= \theta(t - \lambda y) \int_0^{q_t} dq\, J_0\left(fq\right) \left(\frac{qt}{\sqrt{q^2 + \lambda^2 y^2}} - q \right), \\
q_t &= \sqrt{t^2 - \lambda^2 y^2}
\end{aligned}
\tag{D.10}
$$

It is important, that the integrand vanishes at the upper boundary. An approximation for the first term can be found from the integral

$$
\int_0^\infty dx \frac{x}{\sqrt{x^2 + a^2}} J_0(fx) = \frac{1}{f} e^{-fa}.
\tag{D.11}
$$

For the second integral we use the relation

$$
\int dx\, x\, J_0(x) = x J_1(x),
\tag{D.12}
$$

and find

$$
\begin{aligned}
C^{(1)} &= \theta(t - \lambda y) \left(\frac{t}{f} e^{-f\lambda y} - \int_{q_t}^\infty dq \frac{qt\, J_0\left(fq\right)}{\sqrt{q^2 + \lambda^2 y^2}} \right) \\
&\quad - \theta(t - \lambda y) \frac{1}{f} \sqrt{t^2 - \lambda^2 y^2}\, J_1\left(f\sqrt{t^2 - \lambda^2 y^2} \right).
\end{aligned}
\tag{D.13}
$$

Obviously, all contribution diverge for large times t. This is not a satisfying result, away from the coast the response to wind field should vanish. (Remember the original boundary conditions). Hence, we try to reorder the terms. To this end, we use the recurrence relation of the Bessel functions,

$$
J_0(x) = J_1'(x) + \frac{J_1(x)}{x}.
\tag{D.14}
$$

This gives

$$
\int_{q_t}^\infty dq \frac{qt\, J_0\left(fq\right)}{\sqrt{q^2 + \lambda^2 y^2}} = \int_{q_t}^\infty dq \frac{qt}{\sqrt{q^2 + \lambda^2 y^2}} \left(\frac{1}{f} \frac{\partial}{\partial q} J_1\left(fq\right) + \frac{J_1\left(fq\right)}{fq} \right).
\tag{D.15}
$$

After integrating the first summand by parts we find

$$\int_{q_t}^{\infty} dq \frac{qt J_0\left(fq\right)}{\sqrt{q^2 + \lambda^2 y^2}} = -\frac{\sqrt{t^2 - \lambda^2 y^2}}{f} J_1\left(f\sqrt{t^2 - \lambda^2 y^2}\right)$$
$$+ \int_{q_t}^{\infty} dq J_1\left(fq\right) \frac{tq^2}{f\sqrt{q^2 + \lambda^2 y^2}^3} \qquad \text{(D.16)}$$

The first term cancels exactly the last term of Eq. (D.13), hence these divergent terms cancel out. The remaining term can be processed by using

$$J_1(x) = -J_0'(x). \qquad \text{(D.17)}$$

Integrating again by parts gives

$$\int_{q_t}^{\infty} dq \frac{qt J_0\left(fq\right)}{\sqrt{q^2 + \lambda^2 y^2}} = -\frac{\sqrt{t^2 - \lambda^2 y^2}}{f} J_1\left(f\sqrt{t^2 - \lambda^2 y^2}\right)$$
$$-\frac{1}{f^2} J_0\left(f\sqrt{t^2 - \lambda^2 y^2}\right) \frac{t^2 - \lambda^2 y^2}{t^2} - \int_{q_t}^{\infty} dq \frac{J_0\left(fq\right)}{q} \mathcal{O}(t/q) \quad \text{(D.18)}$$

The last term vanishes faster then t^{-1} for large times t. Hence, we find the following result for the asymptotic behaviour of $C^{(1)}$,

$$C^{(1)} \approx \theta(t - \lambda y)\left(\frac{t}{f}e^{-f\lambda y} + \frac{1}{f^2} J_0\left(f\sqrt{t^2 - \lambda^2 y^2}\right) \frac{t^2 - \lambda^2 y^2}{t^2}\right). \qquad \text{(D.19)}$$

For large arguments the Bessel function shows a slowly decreasing oscillation,

$$J_0\left(f\sqrt{t^2 - \lambda^2 y^2}\right) \approx \sqrt{\frac{2}{f\pi t}} \cos\left(f\sqrt{t^2 - \lambda^2 y^2} - \frac{\pi}{4}\right)$$
$$= -\sqrt{\frac{2}{f\pi t}} \sin\left(f\sqrt{t^2 - \lambda^2 y^2} + \frac{\pi}{4}\right) \qquad \text{(D.20)}$$

It is important, that we keep the full argument in the *sin*-function. This so called "phase conserving approximation" is needed for the summation over the vertical modes.

$$C^{(1)} \approx \theta(t - \lambda y)\left(\frac{t}{f}e^{-f\lambda y} - \frac{1}{f^2}\sqrt{\frac{2}{f\pi t}} \sin\left(f\sqrt{t^2 - \lambda^2 y^2} + \frac{\pi}{4}\right)\right). \qquad \text{(D.21)}$$

Evaluation of $C^{(2)}$

Similarly (Fennel, 1989) we find for $C^{(2)}$ the representation as a time integral,

$$C^{(2)} = \theta(t - \lambda y)\left(t - \lambda y - \frac{\sin f(t - \lambda y)}{f}\right)$$
$$-\frac{y}{R}\int_{-\infty}^{t} dt'\left(t - t' - \frac{\sin f(t - t')}{f}\right)\theta(t' - \lambda y)\frac{J_1\left(f\sqrt{t'^2 - \lambda^2 y^2}\right)}{\sqrt{t'^2 - \lambda^2 y^2}}. \qquad \text{(D.22)}$$

We need also the time derivative

$$
\begin{aligned}
C_t^{(2)} \;=\;& \theta(t - \lambda y)\left(1 - \cos f(t - \lambda y)\right) \\
& - \frac{y}{R} \int_{-\infty}^{t} dt' \left(1 - \cos f(t - t')\right) \theta(t' - \lambda y) \frac{J_1\left(f\sqrt{t'^2 - \lambda^2 y^2}\right)}{\sqrt{t'^2 - \lambda^2 y^2}}.
\end{aligned}
\tag{D.23}
$$

The asymptotic result for large time reads,

$$
C^{(2)} \;\approx\; \theta(t - \lambda y)\left(te^{-\frac{y}{R}} - \frac{\sin ft}{f} + \frac{y}{Rf}\sqrt{\frac{2}{f\pi t}}\sin\left(f\sqrt{t^2 - \lambda^2 y^2} + \frac{\pi}{4}\right)\right),
\tag{D.24}
$$

$$
C_t^{(2)} \;\approx\; \theta(t - \lambda y)\left(e^{-\frac{y}{R}} - \cos ft + \frac{y}{R}\sqrt{\frac{2}{f\pi t}}\cos\left(f\sqrt{t^2 - \lambda^2 y^2} + \frac{\pi}{4}\right)\right)
\tag{D.25}
$$

Appendix E

Example for the Ekman transport in the open ocean

The steady componenten of a wind driven flow in the open ocean reads:

$$v(x,y,z,t) = -\frac{\tau^x}{\rho_0}\theta(t)\frac{\theta(z+H_{mix})}{H_{mix}f}. \tag{E.1}$$

$$u(x,y,z,t) = \frac{\tau^y}{\rho_0}\theta(t)\frac{\theta(z+H_{mix})}{H_{mix}f}. \tag{E.2}$$

$$p(x,y,z,t) = 0. \tag{E.3}$$

This result, see also Eq.(2.293) in Section 2.4 can be found if the wind field is assumed to be basically uniform. Here we discuss the Ekman transport driven by locally uniform winds. As input we consider the COADS climatological winds, the analysis is done with *ferret*. Here is a sketch of the script.

```
! Load Coads climatology
use coads_climatology ! it is distributed with ferret
show data

!1. Find coriolis parameter
let pi    = 4*atan(1)
let t_sid = (1-1/365.2425)*24*3600
let omega = 2*pi/t_sid

!find coordinates
let x_coord = x[gx=slp]
let y_coord = y[gy=slp]

! define a field with f depending on the coordinates of the wind field
! blank the equatorial area. Division by f is not well defined there.
let f_total = 2*omega* sin(y_coord*pi/180)+ 0*x_coord
```
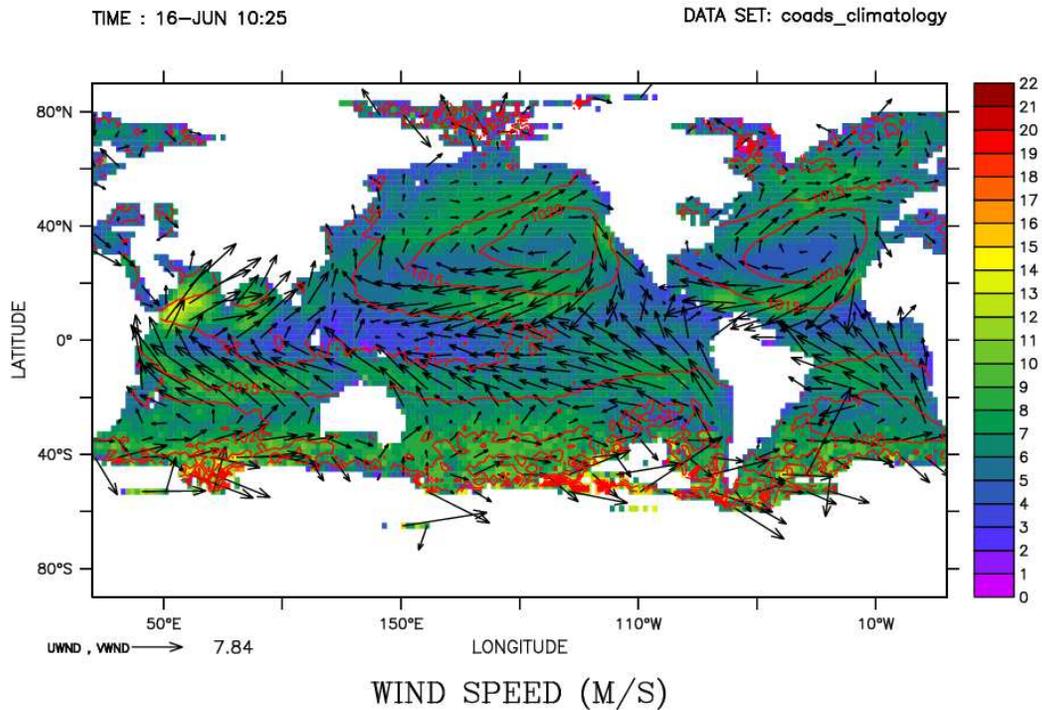
Figure E.1. Coads climatological wind and the global pressure field for June.

```
let f_blank = if abs(f_total) gt 1e-5 then f_total else 1/0

! get the kinematic wind stress (divided by the density)
let rho_a= 1.2  !kg/m3 density of air
let rho_w= 1022 !kg/m3 density of water
let C_d  = 0.001
let taux = wspd*C_d*uwnd*rho_a/rho_w
let tauy = wspd*C_d*vwnd*rho_a/rho_w

! get the Ekman transport
let uek = tauy/f_blank
let vek = (-1)*taux/f_blank

! Display the wind speed
cancel mode logo; set win/asp=0.7/quality=high 1
! Select January or June as example
set region/l=6
shade WSPD
vec/over uwnd, vwnd
!see the geostrophic balance with the air pressure
cont/over/nolab slp
```
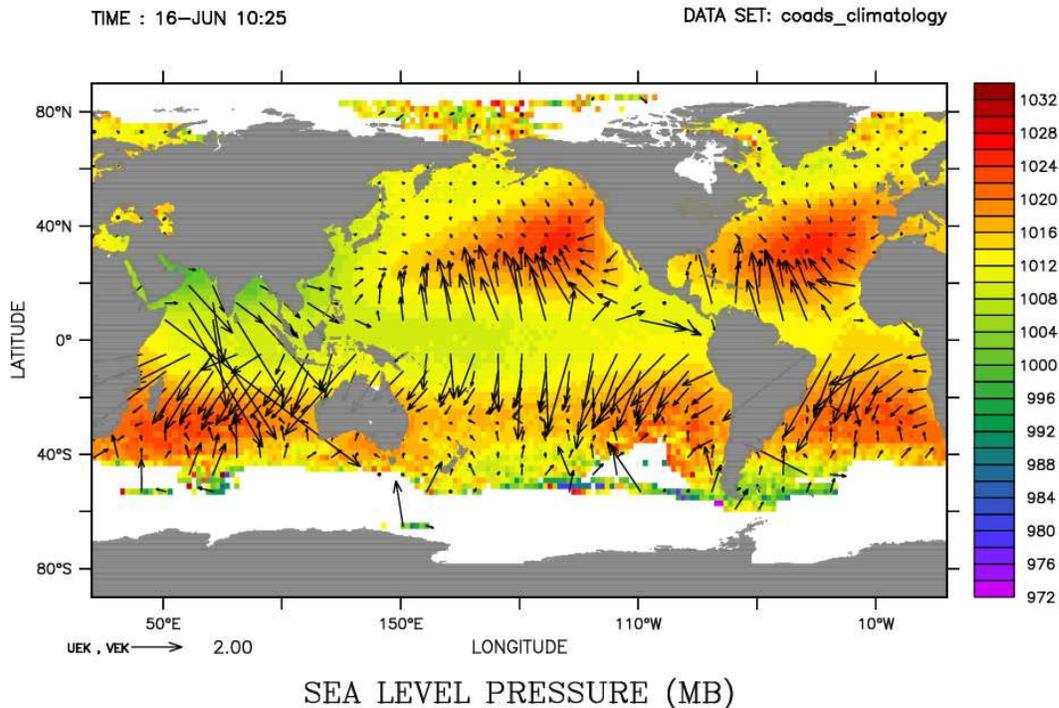
Figure E.2. Ekman transport driven by the climatological winds.

```
vec/over/col=2/len=10 (-100)*slp[y=@ddc]/f_blank/rho_a, 100*slp[x=@ddc]/f_blank/rho_a
```

The winds are in geostrophic balance with the sea level pressure. Permanent wind pattern like the trade winds correspont to permanent high an low pressure areas. Try to locate the Island low, the Azores high or the St. Helena high in the Atlantic ocean! The geostrophically balanced winds encircle the high and low air pressure areas.

```
! Display the sea level pressure and the Ekman transport
set region/l=6
shade slp
vec/over/len=2 uek,vek
go fland 20
```

We see that the Ekman transport is mainly directed into areas with high air pressure and away from areas with low air pressure.

```
! Find the divergence, i.e., vertical velocity at the bottom of the mixed layer
can region
let tauf_x=taux/f_blank
let tauf_y=tauy/f_blank
let curl_tau=tauf_x[y=@ddc,l=@ave]-tauf_y[x=@ddc,l=@ave]
shade/lev=(-4e-6,4e-6,1e-7)/pal=adcp (-1)*curl_tau[x=@sbn:3,y=@sbn:3]
```

```
vec/over/len=2 uek[l=@ave],vek[l=@ave]
cont/over/lev=(1015,1040,5)/line=2/nolab slp[l=@ave]
cont/over/lev=(900,1010,5)/line=3/nolab slp[l=@ave]
go fland 20
```
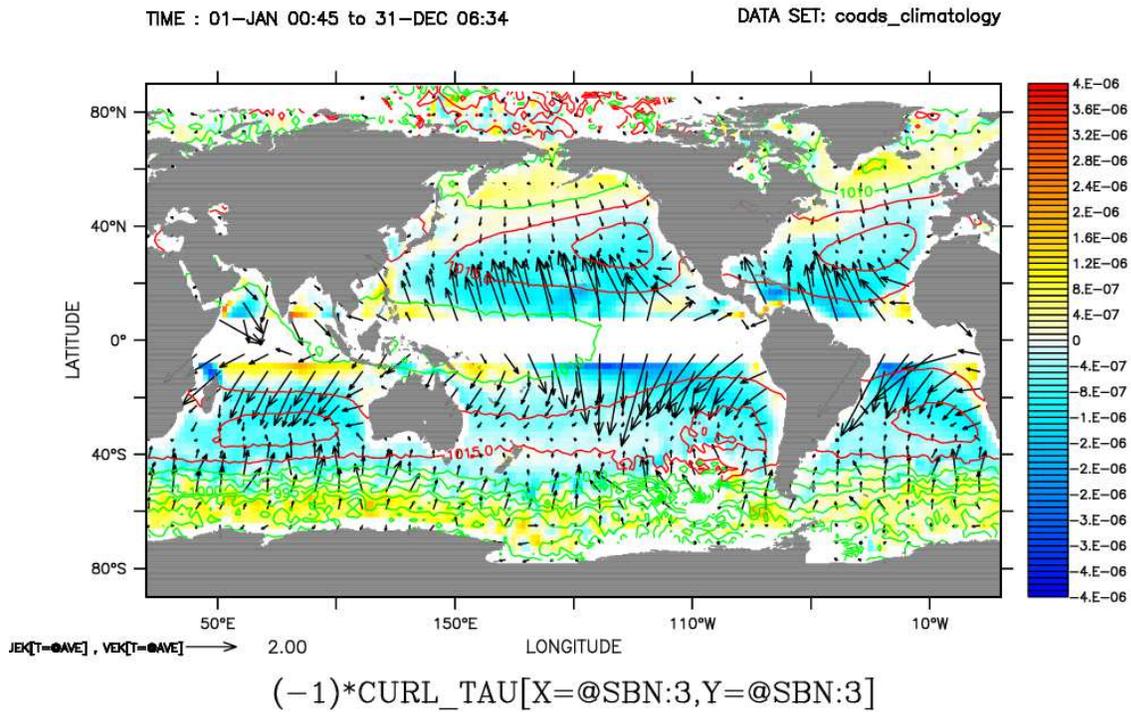

Figure E.3. Negative curl of the wind stress divided by f as measure for upwelling at the bottom of the mixed layer.

REFERENCES

[1] J. R. Apel. *Principles of Ocean Physics*, volume 38 of *International Geophysics Series.* Academic Press, London, 1987.

[2] W. Fennel and H.U. Lass. *Analytical theory of forced oceanic waves.* Akademie-Verlag, Berlin, 1989.

[3] A. Gill. *Atmosphere-Ocean Dynamics*, volume 30 of *International Geophysics Series.* Academic Press Inc., London, 1982. 662 + xv pp.

[4] Kundu, Pijush K. *Fluid Mechanics.* Academic Press, San Diego, 1993.

[5] James Lighthill. *Waves in Fluids.* Cambridge University Press, 2001.

[6] Dirk Olbers, Jürgen Willebrand, and Carsten Eden. *Ocean Dynamics.* Springer, 2012.

[7] Emery W.J. Swift J.H. Talley L.D., Pickard G.L. *Descriptive Physical Oceanography: An Introduction (Sixth Edition).* Elsevier, 2011.

[8] Matthias Tomczak and J. Stuart Godfrey. *Regional Oceanography: An Introduction.* Pergamon Press, Oxford, England, 1994. 422 + vii pp.

[9] Geoffrey K. Vallis. *Atmospheric and Oceanic Fluid Dynamics.* Cambridge University Press, 2006.